Porins in der Gattung *Borrelia,*
Charakterizierung von P13 und P66

Porins in the genus *Borrelia*

Characterization of P66 and P13

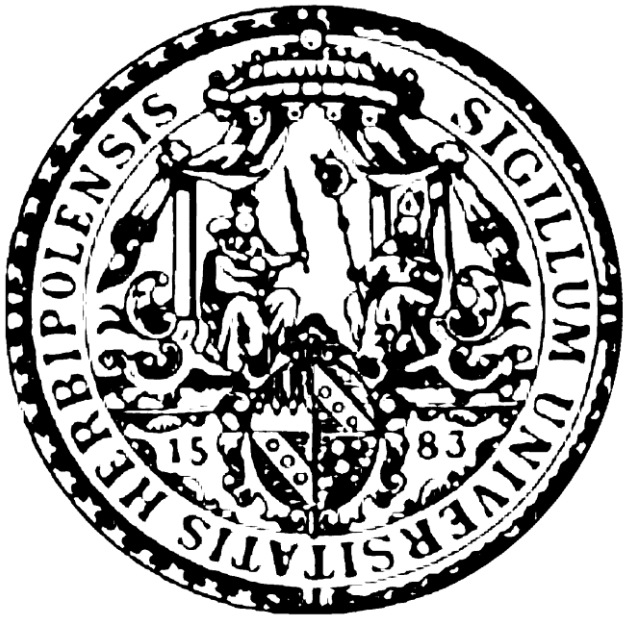

Iván Bárcena Uribarri
from Santander
Graduate School of Life Sciences – University of Wuerzburg
Infection and Immunity
October 2010

Submitted on: ……..

Office stamp

Members of the Thesis Committee:

Chairperson:	Prof. Dr. Jörg Schultz
Primary Supervisor:	Prof. Dr. Roland Benz
Supervisor (Second):	Prof. Dr. Thomas Rudel
Supervisor (Third):	Prof. Dr. Miquel Viñas

Date of Public Defense: ……

I hereby declare that my thesis entitled “Porin in the genus *Borrelia*. Characterization from P13 and P66” is the result of my own work. I did not receive any help or support from commercial consultants. All sources and/or materials applied are listed and specified in the thesis.

Furthermore, I verify that this thesis has not yet been submitted as part of another examination process neither in identical nor in similar form.

Wuerzburg, October 2010.

Nere amari eskeinita.

Bere ahalegin eta ekimenik gabe, bere babesa eta ulermenik gabe, tesi hau ez litzaidake posible izango. Momentu onetan eta batez ere zailtasun uneetan, nere alboan egoteagatik eta laguntzeagatik.

Maite zaitut, zure.

Publications

- Bárcena-Uribarri* I, Thein* M, Sacher A, Bunikis I, Bonde M, Bergström S, Benz R. P66 porins are present in both Lyme disease and relapsing fever spirochetes: a comparison of the biophysical properties of P66 porins from six *Borrelia* species. Biochim Biophys Acta. 2010 Jun;1798(6):1197-203. Epub 2010 Feb 25.

- Thein* M, Bárcena-Uribarri* I, Maier E, Bonde M, Bunikis I, Bergström S and Benz R. Use of non-electrolytes reveals the channel size and oligomeric structure of the *Borrelia burgdorferi* P66 porin. Biophysical Journal (Submitted).

*both authors contributed equally.

Index

Abstract

• **English:**

The genus *Borrelia* belongs to the *Spirochaetes* phylum which is far related to Gram negative bacteria. This phylum possesses a characteristic long helically coiled shape with lengths that vary from 5 to 250 µm. Other pathogens as *Treponema* and *Leptospira* which cause syphilis and leptospirosis, also belong to the *Spirochaetes*. *Borrelia* itself is the causative agent of two human diseases, the Lyme disease and relapsing fever.

Borreliae are pathogenic bacteria which cycle between their arthropod vector, in most cases a tick, and a mammal host, very often small rodents. This complex life cycle requires an extraordinary protein up- and down-regulation in order to survive in such different organisms and avoid their immunologic systems.

Lyme disease is a multisystemic disease that can affect different organs like skin, joints and nervous system. A red rash with concentric rings, called *erythema migrans* is a distinctive manifestation that allows clinical diagnosis. It appears after the bite of an infected tick and spreads out to diameters that can reach 15 cm. Relapsing fever is characterized by sudden recurrent fever peaks accompanied with chills, headache, muscle and joint pain and nausea. Both diseases are easily treated with antibiotics in early infection stages.

Borrelia species possess a small genome. Many of their genes are related with virulence and the adaptation to the different hosts. The absence of genes in *Borrelia* involved in the biosynthesis of amino acids, fatty acids or nucleotide is very remarkable. This metabolic deficiency makes *Borrelia* species dependent on substances produced by the host.

The first step in nutrient uptake is accomplished by porins. Bacterial porins are water-filled channels that facilitate the transport of essential molecules through the outer membrane. Four porins have been described in *Borrelia* up to this point. P66, P13 and Oms28 have been found in *Borrelia burgdorferi* while Oms38 was discovered in relapsing fever spirochetes. P66 is a singular porin with an extremely high single channel conductance of 11 nS. P13 is a small protein with an α-helical secondary structure which does not fit into the general porin model. The function of Oms28 as a porin has been questioned recently due to its periplasmic membrane-associated location. Finally, Oms38 is a specific porin for dicarboxilates with homologues in Lyme disease species.

The aim of this thesis was to broaden the knowledge of the P66 and P13 porins described in the genus *Borrelia*. Both differ in structure and size from the general Gram negative porin model and could be highly involved in specific tasks in the genus *Borrelia*.

In the first project of this thesis, the presence and pore forming capacity of P66 was studied in several *Borrelia* species including members of the relapsing fever group. P66 is the best studied porin in *Borrelia* with a dual function as porin and adhesin. This knowledge is restricted to *B. burgdorferi* and little or nothing is known about homologues in other *Borrelia* species. Therefore, three Lyme disease and three relapsing fever species were chosen as representative agents of the genus and the pore forming activity of their P66 homologues was studied. Five out of the six homologues exhibited a similar single channel conductance in a range from 9 to 11 nS. All of them showed no selectivity for cations or anions, and they were voltage dependent starting at different voltages from 30 to 70 mV. Only in the case of the *B. hermsii* homologue no pore forming activity could be established. It remains unclear if the lack of activity was due to an evolutionary loss of its porin function or to a higher sensibility to the detergents used for purification.

In another project, the controversial P66 pore diameter of *B. burgdorferi* was analyzed with an empirical method. In a former study, the diameter of the P66 channel was estimated to be 2.6 nm based on theoretical considerations. This diameter is rather large and could impair the outer membrane protective function. Different non-electrolytes were used to study the P66 pore diameter indicating a 1.8 nm entrance diameter and a 0.8 nm inner constriction. In addition, the blockage of the channel with some of those non-electrolytes disclosed an oligomeric organization formed by approximately eight independent channels. Such a structure has not been observed so far in any other living organism and could be exclusive of *Borrelia* or spirochetes.

The third project of this thesis deal with the recombinant production of a *B. burgdorferi* protein with immunogenic potential. This protein might be used to develop new diagnosis tests and therapeutic treatments. P13 is an outer membrane protein present in LD and RF species and it does not have any other known bacterial homologue. These facts make of P13 a good candidate to be used as a therapeutic target. For such purpose, P13 was cloned in two organisms. First, in *Escherichia coli* were two different constructs were designed to establish the role of a periplasmic cleaved C-terminus. Second, in a virus based vector delivered by *Agrobacterium tumefaciens* into tobacco plant cells. The vector replicates inside the plant cells spreading the infection to adjacent cells and at the same time producing the recombinant

protein. This second expression method should enable the production of large amounts of the recombinant protein reducing time and costs.

The last project of this thesis looked into the outer membrane complexome of *B. burgdorferi* focusing on the P13 and P66 porin complexes. Blue Native Page and second dimension SDS-Page were the technique chosen for this purpose. P66 could be shown to be the only protein involved in the formation of the 11 nS pore which complex is probably formed by eight monomers. It was also possible to divide this complex in two halves with approximately half the molecular weight and a conductance of 5.5 nS. In the case of the P13 complex, a possible association with the lipoprotein OspC was revealed. The gel extraction of the P13 complex and its test with the Back Lipid Bilayer assay exhibited a 0.6 nS activity. This is in high contrast with the 3.5 nS activity previously described for this protein.

To sum up, P66 is a porin present in many *Borrelia* species including not only LD but also RF species and which homologues show similar biophysical properties. The diameter of this pore is smaller than previously thought and it has molecular weight sieving properties. In the case of P13, its recombinant procurement will allow the use of P13 as a diagnostic and therapeutic target. The possible association with OspC could facilitate to unravel in future experiments the function of this intriguing protein.

• **Deutsch:**

Die Gattung *Borrelia* gehört zur Familie der *Spirochaetes*, welche sich den Gram-negativen Bakterien zuordnen lassen. Für diese Familie charakteristisch ist eine längliche, helikale Form, die Längen von 5 – 250 µm erreichen kann. Den Spirochaeten gehören diverse Pathogene an wie *Treponema* und *Leptospira*, die Erreger der Syphillis und der Leptospirose. Borrelien verursachen beim Menschen zwei schwere Krankheiten: Die Lyme-Borreliose (LB) und das Rückfallfieber (RF).

Als Pathogen besitzen Borrelien einen Lebenszyclus, in dem sie zwischen Gliederfüßern als Vektoren und Säugetieren (oft kleinen Nagetieren) als Wirt wechseln. Um das Überleben in derart unterschiedlichen Organismen zu sichern und die Immunantwort des Wirtes zu unterdrücken, benötigt ein Organismus mit einem solch komplexen Lebenszyklus eine außergewöhnliche Regulierung der Proteinexpression.

Die Lyme-Borelliose stellt eine multisystemische Krankheit dar, die verschiedene Organe, wie Haut, Gelenke und das Nervensystem betreffen kann. Häufig kommt es zu einer sich kreisförmig ausbreitenden Rötung, die *erythema migrans* genannt wird, die zur klinischen Diagnose genutzt wird. Sie erscheint nach einem Zeckenbiss und kann einen Durchmesser von bis zu 15 cm weit erreichen. Rückfallfieber erkennt man an plötzlich auftretenden Fieberschüben, die von weiteren Symptomen wie Schüttelfrost, Kopfschmerzen, Muskel und Gelenkschmerzen oder Übelkeit begleitet werden. Beide Krankheiten können in frühen Stadien der Infektion leicht mit der Gabe von Antibiotika behandelt werden.

Die verschiedenen Arten der Gattung *Borrelia* besitzen ein relativ kleines Genom. Da außerdem viele der vorhandenen Gene für Virulenzfaktoren und wirtsspezifische Anpassungen codieren, fehlen den Borrelien wichtige Genen für die Biosynthese von Aminosäuren, Fettsäuren oder Nukleotiden. Diese metabolischen Defizite werden durch die Aufnahme von durch den Wirt produzierten Nährstoffen ausgeglichen.

Den ersten Schritt der Nährstoffaufnahme übernehmen Porine. Dies sind wassergefüllte Kanäle, die die Aufnahme und den Transport von essentiellen Molekülen über die äußere Membran ermöglichen. P66, P13 und Oms28 wurden bei *Borrelia burgdorferi*, Oms38 bei Rückfallfieber verursachenden Spirochaeten gefunden. P66 ist ein einzelnes Porin mit einer extrem hohen Leitfähigkeit von 11 nS. P13 ist ein kleines Protein (13kDa) mit einer α-helikalen Sekundärstruktur, die keinerlei Ähnlichkeit zu den bisherigen Modellen von bekannten Porinen

aufweist. Aufgrund seiner Assoziation mit der periplasmatischen Seite der Membran wurde die Funktion als Porin für Oms28 in letzter Zeit stark angezweifelt. Oms38 ist ein Dicarboxylat-spezifisches Porin mit Homologen bei Lyme-Borreliose verursachenden Arten.

Das Ziel der vorliegenden Arbeit war das vorhandene Wissen über P66 und P13 als Porine der Gattung *Borrelia* zu erweitern. Die beiden Proteine unterscheiden sich strukturell stark von den bisher bekannten Porine Gram-negativer Bakterien und sind daher geeignete Forschungsobjekte, um die speziellen Anforderungen an Borrelienporinen zu erforschen.

Das Ziel dieser Arbeit war die Erforschung der beiden in Borrelien beschriebenen Proteine P66 und P13. Gerade weil sich beide in Aufbau und Größe von bekannten Porinen Gram-negativer Bakterien unterscheiden und somit in spezifische Prozesse bei der Gattung *Borrelia* involviert sein könnten, ist die Forschung auf diesem Gebiet auch weiterhin von höchstem Interesse.

Im ersten Projekt dieser Arbeit wurden das Vorkommen und die porenformende Aktivität von P66 in verschiedenen *Borrelia*-Arten (Lyme-Borreliose und Rückfallfieber) untersucht. Bei P66 handelt es sich um das am besten untersuchte Porin der Borrelien, das eine Doppelfunktion als Porin und als Adhesin besitzt. Da sich alle bisherigen Ergebnisse auf *B. burgdorferi* beziehen, ist wenig bis gar nichts über homologe Proteine in anderen Borrelien-Arten bekannt. Deswegen wurden jeweils drei Arten, die Lyme-Borreliose und Rückfallfieber verursachen, ausgewählt und an deren P66-Homologe die porenformende Aktivität überprüft. Fünf von sechs zeigten dabei eine ähnliche Einzelkanalleitfähigkeit wie P66, die im Bereich von 9 – 11 nS lagen, bei gleichzeitig kaum vorhandener Selektivität für eine bestimmte Ionensorte. Auch eine Spannungsabhängigkeit, die bei 30 – 70 mV begann, war messbar. Nur im Fall von *B. hermsii* konnten keine Poren gefunden werden. Dabei ist noch nicht geklärt, ob das Fehlen der porenbildenden Aktivität einem evolutionären Verlust der Funktion als Pore oder einer höheren Anfälligkeit gegenüber den verwendeten Detergenzien geschuldet ist.

In einem weiteren Projekt wurde der kontrovers diskutierte Porendurchmesser von P66 aus *B.burgdorferi* mit empirischen Mitteln analysiert. In früheren theoretischen Studien wurde der Kanaldurchmesser auf 2,6 nm geschätzt. Dieser sehr große Durchmesser würde allerdings die Schutzfunktion der Außenmembran verhindern. Mit Hilfe von ungeladenen Substanzen gelang eine Bestimmung des Innendurchmessers von P66 auf 1,8 nm am Eingang und 0,8 nm an der Engstelle der Pore. Zusätzlich führte eine unerwartete Blockierung der Pore durch einige dieser Substanzen zu der Erkenntnis, dass P66 einen oligomeren (wahrscheinlich oktameren) Aufbau besitzt. Ein solcher Aufbau konnte bisher noch nie nachgewiesen werden und könnte von daher ein einzigartiges Merkmal von Borrelien oder Spirochaeten sein.

Das dritte Projekt beschäftigte sich mit der rekombinanten Produktion eines Proteins von *B. burgdorferi* mit immunogenen Eigenschaften. Dieses könnte dazu verwendet werden, neue Diagnose Tests und Therapien zu entwickeln. P13 kommt in verschiedenen LB- und RF-Arten vor und besitzt kein bekanntes bakterielles Homolog. Diese Fakten machen aus P13 einen geeigneten Kandidaten als therapeutisches Ziel. Aus diesem Grund wurde das P13-Gen in zwei unterschiedliche Organismen kloniert. Zum einen in *E. coli*, wo zwei verschiedene Konstrukte zur Klärung der Rolle des periplasmatisch verdauten C-Terminus dienen sollten. Zum anderen in Tabakpflanzen über *Agrobacterium tumefaciens*, mittels eines Virus. Dabei vermehrt sich der Vektor in den Zellen der Pflanze, breitet sich aus und produziert gleichzeitig das gewünschte Protein. Mit Hilfe dieser zweiten Expressionsmethode sollte es möglich sein, große Mengen des rekombinanten Proteins zu erzeugen und gleichzeitig die Kosten und den Zeitbedarf zu senken.

Das letzte Projekt beschäftigte sich mit dem Außenmembran-Komplexom von *B. burgdorferi* und konzentrierte sich dabei auf die Komplexe von P13 und P66. Blue Native PAGE und 2D-SDS PAGE wurden als Techniken ausgewählt. Es konnte gezeigt werden, dass P66 das einzige Protein ist, das am vermutlich oktameren Aufbau der 11 nS Pore beteiligt ist. Zusätzlich gelang es, den Komplex in zwei Hälften zu spalten, die ungefähr das halbe Molekulargewicht bei einer Leifähigkeit von 5,5 nS zeigten. Im Fall des P13-Komplexes konnte eine mögliche Verknüpfung mit OspC entdeckt werden. Die Gelelution des Komplexes und anschließende Tests mit Hilfe der Black-Lipid-Bilayer-Methode ergaben eine Aktivität von 0,6 nS. Dies steht im starken Gegensatz zu der vorher für P13beschriebenen Größe von 3,5 nS.

Zusammenfassend lässt sich sagen, dass P66 ein in vielen Borrelienarten vorkommendes und damit weit verbreitetes Porin mit Homologen in LB- und RF-Spezies ist, die ähnliche Charakteristika besitzen. Der Durchmesser dieser Pore konnte unter Berücksichtigung der Eigenschaften eines molekularen Siebes genauer bestimmt werden. Im Fall von P13 könnte dessen rekombinante Produktion es erlauben, dieses Protein als Hilfsmittel zur Diagnose und zur medizinischen Therapie einzusetzen. Zusätzlich könnte der gefundene Bezug zu OspC dazu beitragen, in Zukunft mehr über die Funktion dieses interessanten Proteins herauszufinden.

• **Español:**

El género *Borrelia* pertenece al filo *Spirochaetes*, que esta lejanamente relacionado con las bacterias Gram negativas. Este filo posee una forma característica enroscada con longitudes que varían desde los 5 hasta los 250 µm. Otros patógenos como *Treponema* y *Leptospira*, agentes etiológicos de la sífilis y la leptospirosis, pertenecen también a filo *Spirochaetes*. *Borrelia* por su parte puede producir dos enfermedades, la enfermedad de Lyme o fiebres recurrentes.

Las especies de *Borrelia* son agentes patógenos cuyo ciclo de vida transcurre entre un vector artrópodo, en la mayoría de los casos una garrapata, y un hospedador mamífero, en muchos casos pequeños roedores. Este complejo sistema de vida requiere una extraordinaria regulación proteica para poder sobrevivir en organismos tan diversos y a su vez poder esquivar su sistema inmunológico.

La enfermedad de Lyme es una enfermedad que afecta a diversos órganos incluyendo entre otros la piel, las articulaciones y el sistema nervioso. Una erupción roja con anillos concéntricos, denominada eritema migrans, es una manifestación típica que permite un diagnostico clínico. Aparece después de la picadura de la garrapata y se va extendiendo hasta alcanzar diámetros de hasta 15 centímetros. Las fiebres recurrentes se caracterizan por picos febriles que aparecen repentinamente y que van acompañados de escalofríos, dolor de cabeza, dolor muscular y de las articulaciones, así como de nausea. Ambas enfermedades son fáciles de tratar con antibióticos en estadios tempranos de la infección.

Las especies de *Borrelia* poseen un genoma muy reducido. Además, muchos de sus genes están relacionados con su virulencia y con la adaptación a los diferentes organismos en los que viven. La ausencia de genes relacionados con la biosíntesis de aminoácidos, ácidos grasos y nucleótidos resulta sorprendente. Esta deficiencia metabólica hace de las especies de *Borrelia* dependientes de las sustancias producidas por el hospedador.

El primer paso en la captación de alimentos en bacterias es realizado por las porinas. Las porinas bacterianas son canales rellenos de agua que permiten el transporte de sustancias esenciales a través de la membrana externa. Hasta la fecha, cuatro porinas han sido descritas en el género *Borrelia*. P66, P13 y Oms28 fueron encontradas en *Borrelia burgdorferi* mientras que Oms38 fue descubierta en especies que causan fiebres recurrentes. P66 es una porina atípica por una conductancia fuera de lo común de 11 nS. P13 es una pequeña proteína de 13

kDa con una estructura secundaria en α-hélice que no encaja en el modelo general de porina. La función de Oms28 ha sido puesta en tela de juicio recientemente debido a una posible localización periplásmica asociada a la membrana externa. Finalmente, Oms38 es una porina con especificidad por los dicarboxilatos con homólogos en las especies que causan la enfermedad de Lyme.

El objetivo de esta tesis era ampliar el conocimiento de las porinas P66 y P13 descritas en el género *Borrelia*. Ambas difieren en estructura y tamaño del modelo general de porina en bacterias Gram negativas y por lo tanto podrían tener un papel muy relevante en este género.

En el primer proyecto de esta tesis la presencia y capacidad formadora de poros de P66 fue estudiada en varia especies incluyendo miembros del género que causan fiebres recurrentes. P66 es la porina mejor estudiada en *Borrelia*, con una función dual como porina y adhesina. Este conocimiento está restringido a *B. burgdorferi* y nada o muy poco es conocido sobre sus homólogos en otras especies de *Borrelia*. Por ello, tres especies representantes de la enfermedad de Lyme y tres de las fiebres recurrentes fueron seleccionadas como representantes del género y la capacidad formadora de poros de sus homólogos de P66 fue estudiada. Cinco de los seis homólogos mostraron una conductancia de canal en un rango de entre 9 y 11 nS. Todos ellos resultaron ser no selectivos para cationes o aniones y una dependencia de voltaje comenzando a diferentes voltajes desde 30 a 70 mV. Tan solo en el caso del homólogo de *B. hermsii* no pudo ser establecida una actividad formadora de poros. Se desconoce si la falta de esta capacidad para formar poros es consecuencia de una perdida de la función como porina a lo largo de la evolución o si por el contrario este homólogo es más sensible a la presencia de los detergentes que se requieren para el proceso de purificación.

En otro proyecto, el controvertido diámetro del poro formado por P66 en *B. burgdorferi* fue analizado con un método empírico. En un estudio previo, el diámetro de P66 fue estimado en 2,6 nm basándose exclusivamente en consideraciones teóricas. Este diámetro para un poro es considerablemente grande y podría afectar a la función protectora de la membrana externa. Varios no electrolitos fueron usados para estudiar el diámetro del poro formado por P66 poniendo de manifiesto un diámetro de la entrada del poro de 1,8 nm y una constricción interna de 0,8 nm. Además, el bloqueo del canal por alguno de los no electrolitos reveló una conformación oligomérica formada por aproximadamente ocho canales independientes asociados en un solo complejo. Una estructura tal no había sido previamente observada en ningún otro organismo y podría ser exclusiva de *Borrelia* o de las espiroquetas.

El tercer proyecto de esta tesis se centró en la producción recombinante de una proteína de *B. burgdorferi* con potencial inmunogénico. Esta proteína podría ser usada en el desarrollo de nuevas estrategias de diagnóstico y terapias. P13 es una proteína situada en la membrana externa de especies causantes de la enfermedad de Lyme y las fiebres recurrentes y no se conoce ningún otro homologo en otra bacteria. Esto hace de P13 un buen candidato para ser usado como diana terapéutica. Para tal fin, P13 fue clonado en dos organismos. Primero, en *Escherichia coli* donde dos injertos diferentes fueron diseñados para esclarecer la función de un péptido C-terminal digerido en el preriplasma. Y segundo, en un vector basado en el virus de la patata introducido en las células de la planta del tabaco a través de *Agrobacterium tumefaciens*. Este vector se replica dentro de las células vegetales infectando a las adyacentes a la vez que produce la proteína recombinante. Este segundo método hace posible la producción de grandes cantidades de la proteína recombinante reduciendo tiempo y costes.

La ultima parte de esta tesis profundiza en el estudio de los complejos proteicos en la membrana externa de *Borrelia burgdorferi* centrándose en P13 y P66. *Blue Native Page* y *SDS-Page* en segunda dimensión fueron las técnicas elegidas para tal propósito. Se demostró que P66 era exclusivamente la responsable de la formación del complejo que forma poros de 11 nS y que probablemente se trate de un octámero. Fue posible dividir el complejo en dos partes iguales con la mitad del peso molecular y una conductancia de 5,5 nS lo que denota una cierta simetría. En el caso del complejo formado por P13, una posible relación con la lipoproteína OspC fue puesta de manifiesto. La extracción del complejo formado por P13 y su análisis en membranas artificiales mostró una actividad formadora de poros de 0,6 nS. Este resultado contradice la conductancia de 3,5 nS atribuida a P13 en un estudio previo.

En conclusión, P66 es una porina presente en muchas especies de *Borrelia* incluyendo no solo miembros causantes de la enfermedad de Lyme, sino también de las fiebres recurrentes y cuyos homólogos presentan propiedades biofísicas similares. El diámetro de este poro es más pequeño de lo que se consideraba actuando como filtro de sustancias en referencia a su peso molecular. En el caso de P13, su producción recombinante permitirá su uso para desarrollar nuevos test de diagnóstico más seguros y terapias contra la infección por esta bacteria. La posible asociación con OspC podría facilitar esclarecer en futuros experimentos la función de esta proteína tan fascinante.

Introduction

1.1 The genus *Borrelia*

1.1.1 Characteristics

The genus *Borrelia* is included in the *Spirochaetacea* family. It is composed by 37 species described to the present. They have a very characteristic long and screwed shape [1] (Fig. 1-1). The size of an individual cell goes from 8 to 30 µm in length and from 0.2 to 0.5 µm wide.

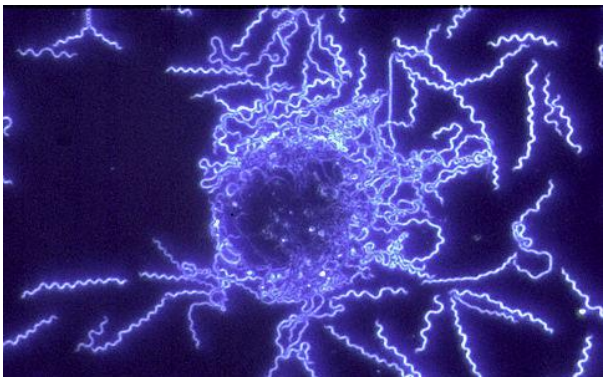

Fig. 1-1: Dark-field microscope image of *B. burgdorferi* cultivated in the laboratory.

They have a peculiar small genome. Each cell holds a 0.9 Mbp chromosome and a set of linear and circular plasmids up to 21 described for *B. burgdorferi* B31 MI [2, 3]. The C+G content is around 27%. Having a reduced genome decreases the metabolic capacity of these species, which force them to live in association with a host that provides essential nutrients and substances [4-7].

Also typical from this genus is the periplasmic endoflagella. They are situated in both ends of the cells in groups of 7 to 11 endoflagella and they coil around the cell in the periplasmic space[8-10]. These flagella rotate around the longitudinal axis propelling the cell forward which makes *Borrelia* exhibit chemotaxis [11].

Borrelia in vitro culture is complicated and it is cultivated in a rich growth medium called Barbour-Stoenner-Kelly II (BSK II) supplemented with rabbit serum [12]. The generation time of *Borrelia* is around 10 hours, much slower than the around 40 minutes required by *E. coli* [13].

Is also distinctive the fact that *Borrelia* had antigenic variation which helps avoiding the host immune system [14].

1.1.2 Classification

Spirochetes have been included in the group of the Gram negative bacteria because of possessing an outer membrane although they have many particular characteristics [15]. Inside this Phylum several genus are included like *Treponema*, *Leptospira*, *Brachyspira* and *Borrelia*. *Borrelia* is the subject of study in this thesis and it is as following classified:

Kingdom	**Bacteria**
Phylum	Spirochaetes
Class	Spirochaetes
Order	Spirochaetales
Family	Spirochateaceae
Genus	*Borrelia*

Table 1-1: Classification of the genus *Borrelia*.

1.2 Human infection

The genus *Borrelia* is known to cause two illnesses, the Lyme disease and relapsing fever. Both of them affect several organs like skin, joints, heart and brain.

1.2.1 Lyme disease and Relapsing Fever symptoms

The Lyme disease, also called borreliosis, is a multisystemic illness caused by some *Borrelia* species, among them *B. burgdorferi*, *B. afzelii* and *B. garinii* are the major agents.

Lyme disease symptoms:

• *Erythema migrans*: is a rash appearing as several annular rings that expand on the skin (Fig. 1-2).

• *Acrodermatitis chronica athropicans*: It appears in the late stage of the disease and is characterized by limb inflammation and a bluish red discoloration (Fig. 1-3).

• Arthritis

• Paralysis

• Heart damage

• Vision problems

Fig. 1-2: *Erythema migrans* on the shoulder of a patient.

Fig. 1-3: Acrodermatitis chronica athropicans.

Relapsing fever is also a multisystemic disease with a typical symptomatology. It is caused mainly by *B. duttonii*, *B. hermsii* and *B .recurrentis*.

Relapsing fever symptoms:

• Periods of high fever due to spirochetemy.

• Headache, muscle- and rheumatic pains that can last 2 to 9 days.

• Clouding of consciousness

• Brain and meninges inflammation

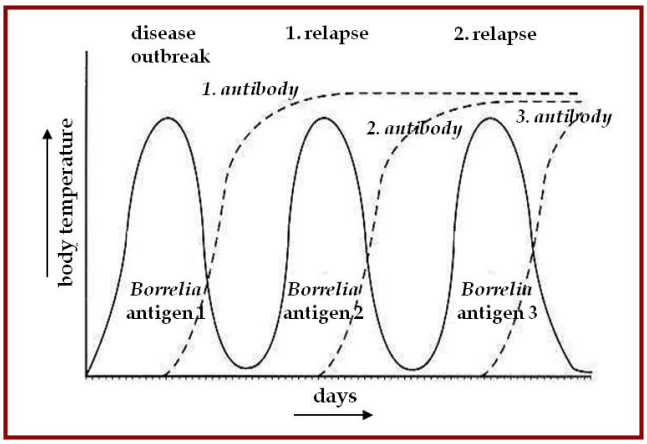

Fig. 1-4: Fever cycles typical of infections due RF spirochetes.

1.2.2 Lyme disease species and relapsing fever species

Inside the *Borrelia* genus the different species are commonly divided depending on the illness they caused as seen in Table 1-2.

Relapsing fever	Lyme disease
B. recurrentis	***B. burgdorferi s.s.***
B. hispanica	***B. garinii***
B. crocidurae	***B. afzelli***
B. persica	***B. japonica***
B. duttonii	***B. andersonii***
B. hermsii	***B. valaisiana***
B. turicatae	***B. lusitaniae***
B. parkeri	**etc.**
B. uzbekistania	
B. venezuelensis	
B. anserina	
B. coriaceae	
B. lonestari	
etc.	

Table 1-2: Classification of *Borrelia* species depending on the human illness they produce.

1.2.3 History of Lyme disease and relapsing fever.

Lyme disease

Is common the mistake of thinking that the first Lyme disease report was from Lyme (Connecticut) during the 70s when Allen Steere described a high incidence of arthritis among children of this location [16].

The first record known of the disease is from 1883 in Breslau, Germany. Back then, a physicist, called Alfred Buchwald described a skin degenerative disorder called now *acrodermatitis chronica athropicans* [17].

Later experiments carried out by a Swedish dermatologist called Arvid Afzelius showed a possible relation between the bite of a tick and the skin lesions that appeared short afterwards [18]. In the early 80s, Willy Burgdorfer proved the relation between the disease and a bacteria transmitted by the tick when he discovered the bacteria during examinations of *Ixodes* midguts [19, 20].

After that discovery, the transmission from vector to host was better studied, and nowadays genetic and molecular studies are being carried out to better understand the biology of *Borrelia*.

Relapsing fever

The first known records of relapsing fever go back to the ancient Greece. This illness was known for some doctors back then and the first clinical disease descriptions coincident with this illness have been documented by Hippocrates [21]. At that time, it was designated as "ardent fever".

During the following centuries different fever outbreaks may have been relapsing fever as well. Those outbreaks were called with different names as "tramp's fever", "gharib ghez", "kimputu". The term "Relapsing fever" was first used by David Craigie [22] to describe an outbreak of this illness in Edinburgh.

In 1868 a German researcher called Otto Obermeier finally identifies in Berlin the cause of relapsing fever. He observed long bacteria mixed with blood cells [23] but was unable to explain the transmission of the spirochetes. This bacterium was called in his honour *Spirocheta obermeieri*, later known as *Borrelia recurrentis*.

Dutton and Todd demonstrated the transmission of relapsing fever spirochetes using *Ornithodoros moubata* and a monkey model [24]. This finding was a consequence of Dutton getting infected [25]. He injured himself while performing an autopsy on a patient who had died from this disease and died himself from relapsing fever.

Sergent and Foley identified in 1910 a second vector for transmission of relapsing fever spirochetes. They described that *Borrelia* could also be transmitted by human body louse [26].

1.3 Vectors and Hosts.

The main *Borrelia* transmission vectors are ticks of two genera. Lyme disease *Borrelia* species are transmitted by ticks of the genus *Ixodes* [19] while relapsing fever *Borrelia* species are transmitted by the genus *Ornithodoros* [27]. In the case of *B. recurrentis* a different transmission vector has been described. *B. recurrentis* is transmitted by the human body louse [28](Fig. 1-5).

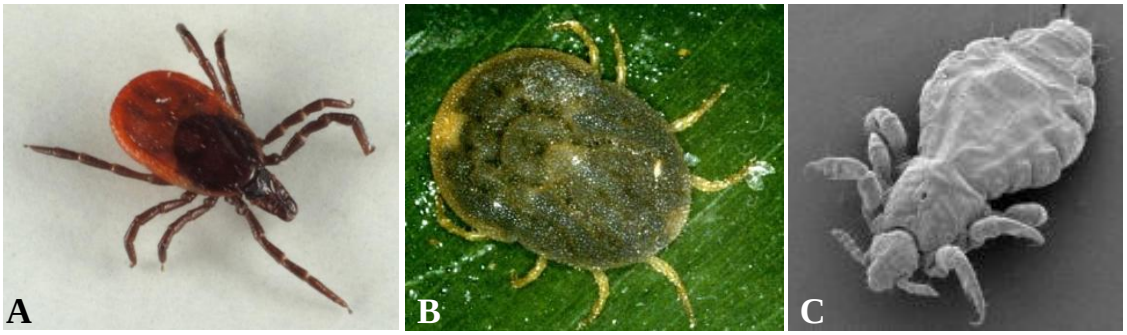

Fig. 1-5: *Borrelia* transmission vectors. A) *Ixodes scapularis*, which transmits Lyme disease *Borrelia* species, B) *Ornithodoros moubata*, transmission vector of relapsing fever *Borrelia* species and C) *Pediculus humanus*, vector for *B. recurrentis*.

There are some differences in the way these two ticks spread the infection. *Ixodes* feeds on the mammal for long periods that last even days. On the other hand, *Ornithodoros* feeds much faster, usually during night periods leaving the host within a few hours. Transmission of the bacteria from the tick to the host takes hours in the case of Lyme disease species but only minutes in the case or relapsing fever species [29].

1.3.1 *Borrelia* life cycle:

The species of the genus *Borrelia* are dependent bacteria that can only be found in association with its vectors and hosts. The vectors get the bacteria when they feed in an infected animal. From that moment, the bacteria will stay in the vector as well as it will infect other animals the tick feeds on.

While the vectors are limited to ticks and the human body louse, the host can be a wide range of mammals and birds [6]. The larvae and nymph usually prefer small rodents like mouse and

squirrels while the adults feed on bigger animals like deers, foxes and dogs. Humans are not a common host, but whenever they get infected they suffer from two possible diseases.

The population of *Borrelia* is maintained in certain areas by the so called reservoirs (Fig.1-6). Those are usually small rodents that live in a restricted area, normally a forest, and they transmit the bacteria when new larvae or nymphs feed on them [6].

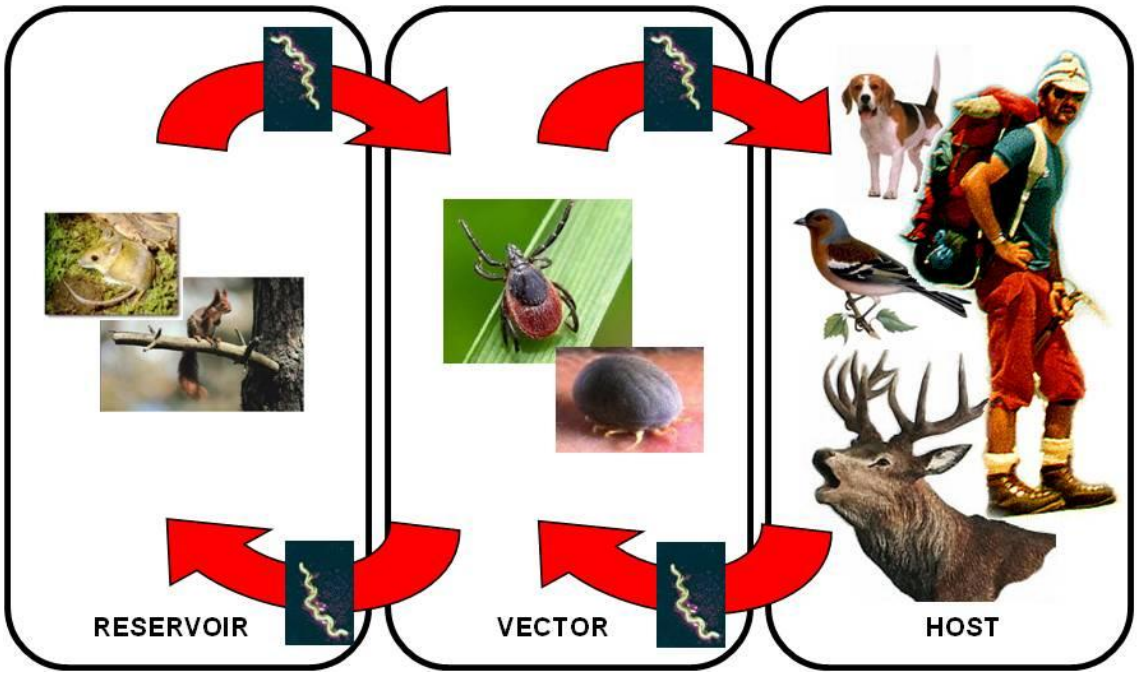

Fig. 1-6: Simplified *Borrelia* life cycle. *Borrelia* persists in small rodents infected with a high incidence denominated reservoirs. Tick vectors spread *Borrelia* to new mammal host, including deers, birds, dogs and even humans. Lime disease *Borrelia* species are transmitted by hard body ticks (*Ixodes*, central panel, above) and relapsing fever by soft body ticks (*Ornithodoros*, central panel, below).

The life cycle of *B. recurrentis* and *B. duttonii* is somehow different. *B. recurrentis* is transmitted along with the human louse [28]and *B. duttonii* has humans as the only mammal host [30, 31].

1.3.2 *Borrelia* world distribution

The development of national health systems and international research nets allows the compilation of infection outbreaks and the production of distribution maps. Depending on the illness they cause *Borrelia* has different distribution zones.

In the following map, the zone marked in blue corresponds to countries where Lyme disease cases have been reported. This illness is typical of two parallel zones in North America and a long stripe taking most of Europe and the central part of Asia (Fig. 1-7)[6].

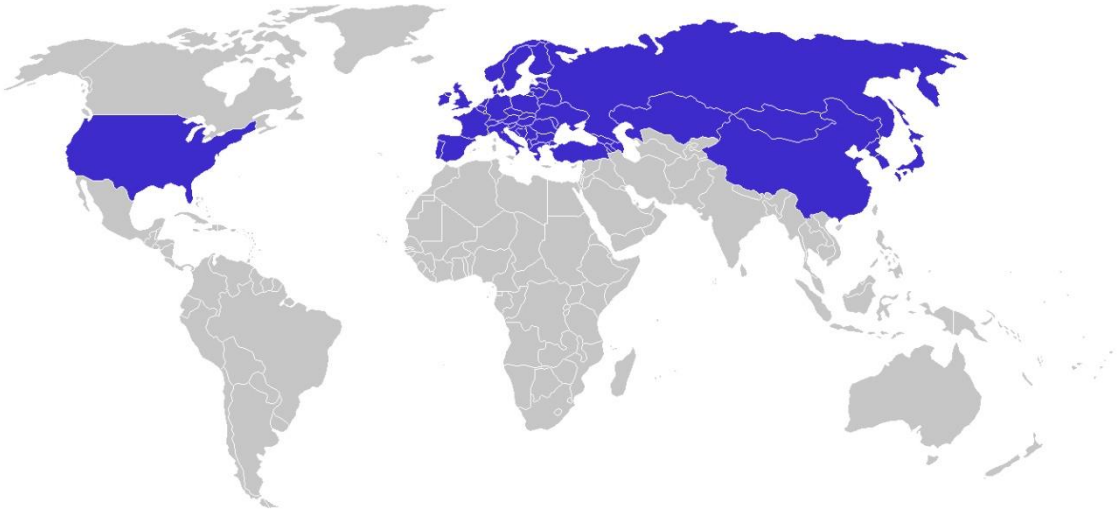

Fig. 1-7: Word distribution of Lyme disease *Borrelia* species.

Relapsing fever distribution is showed in the map of Fig. 1-8 .The species causing this illness are localized in Africa, Asia, Europe as well as Central America and Mexico [32].

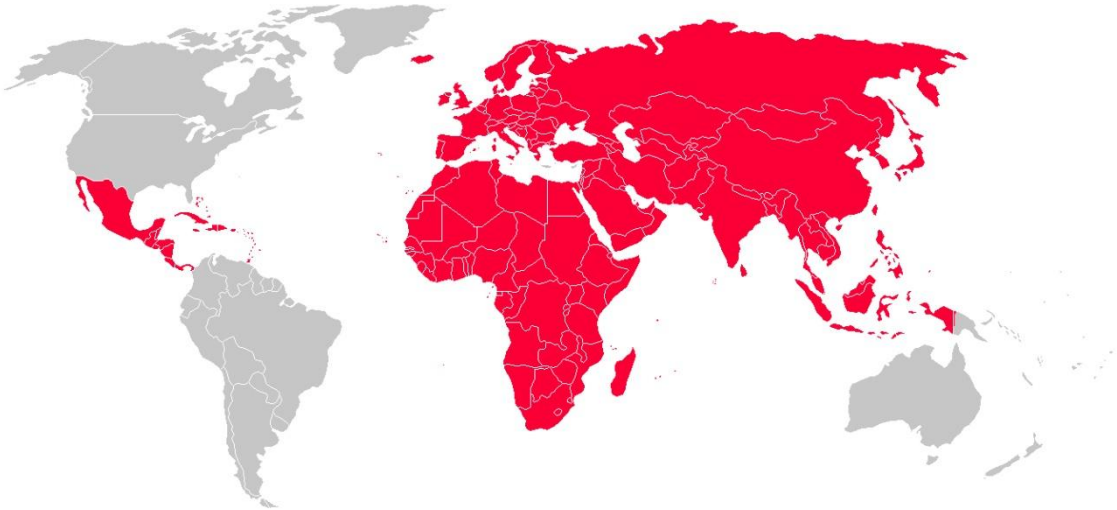

Fig. 1-8: World distribution of relapsing fever *Borrelia* species.

1.4 Outer membrane in *Borrelia*

Spirochetes belong to the Gram-negative bacteria even though they differ from the general model in many aspects.

The genus *Borrelia* has two membranes and a periplasmic peptidoglycan layer as all Gram-negative bacteria. In *Borrelia,* the flagellum is also found in this space, which is a peculiar characteristic of spirochetes (Fig. 1-9).

One big difference between the Gram-negative bacteria and the spirochetes is the absence of lipopolysaccharides [33, 34]. Instead of them, the outer membrane in this genus is very rich in lipoproteins which are the primary interface between the bacterium and the host [35]. *Borrelia* outer membrane is considerably more fluid than in other Gram negative bacteria. They also possess a lower density of membrane spanning proteins [36, 37]. Porins, the focus of this thesis, are also found in the outer membrane of spirochetes with remarkable and unique characteristics.

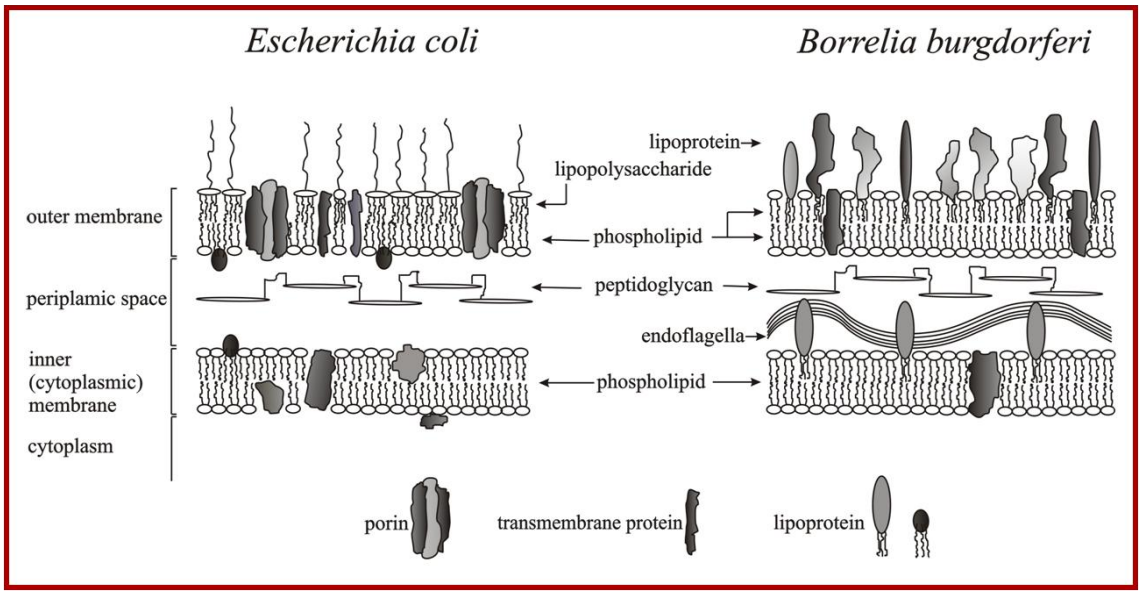

Fig. 1-9: Schematic comparison of the outer membrane in *E. coli* and *B. burgdorferi*. As mayor differences it can be appreciated the replacement of lipopolysaccharides in *Escherichia* by lipoproteins in *Borrelia* and a decrease in this last one of membrane spanning proteins.

1.5 Porins in Gram negative bacteria and porins in *Borrelia*

Porins are a group of proteins located in the outer membrane of Gram negative bacteria that facilitate the transit of substances between the surrounding environment and the periplasmic space. Porins are also found in mycobacteria, chloroplasts and mitochondria [38, 39].

Porins form channels filled with water that allow a passive transport of molecules down their concentration gradient [40, 41]. The transport through the outer membrane does not require the use of energy in contraposition with the substrate translocation via transporters in the inner membrane.

Most of the porins described to date form β barrels from antiparallel β sheets. Frequently, they are associated in oligomers that confer to the whole complex a higher stability (Fig. 1-10). In the outer membrane of Gram negative bacteria, channel-tunnel proteins like TolC in *Escherichia* and BesC in *Borrelia* are also found. They form pores in the outer membrane and are part of bigger complexes involved in drug-resistance known as efflux pumps.

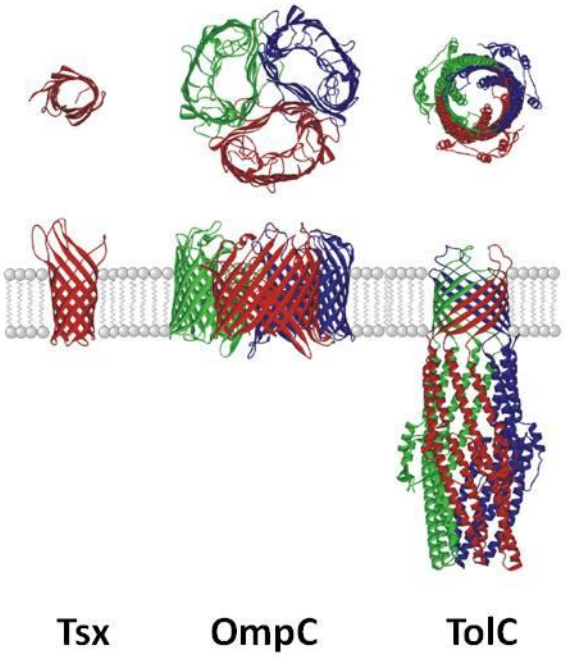

Fig. 1-10: Three examples of pore forming outer membrane proteins. Tsx is a monomeric specific porin for nucleosides [42], OmpC is a trimeric general diffusion pore [43] and TolC is a trimeric protein complex part of an efflux system [44]. OmpC forms a complex with three independent pores while trimeric TolC forms only one. All of them are described in *E. coli*.

Porins can be classified depending on the kind of molecules they transport [45]:

General diffusion porins: are perforations in the outer membrane of bacteria that allow the transport of small molecules, ions and water. Examples of this kind of porins are OmpF and OmpC in *E. coli* [40].

Substrate-specific porins: are those porins that are specialized in the transport of certain molecules. Tsx is an example of this kind of porins in *E. coli* that is specialized in the nucleoside transport from the surrounding media to the periplasmic space [46, 47]. Other examples include porin with specificity for sugars [48], phosphate [49]and antibiotics [50].

1.5.1 Porins in *Borrelia*

To this point, three porins have been identified in *B. burgdorferi* and one in relapsing fever species. Those are P66, P13 and Oms28 in *B. burgdorferi* and Oms38 in *B .duttonii*.

P66 is a porin with an unusual high single channel conductance of around 11 nS [51, 52]. The biophysical characterization showed no ion selectivity and a voltage dependency above 60 mV. It has also been described a second function of this protein as an adhesin that binds integrins [53-55].

P13 has also been described as a porin in *Borrelia* [56]. However, many aspects of this porin remain unsolved such as its possible specificity for substrates or its molecular structure. It has a high number of paralogues that are potentially interchangeable with P13 [57, 58]. The biophysical analysis of P13 showed cation selectivity and no voltage dependency [56].

Oms28 was described as a porin with a conductance of 0.6 nS in 1M KCL [59]. Recent studies have questioned the function of this protein as a porin [60, 61].

Oms38 is the latest porin described in *Borrelia*. It has a small conductance of around 80 pS [62]. Homologues of this protein have also been found in LD species with similar pore forming activity (Thein, M.; unpublished data).

Methods

2.1 *Borrelia* outer membrane isolation

The outer membrane of *Borrelia*, also known as B-fraction [63] is obtained through a collaboration project with Prof. Dr. Sven Bergström from the Molecular Biology department of the University of Umeå. In this department, *Borrelia* species were cultivated and the outer membrane was isolated following the slightly modified protocol given elsewhere [63]:

- *Borrelia* strains were cultivated in BSKII medium supplemented with 6% rabbit serum for Lyme disease strains and 10% rabbit serum plus 1.4% gelatin for relapsing fever strains. They were kept at 37 °C until cell density reached approximately 10^7-10^8 cells/ml.
- 1 liter of BSK II medium was centrifuged at 9000 g for 20 min. at 4°C.
- The cells were washed with 50ml TSM buffer and centrifuged at 9000 g for 15 min. at 4°C.
- 1,2 ml of 8% octyl-β-D-glucopyranoside (OGP) in TSEA buffer was added to the washed cells and incubated 60 min. at 37°C
- Cell lisates were centrifuged at 48000 g during 30min at 25°C
- Supernatant was collected and incubated for 30 min at 56°C
- The solution was centrifuged at 48000 g, 30 min. at 25°C
- Supernatant was filtered through a nitrocellulose filter with a 0.45 µm pore diameter.
- The filtered solution was dialyzed at 4°C in H_2O during 48H.
- The solution was centrifuged at 48000 g during 30 min. at 25°C.
- The supernatant was discarded and the pellet was resuspended in 1ml H_2O.
- The pellet contained the outer membrane and was conserved at -20°C.

2.2 Fast Performance Liquid Chromatography

The Fast Performance Liquid Chromatography (FPLC) is a common technique used in the laboratory to purify or separate proteins from a complex mixture. The diluted samples flow through a stationary phase made of gel beads. Depending on the properties of the beads used the proteins can be separated base on their size, hydrophobicity, charge or affinity to certain compounds. A pressure is applied to accelerate the process.

The eluted proteins are collected in different Eppendorf tubes in defined time intervals. In this way, the proteins are separated in different fractions. Fractions containing proteins are detected by a UV detector that shows a protein elution peak in the register.

In this thesis, B-fractions were purified using different columns:

- MonoQ 5/50 GL, Amersham Biosciences. Anion exchange chromatography. The matrix is positively charged binding proteins charged negatively. Using a salt gradient (0-1 M NaCl) the proteins are eluted and separated depending on their negative charge.
- Superdex^{TM} 75 10/300, GE Healthcare. Gel filtration column used to separate proteins base on their size.

To identify how many proteins were contained in each fraction and its molecular weight, SDS-Page was performed. Low concentrated proteins samples were concentrated by the Wessel-Flügge method.

2.3 Wessel-Flügge protein precipitation

Some FPLC fractions contained diluted proteins. Sometimes, in order to see clearly some protein bands in SDS-Page bigger samples volumes were concentrated. The concentration method used was previously described by D. Wessel and U. I. Flügge [64] and it was performed as following described:

- 400 µl of methanol were added to 100 µl of sample. The sample was mixed shortly using a vortex and centrifuged 10 s at 8600 g.
- 100 µl of chloroform were added. The mixture was vortexed and centrifuged 10 s at 8600 g.

- 300 µl of H_2O_{dd} were added and mixed with a vortex. The sample was then centrifuged 1 min at 8600 g.
- At this point, two phases could be observed in the sample. In the interphase were located the proteins. The supernatant was removed carefully with a Pasteur pipette avoiding the disruption of the interphase.
- 300 µl methanol were added to the remaining solution and homogenized using a vortex. The sample was centrifuged 10 min at 8600 g.
- The supernatant was discarded and the pellet, where the proteins were, was dried at room temperature approximately for one hour.

2.4 SDS-Page

Sodium Dodecyl Sulfate Polyacrylamide gel electrophoresis (SDS-Page) is a technique widely used in molecular biology to separate proteins according to their molecular weight. When a protein mixture is heated to 100 °C in presence of SDS, the detergent wraps around the polypeptide backbone. It binds to polypeptides in a constant weight ratio of 1.4 g/g of polypeptide. In this process, the intrinsic charges of polypeptides become negligible when compared to the negative charges contributed by SDS. These polypeptides after treatment become a rod like structure possessing a uniform charge density that has the same net negative charge per unit length. Mobilities of these proteins will be a linear function of the logarithms of their molecular weights.

The SDS-Page has two regions. The upper part of the gel is the stacking gel and the lower part is called resolving gel. In this thesis, the stacking gel had always a 3% acrylamide concentration and the resolving gel had either 12% or 15% acrylamide (when not otherwise specified). 12% acrylamide gels were used with P66 samples while P13 samples were better visualized in 15% acrylamide gels.

The SDS-Page in this thesis was performed according to the Laemmli gel system [65]. The samples were mixed with a reducing sample buffer (Redmix) prior to load the gel. The voltage used was 80 mV through the stacking gel and 120 mV through the resolving gel.

LMW-marker (Amerham Biosciences) was used in most of the gels. Prestained PageRuler (Fermentas) was used whenever the gel was used to do a Western blot.

The recipes to cast the gels, to prepare the running and the sample buffers are included in section 7.5.

2.5 BN-Page and second dimension SDS page

Blue Native Polyacrylamide Gel Electrophoresis (BN-Page) is a technique developed by Schägger and von Jagow in 1991 [66]. In these gels the SDS is substituted by Coomassie® G-250 as a charge-shift molecule.

Coomassie® G-250 binds to proteins and confers it a negative charge while maintaining the protein native state. In this way, protein complexes and protein interactions can be studied [67].

Mild non-ionic detergents are used to solubilize membrane proteins complexes without disrupting them [68]. Digitonin and n-dodecyl-β-D-maltoside are commonly used maintaining protein complexes in their native state [69].

Three running buffers are needed to run these gels, the anode buffer, without Coomassie, and two cathode buffers, a dark-blue one containing 0.02% Coomassie and a light-blue buffer containing 0.002% Coomassie. The dark-blue buffer is replaced by the light-blue when the run-front has reached two thirds of the total gel length in order to reduce the Coomassie background [70].

The B-fraction samples were solubilized in different concentrations of digitonin after the extraction process of the outer membrane proteins described in the section 2.1.

BN Page and 2D SDS-Page gels were bought precast from Invitrogen (NativePAGE™ Novex® 4-16% Bis-Tris Gels 1.0 mm, 10 well, Cat. No. BN1002BOX and NuPAGE® Novex 12% Bis-Tris Gel 1.0 mm, 2D well, Cat. No. NP0346BOX). The marker used was NativeMark™ Unstained Protein Standard, Cat. No. LC0725). The running buffers were self-made as described elsewhere [70].

BN gels were stained with silver nitrate with a different protocol of the one described in the section 2.6 [71].

Second dimension SDS-Page from the BN-Page was performed as described in the Invitrogen user's manual [67]. The BN-Page strips were incubated in three denaturing solutions previous

to the second dimension electrophoresis as described in the manual cited. MOPS SDS running buffer was used (see section 7.5).

2.6 SDS-Page silver nitrate staining and gel drying

Proteins separated by SDS-Page depending on their molecular weight were stained with silver nitrate [72]. This staining method has been proved to be very sensitive, detecting proteins in nanogram concentrations.

The following protocol was used to stain SDS-Page. The composition of the A to D solutions is described in section 7.5:

- The gel was immersed in 50 ml of Solution A during 10 min. to fix the proteins to the gel matrix.
- The SDS-Page was washed twice with H_2O_{dd} during 5 min.
- The water was discarded and the gel submerged in Solution B during 1min.
- The gel was washed twice in H_2O_{dd} for 20 sec.
- The gel was incubated in solution C for 10 min.
- A wash step was required with approximately 40 ml $H2O_{dd}$ and 10 ml of Solution D for a few seconds.
- The gel was developed in 40 ml Solution D supplemented with 100 µl $Na_2S_2O_3$ (10 mg/ml) and 25 µl formaldehyde (35%).
- The staining reaction was stopped when the bands were visible with 2.5 ml of citric acid (2.3 M).

All the steps were carried out at room temperature and the incubations in the different solutions were done on a shaker.

Once the proteins were purified to homogeneity, their pore forming activity could be tested using the “Black Lipid Bilayer” assay.

2.7 Black Lipid Bilayer assay

The Black Lipid Bilayer assay (BLB) owes its name to the brownish color that the artificial membrane acquires when it reaches the bilayer state. This method has been described before

[73] and is used to test the pore forming activity of some proteins (porins, toxins and some peptides) from different bacteria, plant and animal cells.

Method principles:

This method is based on the ion-impermeable properties of lipid membranes which impede the electric current through them. Pore forming proteins get inserted in the membrane forming holes which increase the membrane conductance. The particular conductance of each porin depends on the size of the hole formed in the membrane and it can be influenced by internal charges. Insertions of porins in the membrane can be observed in a register as increasing-conductance steps with a typical value depending on the porin.

Porins differ from each other in conductance and biophysical behavior. For example, the single channel conductance of Tsx of *Escherichia coli* is around 10 pS while a porin from *Thermus thermophilus* has an unusual conductance of 20 nS. Some of them are selective for anions or cations or are not ion selective. Some of them have a rigid structure that resists high voltages without any changes in conductance. Some of them are specialized in the transport of certain type of molecules. All these characteristics can be studied using the BLB assay.

Devices and material used for this assay:

A Teflon chamber divided into two compartments is required. The wall dividing both compartments has a 0.5 mm^2 hole. Upon this hole an artificial membrane is spread. The central wall forms a light angle with the vertical wall to avoid the reflection of the light which could hinder the membrane observation. To observe the membrane at any time, the front wall of the chamber is a transparent window (Fig. 2.1).

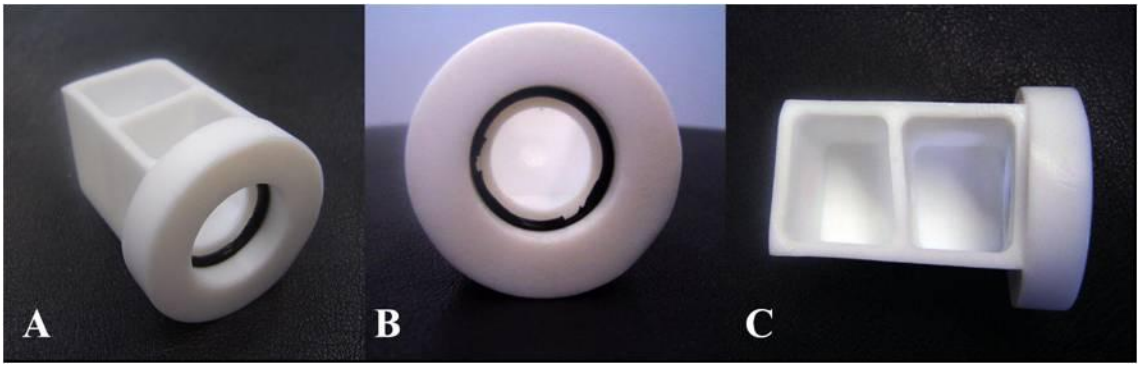

Fig. 2-1: Teflon chamber used in the BLB assay. A) Lateral vision of the chamber, B) frontal view, where the window and the hole where the membrane is established can be appreciated, C) superior view showing the dividing wall of the chamber.

The Teflon chamber is inserted in a metal support inside a metal box called Faraday cage. This metal container prevents the influx of external forces in the measurements and supports the rest of the components (Fig. 2-2). The Teflon chamber is filled with a salt solution in which two Ag/AgCl electrodes are immersed.

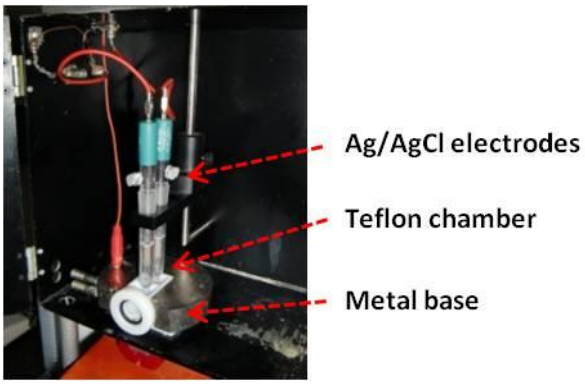

Fig. 2-2: Interior of the Faraday cage where the electrodes and the Teflon chamber are located.

One of the electrodes is connected to a voltage source; the second detects increases in membrane conductance and send the signal to an amplifier. The amplifier also filters the signal and is connected to a register where it is possible to observe single insertions of pore forming proteins in the artificial membrane (Fig.2-3). The records of the register can be afterwards mathematically analyzed.

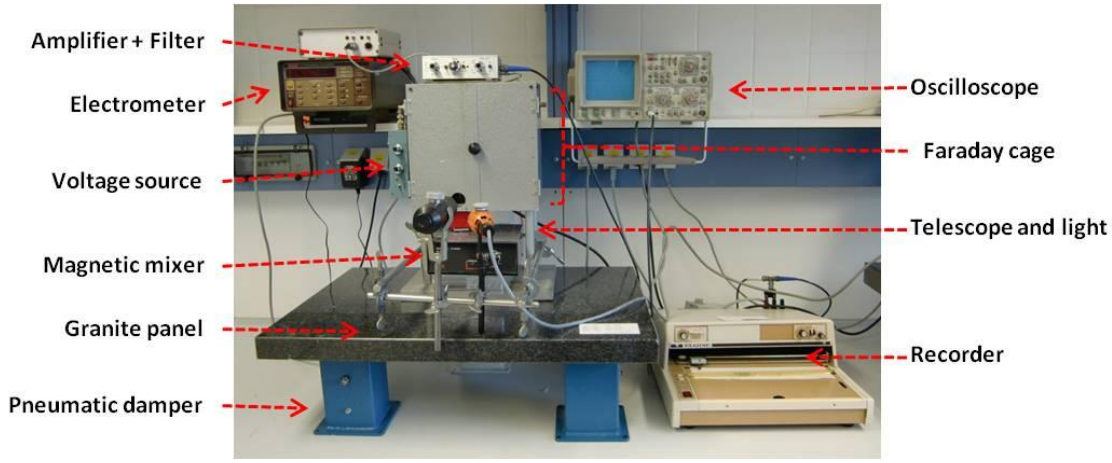

Fig. 2-3: Black Lipid Bilayer setup. Basic scientific instruments used to test the pore forming activity of proteins, toxins and peptides.

In the BLB setup several other apparatus are required. An electrometer is used to verify the electrochemical symmetry of the electrodes. An oscilloscope helps to distinguish fast insertions in the membrane when the activity of the samples is too high to be recognized as individual pores by the recorder. A telescope and light help to check the formation of artificial membranes and the absence of bubbles attached to it. The granite panel and the pneumatic dampers hinder the influence of floor vibrations. A magnetic mixer is used during ion selectivity or titration experiments to quickly diffuse substances added to the salt solution.

Artificial membranes:

Several lipids with different characteristics (charge, length, etc) can be used to form artificial membranes in this method. Diphytanoyl phosphatidylcholine (DiphPC) was the only one used in this thesis.

An impregnation of the hole in the Teflon chamber is required before spreading the membrane. For the impregnation, 5 µl of 2% DiphPC in chloroform is deposited in the hole and let dry for 15 minutes. After this time, the lipid has formed a lipid ring around the hole which increases the stability of the membrane.

A solution of 1% DiphPC in n-decane and 10% butanol is used to form the membrane. Once the Teflon chamber is filled with the salt solution, 5µl of the lipid solution are placed upon a wire-handle and spread with its help over the impregnated hole.

The membrane stops the ion flux through the hole and the conductance decreases to a negligible value. At the beginning the membrane shows a multicolor state indicative of a lamellar structure. After a short period of time the membrane starts to have black spots and finally turns completely dark (Fig. 2-4). This color is indicative of a single bilayer membrane, and is also the reason why the method is called “Black Lipid Bilayer”.

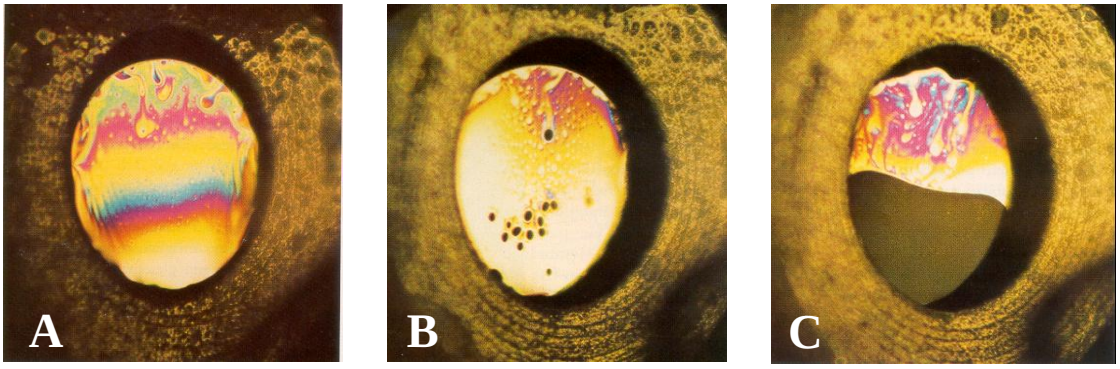

Fig. 2-4: Formation of a single bilayer. Multiple layers are spread over the hole in the dividing wall showing multiple colors (A). As the membrane stabilizes, dark spots appear where a single bilayer is present (B). Eventually, the membrane stabilizes in a single bilayer presenting a dark color (C).

The membrane must be observed through the front window to make sure that no bubbles are on the membrane which can interfere with the pore forming activity measurements.

Before adding the protein sample, a period of time is waited as negative control (cero line). If after 5 minutes no activity due to contaminations appears in the register, the measure can proceed.

With this method the pore forming activity of membrane proteins can be tested. If the protein tested shows some activity, some biophysical characterization can be done. Among the different characteristics that can be studied are the following;

- Single channel conductance
- Voltage dependency
- Ion selectivity
- Substrate specificity (Substrate titration)
- Current noise analysis
- Pore diameter

2.7.1 Single channel measurements

Each pore forming protein has a defining conductance depending on how big is the ion flow through it. This varies depending on the channel diameter, channel internal charges and oligomeric constitution of a porin.

A porin must be first purified to homogeneity and then added to the salt solution in the Teflon chamber to measure its single channel conductance. The proteins get inserted in the membrane increasing its conductance in a step-like manner. Each step corresponds to a protein or protein complex insertion.

The single channel conductance of a porin is defined as the most common conductance value observed in a purified sample. Mathematically, the conductance of a porin can be defined as:

(Eq. 1) $G = \frac{I}{U_e}$ where: G = conductance (S)

I = current (A)

U_e = applied voltage (V)

The current of the system (I) is amplified and transformed in voltage, which is registered. This voltage (U_a) is proportional to the current (I). V_f (V A^{-1}) is the conversion factor. The current is therefore defined as following:

(Eq. 2) $I = \frac{U_a}{V_f}$ where: U_a = output voltage (V)

V_f = amplification factor (V A^{-1})

Substituting (2) in (1):

(Eq. 3) $G = \frac{U_a}{V_f \cdot U_e}$

In the praxis, the conductance U_a is evaluated using the records in the register. The record-paper is divided in 100 boxes. The conductance per box results from dividing the total deviation U_v by 100. If U_a is substituted by U_v in the formula 3, the conductance per box (G_k) is the following:

(Eq. 4) $G_k = \frac{U_v}{V_f \cdot U_e \cdot 100}$ where: G_k = Conductance pro box (S).

U_v = full scale of the register (V).

The single channel conductance of a certain porin can be obtained multiplying G_k by the number of boxes increased in the recorder when it gets inserted.

2.7.2 Ion selectivity

While some porins show no discrimination between different ions, others are more permeable to anions or cations. The reason for that behavior depends on the charge distribution in the entrance and interior of the channel.

To test the ion selectivity of a channel, a concentration gradient is established between both sides of a membrane as described previously elsewhere [74, 75]. The kind of ion for which the porin shows specificity is preferentially transported to the diluted side of the chamber to equilibrate the concentration creating a potential difference. The potential difference works against the concentration gradient. This process stops when the electrochemical potential is equal in both sides. The potential difference can be then measured with an electrometer and a permeability coefficient (P_c/P_a) can be calculated using the Goldmann-Hodgin-Katz equation;

(Eq. 5) $V_m = \frac{RT}{F} \ln \frac{P_c C_t + P_a C_c}{P_c C_c + P_a C_t}$ where: Vm = Membrane Potential

R = Gas Constant.

T = Thermodynamic temperature

F = Faraday constant.

P_c = Permeability constant of the cations.

P_a = Permeability constant of the anions.

C_c = Concentration in the Cis-compartment

C_t = Concentration in the Trans-compartment

where $C_t > Cc$

In the practice, the chamber is filled with 5 ml of salt solution 0.1 M in each side of the wall and the protein sample is added to the solution once the membrane is in place. After reaching at least 100 insertions in the membrane and a stationary phase (no new insertions), the measurement can start. In this experiment, the voltage applied in other measurements like single channel measurements or voltage dependency is not required and therefore it is switched off. 100 µl 3M salt solution are added to the cis-side of the chamber. At the same time, 100 µl 0,1M KCl are added to the trans-side, equilibrating the volume and avoiding ion transport due osmotic pressure. The voltage value is note down after the electrochemical potential is reached. The process is repeated several times increasing proportionally the salt concentration gradient. If the voltage increases in a positive manner the porin is considered cation selective ($P_c/P_a > 1$). In contrast, if the values are negative the porin is an anion selective porin ($P_c/P_a < 1$). A non-selective channel will display voltages values close to 0 and a P_c/P_a close to 1.

Other salts are used in these measurements apart from the KCl, where the hydrodynamic radius of its cations and ions are different. In LiCl the cation (Li^+) is bigger than the anion (Cl^-) and in KCH_3COO the anion (CH_3COO^-) is much bigger than the cation (H^+). That way the transport of the different ions through the membrane is influenced. Non selective porins for example will show a negative membrane potential in presence of LiCl and values of $P_c/P_a < 1$ because the transit of Cl^- through the membrane is favored due to its smaller size.

2.7.3 Voltage dependency

Another test done using the BLB assay is the voltage dependency of a channel. Some pore forming proteins close partially or totally increasing the applied voltage during a measurement. The voltage at which they close is characteristic of the channel.

In practice, a sample is added to the bathing solution where the membrane was previously formed. The measurement can start after reaching hundred pore insertions in the membrane and a stationary phase where no new insertions are appreciated. A positive 10 mV voltage is applied and the membrane is observed for a short period of time for closure of the pores. When the conductance is stabilized, the measurement is repeated with the same negative voltage (-10 mV). Increasing voltages (20, -20, 30, -30 and so on) are tested up to 100-150 mV. After finishing the measurements, a graphic can be done where the closure percentage of the pores is showed.

This graphic can show symmetric or asymmetric voltage dependence for positive and negative values or voltage independence.

2.7.4 Substrate specificity

Porins can be of two types, general diffusion porins or substrate-specific porins. The transport through general diffusion porins is fast and it does not decrease with an increase in the solute concentration. In the case of specific porins, the transported molecule had different binding sites in the channel and therefore the transport is slower (Fig. 2-5). The ion flow is interrupted and the conductance of the membrane decreases at certain concentrations of solutes for which the porin shows specificity. This characteristic can be used to determine if a porin is specific for particular solutes.

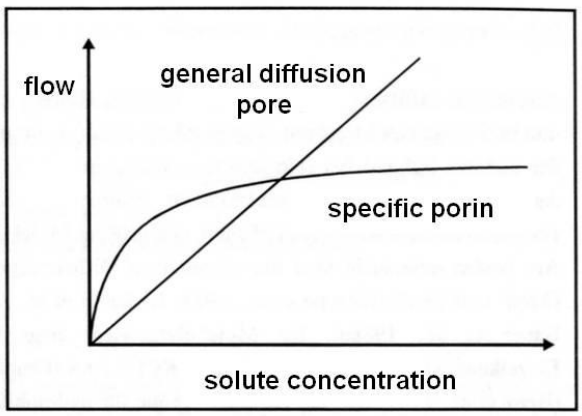

Fig. 2-5: Relation between solute flow through a porin and the concentration of the solute in the salt solution. In general diffusion pores the flow had a linear correlation with the solute concentration while in specific porins the channel gets saturated with increasing concentrations of the solute.

To test if a porin is specific for a substrate, a membrane is permeabilized with a porin sample. At least hundred pores must be inserted in the membrane and insertions must have reached a stationary phase. After that, increasing amounts of a compound are added to the 0.1M KCl salt solution in which the membrane was formed. If a porin transports a substance specifically through the membrane the ion flux will be interrupted, decreasing the total membrane conductance.

A solution 1M of the possible specific substrate is prepared in standard measurements. In the first place, 1µl is added to each side of the chamber under stirring conditions. A few minutes must be waited to see if there is an effect in the membrane conductance. When the conductance is stable the same is repeated adding 2, 4, 8, 16, 32, 64 and 128 µl of the substrate.

After that, the binding constant can be calculated using the Michaelis-Menten constant, which relates the total membrane conductance with the increasing substrate concentration (1+K·c);

(Eq. 6) $G_c = \frac{G_{(max)}}{1+K \cdot c}$ where

$G_{(c)}$ = Membrane conductance after adding the substrate

$G_{(max)}$= Membrane conductance before adding substrate

K= stability constant (l mol^{-1})

c= substrate concentration (mol l^{-1})

2.7.5 Noise analysis.

Titration experiments allow identifying a possible specificity of a channel for different substrates but do not allow the evaluation of the on- and off- binding rate constant. To get some information about the binding kinetics, the current noise is measured. Parallel to titration measurements, the frequency-dependence of the spectral density is evaluated using a Fourier transformation. A reference is taken from a membrane saturated with channels before adding any substance to the salt solution. This reference always exhibits a 1/f noise in a low frequency range. An increase in the spectral density can be observed above 200 Hz. This increase is caused by intrinsic noise of the preamplifier that produces frequency-dependent current noise through the membrane capacity C_m. The reference spectrum is subtracted from each spectrum taken after the addition of the substance to be tested.

While channels that show no specificity for a certain substance exhibit a 1/f noise, the porins that bind a substrate show a current noise spectrum that can be fitted to a single Loretzian function [76, 77].

The experiments are done with the same bilayer setup used for titration measurements. A special amplifier and filter that allow working with high frequencies is needed. The amplifier is connected to a PC with an AD-converting card. A self-made computer program is used to measure the noise spectra in a frequency range (0-1000 Hz). The spectra were composed of 400 points and they were averaged either 128 or 256 times. The values are represented in a plot using commercial graphic programs. An example can be seen in figure 4-5.

2.7.6 Channel diameter determination using non-electrolytes

This method was described by Krasilnikov et al. in 1998 [78]. It has been used successfully to determine the channel diameter of several membrane pore forming proteins like colicin Ia [78]. It is especially appropriate because it avoids the potentially strong coulombic interactions that occur when using ionic probes and ion channels with fixed charges.

The method is based in two principles; first, a salt solution containing 20% of a determinate non-electrolyte has a reduced conductivity between 40 and 70% of the original. And second, this decrease will only affect the conductance of a porin if the non-electrolyte is small enough to enter the channel.

Using these two principles, solutions containing 1M KCl and 20% of a given non-electrolyte were used. Single channel measurements were carried out using each time non-electrolytes with increasing hydrodynamic radius. The non-electrolytes used, their hydrodynamic radius and the conductivity of each mixture are shown in the following table (Table 2-1).

Nonelectrolyte	r (nm)	χ (mS cm^{-1})
None	-	110.3
Ethylene glycol	0.26	57.2
Glycerol	0.31	49.1
Arabinose	0.34	63.7
Sorbitol	0.39	57.8
Maltose	0.50	73.8
PEG 300	0.60	45.5
PEG 400	0.70	46.4
PEG 600	0.80	54.1
PEG 1000	0.94	49.5
PEG 3000	1.44	48.9
PEG 6000	2.50	50.5

Table 2-1: Non-electrolytes used to determine the channel radius of porins and toxins. The hydrodynamic radii of these NEs goes from 0.2 to 2.4 nm and the conductivity of the mixture is on a rage from 40 to 70 % of the original when only the salt solution without any NE is present (1M KCl at 25 ˚C).

As seen in the following graphic, the conductance of a pore in 1M KCl (horizontal line) is reduced with the small non-electrolytes that have access to the channel interior. The

conductance of the porin is not influenced anymore from a determined NE diameter because the NEs have no access to the channel interior (Fig.2-6).

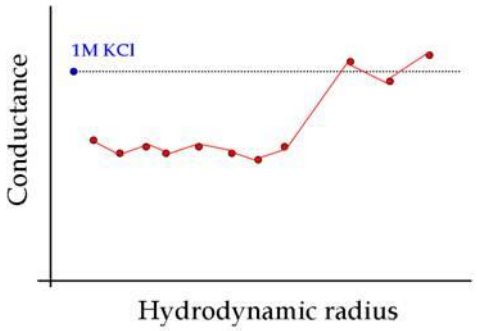

Fig. 2-6: Effect of different NE in the conductance of a porin. Small NEs enter the pore reducing the conductance of the porin. When the hydrodynamic radius of the NEs is too big to enter the channel, the conductance of the porin goes back to the original (horizontal line).

A second concept introduced in this method is the "channel filling" (F). The channel filling describes the portion of a channel that is occupied by a particular NE. It is used to determine possible inner constrictions inside the channel.

To calculate the channel filling, it is assumed that an ion channel can be treated as an equivalent ohmic resistor with resistance (R). This assumption can be extended to all channels with a linear current-voltage relationship. R can be seen as composed of two parts. One part corresponds to the portion of the channel length filled with the NE (F) and one part corresponds to the portion without NE (1-F). Thus, R can be written as:

(Eq. 7) $R = [F/(AX_i) + (1-F)/(AX_o)]$

where $A = \pi r^2/l$, l is the channel length and r its radius, and X_o and X_i are the conductivities of the solution without and with a particular NE respectively. In assumption that AX_o is equal to the ion channel conductance in a solution without NE (G_o), it can be shown that the filling (F) is given by:

(Eq. 8) $F = [(G_o-G_i)/ G_i]/[(X_o -X_i)/ X_i]$

where G_o is the single-channel conductance in a solution without NE (1 M KCl), G_i is the single-channel conductance in the presence of a solution containing 20% (w/v) of an NE, X_o is the conductivity of the solution without NE (1 M KCl), and X_i is the conductivity of the solution containing 20% (w/v) of a given NE.

Assuming that the filling of the channel by two of the smallest NE (in this study ethylene glycol and glycerol) is close to the maximum possible level (100%), the filling can be calculated in terms of percentage (F%):

(Eq. 9) $F\% = 2F_i/(F_1+F_2)*100\%$

where F_i is the filling in the presence of a given NE and F_1 and F_2 represent the filling in the presence of ethylene glycol and glycerol in the bathing solution respectively.

Most of the channels are not perfect cylinders, but funnel-like structures. Analyzing the filling of a funnel-like channel three events are possible (Fig. 2-7). If the NE is smaller than the narrowest part of the channel, the channel will be completely filled (F%=100%). In contrast, if the NE is bigger than the entrance, there will be no NE inside the channel (F%=0%). Intermediate-sized NEs will fill the channel to an extent inversely related to theirs sizes (F% between 0 and 100%). These NEs don't fill the channel completely because its size is too big and they get stopped somewhere along the channel interior.

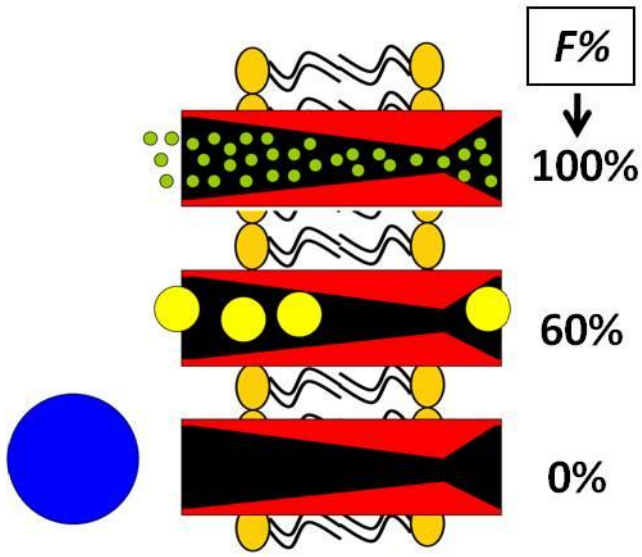

Fig. 2-7: Possible channel filling events with NEs. When the NEs are smaller than the constriction zone they will fill 100% of the channel (green). If they are bigger than the entrance, the NEs remain outside and the channel filling is 0% (blue). NE with sizes in between will fill the channel to an extent inversely related to their sizes (yellow).

According to this method, the radius of the constriction zone should be equal to the radius of the smallest NE that does not pass freely through the channel.

2.8 Western-Blot

The Western-blot (WB) is a technique used in molecular biology to detect a specific protein in a sample using specific antibodies against this protein. The WB in this thesis were performed as previously described [79].

First the protein or proteins were separated in an acrylamide gel by molecular weight (SDS-Page or BN-Page). Afterwards, the proteins were horizontally transferred or blotted to a PVDF or nitrocellulose membrane. Depending on the protein size, the transfer time varied. P13 which is a 13 kDa protein was transferred in 12 minutes at 350 mA while P66 which has 66 kDa required 45 minutes.

To blot the proteins from a gel to a membrane, the cassette and tank must be prepared as following:

- PFDF membranes (7.5 x 8.5 cm) were pre-wetted in methanol for 5-10 seconds. Briefly afterwards, the membrane was place in deionized water for 2-3 minutes and then a few minutes more on the transfer buffer.
- The gel and membrane were introduced in a cassette which was filled with the different components as described by the manufacturer. Proteins run towards the anode and consequently the membrane was situated closer to it than the gel.
- The cassette was placed inside the tank and the tank was filled with Towbin buffer. An ice block was placed inside the tank to avoid overheating.

The WB from BN-Page and second dimension SDS-Page were done following the instructions from the manual provided by Invitrogen [67]. The buffer used was Nu-Page Transfer Buffer (Invitrogen) and the proteins were blotted one hour at 30 V.

Immunodetection:

- Once the proteins were on the membrane, the rest of the surface was blocked with protein to avoid unspecific antibody binding to the membrane. 5% milk in TBS buffer was used during an incubation time from 1 to 12 hours (overnight).
- After the blockage the membrane was washed 3 times during 10 minutes with TBS + 1% Tween 20. During the washing steps the membrane was placed on a shaker.
- The membrane was incubated during 1 hour in the first antibody. The antibody is properly diluted in TBS + 2.5% milk or BSA. Dilutions for the antibodies used in this thesis are indicated in section 7.10.

- The membrane was washed 3 times in TBS + 1% Tween 20 for 10 minutes each time.
- After that, the membrane was again incubated for 1 hour in the second antibody. This antibody was diluted according to the manufacturer in TBS + 2.5% milk or BSA.
- The membrane was washed twice in TBS + Tween 20.

Development:

The membrane was placed on a clean surface where the electrochemiluminescence reagents were added. The secondary antibody had linked a horseradish peroxidase and it was developed with the "ECL-detection kit" (GE healthcare). Equal volumes of reagent 1 and reagent 2 were mixed and incubated with the membrane for 1 minute.

The remaining reagent solution was removed and the membrane was introduced in an x-ray cassette. An x-ray film was exposed to the membrane inside the cassette in a dark room and then it was developed as a traditional photo. First, it was submersed in the developing solution (Kodak), rinsed with water, immersed in the fixing solution (Kodak) and again rinsed with water before letting it dry.

2.9 Gen cloning

Multiple steps were taken to clone *p13* in *E. coli* and *A. tumefaciens*. An overview of all those steps is shown in section 2.9.1. Fig. 2-8 shows the cloning process in *Escherichia* while Fig. 2-9 shows the steps to clone *p13* in *Agrobacterium*.

2.9.1 P13 cloning outline

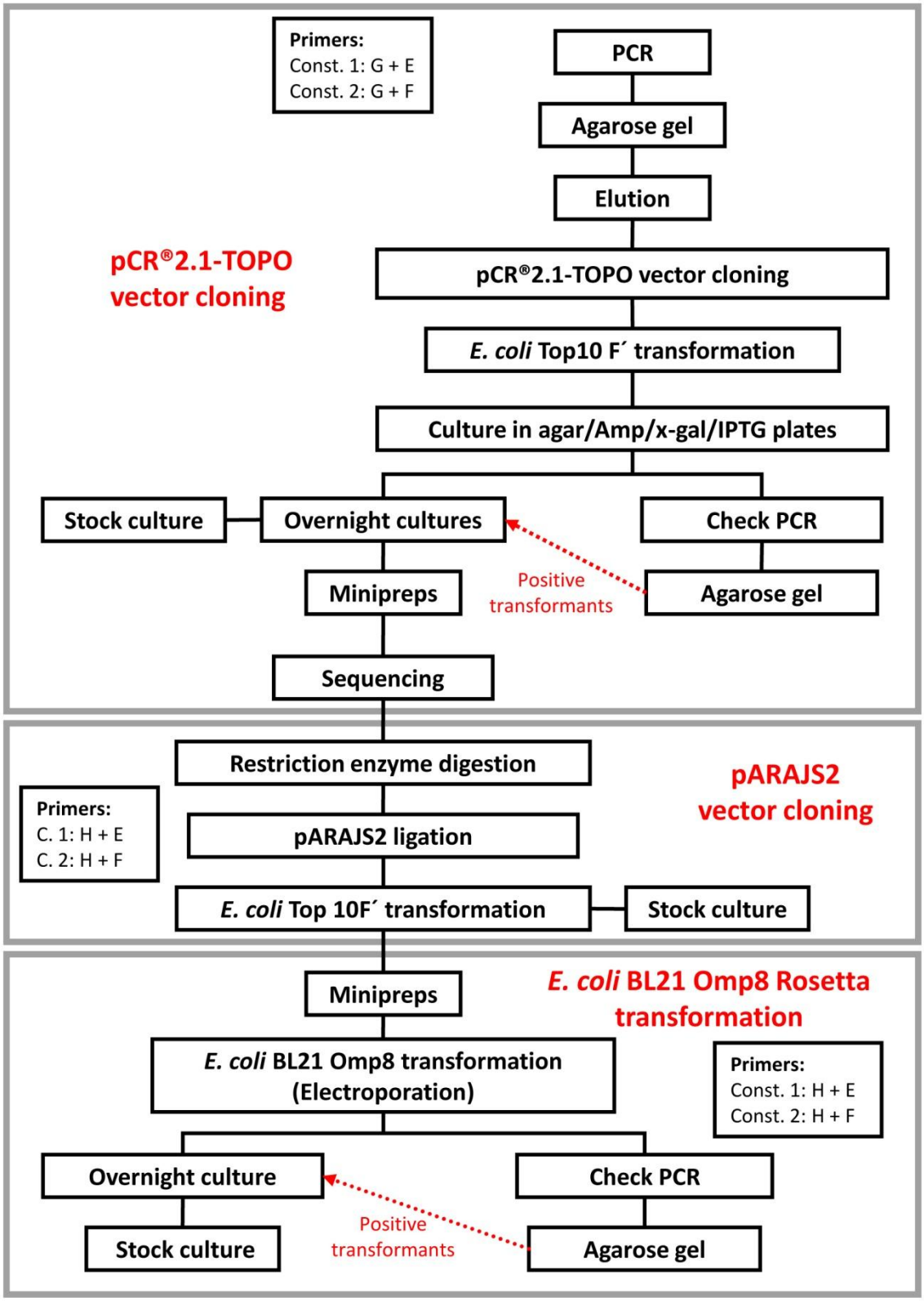

Fig. 2-8: *p13* cloning in *E. coli*.

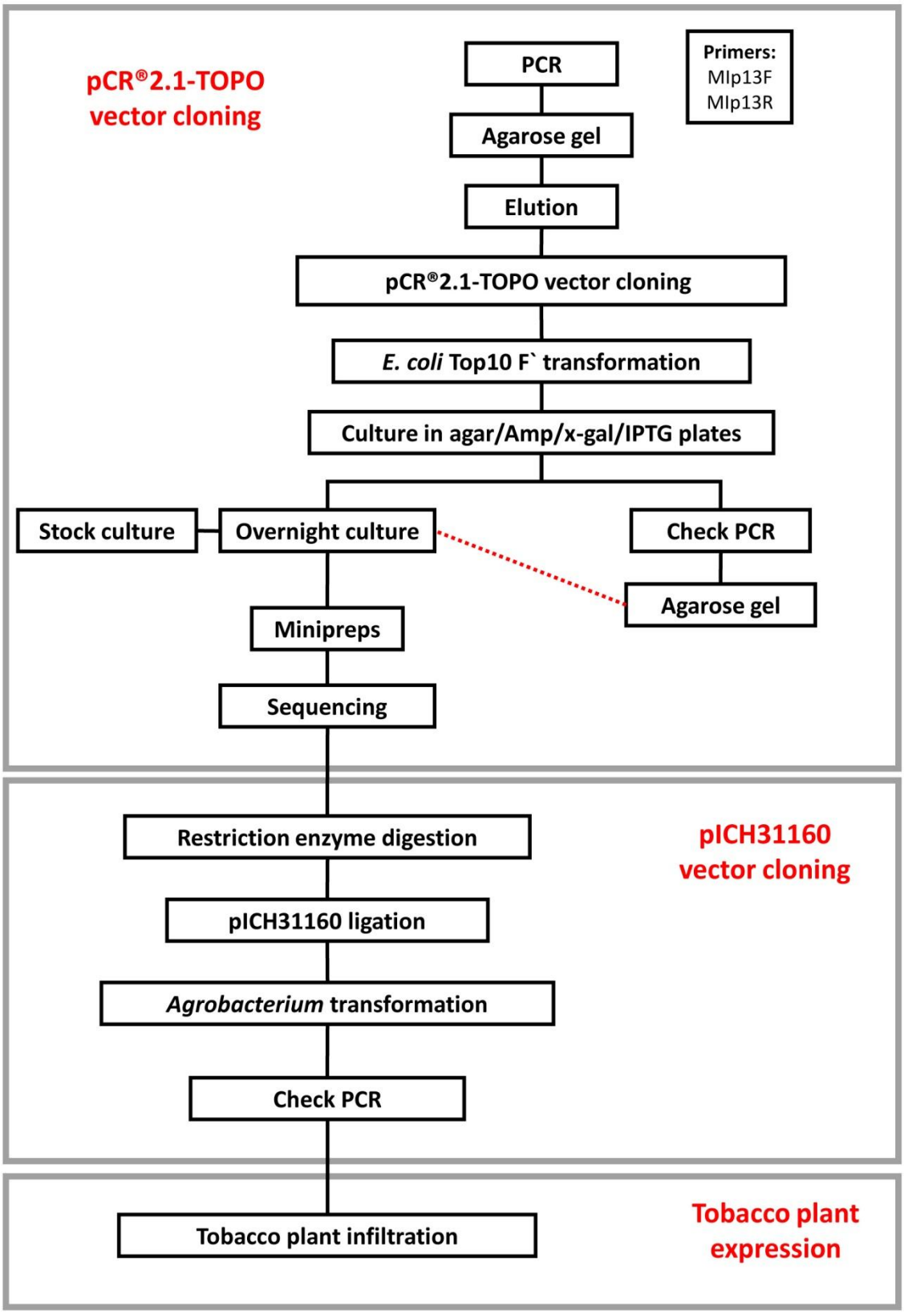

Fig. 2-9: *p13* cloning in *Agrobacterium*

2.9.2 Constructs and primer design

Cloning in *E. coli*

Different structures were designed to be clone in *E. coli*. The first construct included the *p13* gen that originates the mature P13 protein. Construct 2 included the *p13* gen and a 28 amino acid C-terminus that in *Borrelia* is cleaved after crossing the inner membrane, probably in the periplasm. The function of this C-terminus remains still unclear. This second structure had the aim of clarifying if this C-terminus was involved in the formation or oligomerization of the channel. Both constructs included an *E. coli* signal sequence required to transport the protein trough the inner membrane and a His_{10}-tag for later purification. The signal sequence and the His-tag were added to the constructs by the pARAJS2 vector when the product of the first amplification was ligated to it. The primers, restriction enzymes and protease needed for the whole process shown in Fig. 2-8 are indicated in Fig. 2-10.

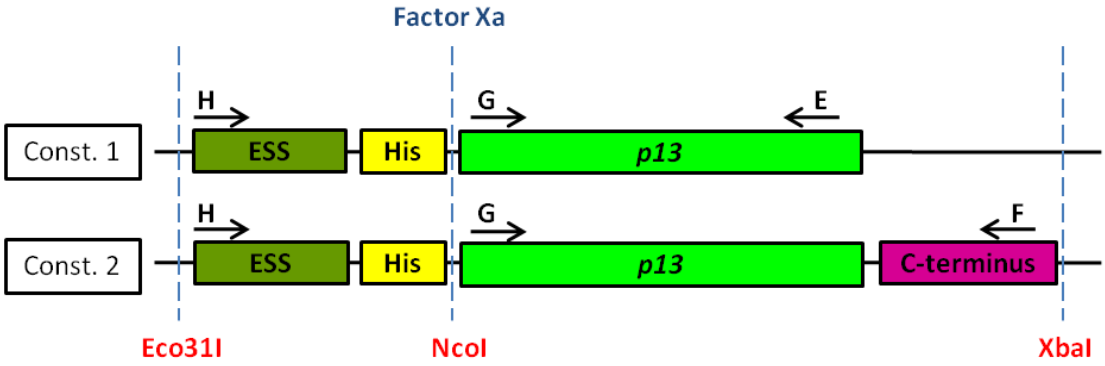

Fig. 2-10: Constructs to be cloned in *E. coli*. Primers are indicated by an arrow in black. The restriction enzymes used are written in red and the protease to cleave the His-tag in blue. The places where the DNA or protein is cut are indicated by the broken lines.

Primers G, E and F were designed to amplify the gen from the *Borrelia* DNA and to do check PCRs while the gen was included in the pCR®2.1-TOPO. Primer H together with E and F were used to do check the cloning process in the pARAJS2 vector. The nucleotide sequences of the constructs and the primers as well as the amino acid sequences of the proteins produced are included in section 7.8.

Cloning in *Agrobacterium* (Tobacco plant expression):

The purpose of the expression in tobacco plants was to obtain a high amount of the recombinant protein and therefore only the mature form of P13 (without C-terminus) was cloned. In this case, a His_6-tag was added to the *p13* gen by the MIp13F primer during the first amplification from the *Borrelia* DNA (Fig. 2-11).

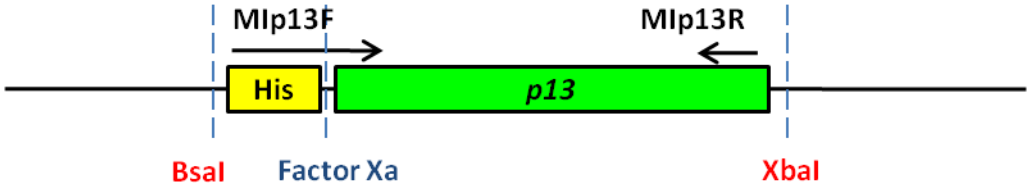

Fig.2-11: Construct to be clone in *A. tumefaciens* to produce P13 in tobacco plants. Primers are indicated with an arrow in black, restriction enzymes are written in red and the protease in blue. The places where the DNA or protein is cut are indicated by the broken lines.

The nucleotide sequence of the construct and the primers as well as the amino acid sequence of the protein produced are included in section 7.8.

2.9.3 Polymerase Chain Reaction

The polymerase chain reaction is a technique used to amplify or copy many times a determined DNA fragment. In this thesis two types of PCR were carried out:

- Standard PCR: In this PCR only one fusion temperature was used. This kind of PCR was used in amplifications to check if the transformation in cells was successful. For this procedure Taq-polymerase which is faster but has a higher mutation rate was used.
- Step PCR: In these PCR two annealing temperatures were used due to the different primers fusion –temperatures. This type of PCR was used to amplify *Borrelia* DNA and the polymerase used was the Pfu-polymerase.

The mixture of the different components and the PCR cycles (time and temperature) are indicated in section 7.9.

2.9.4 Agarose gel electrophoresis and agarose gel elution

The products of the PCR were run in agarose gels to check if the desired gen was correctly amplified. Those gels separate the DNA depending on their size .In that manner, the size of the DNA amplified was compared with a DNA marker to know if the size was correct.

The gels used in this thesis were made of 1% agarose. Two markers were used, MassRuler™ DNA Ladder Mix (Fermentas) or GeneRuler™ 100bp Marker (Fermentas). The running buffer used was TAE and the applied voltage was 100 mV.

To visualize the bands in those gels, they were submerged 15 minutes in an ethidium bromide solution (10 mg/ml) and then placed upon a black light.

After checking the right size of the amplified gen, the DNA was extracted from the agarose gel. To do so the desired DNA band was excised from the gel with a scalpel. The DNA extraction was done using a commercial kit (QIAquick Gel Extraction, Qiagen).

2.9.5 Vector cloning

2.9.5.1 p13 cloning in E. coli

The correct proceeding of the cloning process was confirmed as much as possible with check PCRs and vector sequencing. The *p13* gen was cloned in two vectors. First of all in the pCR®2.1-TOPO which is an easy system to multiply the number of *p13* copies, permits an easy screening of transformed colonies and allows an easy sequencing of the insert to dismiss any point mutation in the gene sequence. The second vector is the pARAJS2 that supplements the construct with an inducible promoter for the expression, a signal sequence to cross the inner membrane in *E. coli* and a His_{10}-tag to facilitate the purification process. A complete diagram of the steps taken to clone *p13* in *E. coli* is found in the section 2.9.1.

***p13* cloning in pCR® 2.1-TOPO vector:**

The TOPO TA cloning® is a highly efficient, fast, one-step cloning strategy that does not require special primers or any ligase to bind to the vector PCR products amplified with Taq-polymerase.

The DNA obtained from *Borrelia burgdorferi* B31A was isolated using a commercial kit (QIAamp DNA Mini Kit). The *p13* gene was amplified using two sets of primers. Primers G and E were used to amplify construct 1 whereas primers G and F were used to replicate construct 2.

Two different annealing temperatures were used to amplify the desired DNA fragments. Construct 1 was obtained with a PCR protocol that included 5 cycles with an annealing temperature of 45 °C and 25 cycles at 50 °C. Construct 2 did not required temperatures as low as construct 1 and the gene was amplified with 5 cycles where the annealing temperature was 50 °C and 25 cycles at 55 °C. The product of the PCR was separated in a 2% agarose gel together with a DNA marker to verify the size of the amplified fragment.

After the verifying that the fragments amplified corresponded to the size of the desired structures, they were ligated to the pCR® 2.1-TOPO vector. This vector was used to transform *E. coli* Top10F´ cells. The transformants were cultivated in agar/Amp/x-gal/IPTG plates at 37 °C overnight. Colonies with a white color have a DNA fragment inserted in the plasmid. Therefore, some white colonies were selected and tested with a PCR (primers G-E and G-F) to amplify the insert. The correct size of the insert was verified in a 2 % agarose gel with a DNA marker run together with the samples.

The colonies that showed a correct size of the insert were cultivated in 5 ml LB medium supplemented with ampicillin at 37 °C overnight. After that, the pCR® 2.1-TOPO vector was extracted using a commercial kit (QIAprep Spin Miniprep Kit, Qiagen). The vector was sent to an external company to sequence the insert (SEQLAB, Sequence Laboratories Göttingen). Only 100% coincidence sequences were used in the following steps rejecting the possibility of point mutations that could alter the protein functionality.

***p13* cloning in pARAJS2:**

The insert from the pCR® 2.1-TOPO plasmid was digested to be inserted in the new expression vector pARAJS2. The fragment and vector were ligated as described in the section 2.9.9 using the T4 polymerase.

Once the vector was prepared, *E. coli* TOP10F' cells were transformed with it. To be sure that the cells had not only the plasmid but also the insert, a check PCR was done (primers H-E and H-F). Only colonies where the fragment was amplified were used for posterior work. The

copies of the plasmid were produced in this strain and then extracted to transform the final strain where the recombinant protein was produced.

A special strain of *E. coli* was used for expression in which eight outer membrane proteins are knocked out (*E. coli* BL21 Omp8 Rosetta) [80]. These cells were transformed by electroporation (see section 2.9.10). As usual, the success of the transformation was checked with a standard PCR where the insert was amplified (primers H-E and H-F).

2.9.5.2 p13 cloning in Nicotiana benthamiana

The cloning of *p13* in *N. benthamiana* was done in a similar way as in *E. coli*. First, *p13* was cloned in the pCR®2.1-TOPO vector. Afterwards, the insert was included in the pICH31160 vector for *Agrobacterium* transformation. A complete diagram of the steps to clone *p13* in *N. benthamiana* is found in the section 2.9.1.

***p13* cloning in pCR®2.1-TOPO and pICH31160:**

Borrelia DNA was used as template to express the mature P13 in the tobacco plant. A His_6-tag was added to the insert by the MIp13F primer. The PCR used consisted in two annealing temperatures, 5 cycles at 45 °C and 25 cycles at 55 °C, respectively.

To check the absence of point mutations in the *p13* gene, the insert included in the pCR®2.1-TOPO vector was sent to be sequenced. A 100 % coincident sequence was digested from the TOPO vector (BsaI and XbaI) and ligated to the final vector, the pICH31160. With this vector *A. tumefaciens* cells were transformed. Colonies from *Agrobacterium* were collected, the fragment amplified by PCR (primers MIp13F and MIp13R) and the presence and size of the insert was proved in agarose gels.

2.9.6 Over Night Cultures and type cultures

Clones containing the vector and desired gen were cultivated overnight. 5 ml LB medium was prepared including the proper antibiotic. After that, the strain was inoculated and cultivated over night at 37 °C in a shutter.

In this thesis, different strains and species were used and transformed with vectors. The vectors used conferred a certain antibiotic resistance:

- pCR®2.1-TOPO vector – Ampicillin
- Rosetta – Chloramphenicol
- pICH31160 - Kanamycin

The final antibiotic concentration in the cultures was 0.1µg/ml ampicillin, 50 µg/ml kanamycin and 40 µg/ml chloramphenicol.

For the type cultures, 1.2ml of LB culture plus antibiotic was mixed with 0.4 ml of glycerol. The sample was well mixed using a vortex and immediately frozen at -80°C.

2.9.7 Plasmid Purification

The pCR®2.1-TOPO and the pARAJS2 vectors were extracted from *E. coli* Top10F using a commercial kit (QIAprep Miniprep Kit, QIAgen) and the protocol followed was provided by the manufacturer.

2.9.8 Digestion with restriction enzymes

To separate the cloned gen from the pCR®2.1-TOPO plasmid, the vector must be incubated with restriction enzymes. This kind of enzymes cut the DNA in concrete places, called restriction sites, and set the fragment free.

The restriction enzymes used in this thesis are shown in Fig. 2-10 and Fig. 2-11.

This procedure takes two hours at 37 °C, which is the optimal temperature for the enzymes to be functional. The size of the fragment was verified with an agarose gel.

Once the insert and the plasmid are prepared, the ligation can start.

2.9.9 Ligation

The *p13* insert was included in the pARAJS2 expression vector after its amplification in the pCR®2.1-TOPO vector. This vector includes a promoter before the gen to make the protein production possible.

The pARAJS2 vector was mixed with the insert in a 1:3 rate. The ligase T4 (Fermentas) and the T4 buffer were added following the manufacturer instructions. In this case 10 µl from the vector and 30 µl from the insert were mixed with 2 µl from the T4 buffer and 1 µl from the T4 polymerase. The final mixture was incubated overnight at 16 °C.

2.9.10 Transformation

In this thesis different types of cell transformations were used.

To transform *E. coli* Top 10F´ a heat shock was used. The competent cells were taken from the -80 °C and placed in ice for 15 minutes. The DNA plasmid was added afterwards on top and the mixture was shuttled very carefully. The cells were placed at 42 °C for 30 seconds and then again in ice for 2 minutes. After that time, 450 µl SOC medium was added and the cells were placed at 37 °C for one hour.

Electroporation was used to transform *E. coli* Omp8 Rosetta cells. The cells were placed in an electric field for 5 milliseconds in presence of the DNA plasmid. Then, 450 µl SOC medium were added to the transformants and they were placed in a shaker for one hour at 37 °C.

Agrobacterium competent cells were obtained and transformed in the laboratory following the Höfgen and Willmitzer protocol [81] with some modifications:

Preparation of *Agrobacterium* competent cells:

- 200 ml of LB medium were inoculated with 1 ml *A. tumefaciens* overnight culture and placed at 28 °C under vigorous shaking.
- The cells were cultivated until they reached the Log phase (OD_{550} 0.5-0.8).
- The cells were spun down at 3000 g during 10 minutes at room temperature.
- The pellet was washed with 1x TE buffer.
- The cells were resuspended in 10% of the initial LB medium volume and divided into Eppendorf tubes in 250-500 µl aliquots.
- The cells were frozen in liquid nitrogen and then stored at -80 °C.

Cell transformation:

- *Agrobacterium* competent cells (250 µl) were thaw in ice and the DNA plasmid was added (10 µl of DNA plasmid extracted from *E. coli*).
- The mixture was kept 5 minutes in ice and then 5 minutes more in liquid nitrogen.
- The sample was incubated 5 minutes more in water at 37 °C.
- 1 ml of LB medium was added to the tube and mixed in a rocking platform shaker during 2 hours at room temperature.
- The cells were spun down and inoculated in LB plates supplemented with kanamycin (pICH31160 vector confers kanamycin resistance).
- The plates were incubated 2 days at 28 °C.
- Some colonies were again inoculated in a new plate and incubated during 2 days at 28 °C.
- LB liquid medium cultures were set. The presence of the plasmid plus insert was checked using PCR.
- From the positive cases, type cultures were set.

2.11 Expression in *Escherichia coli*

The different steps followed to express and purify P13 in *Escherichia* are represented in the diagram of Fig. 2-12. The efficiency of P13 expression, cell fractionation and Ni Sepharose purification was tested using SDS-Page and WB.

2.11.1 Expression outline in *E. coli*

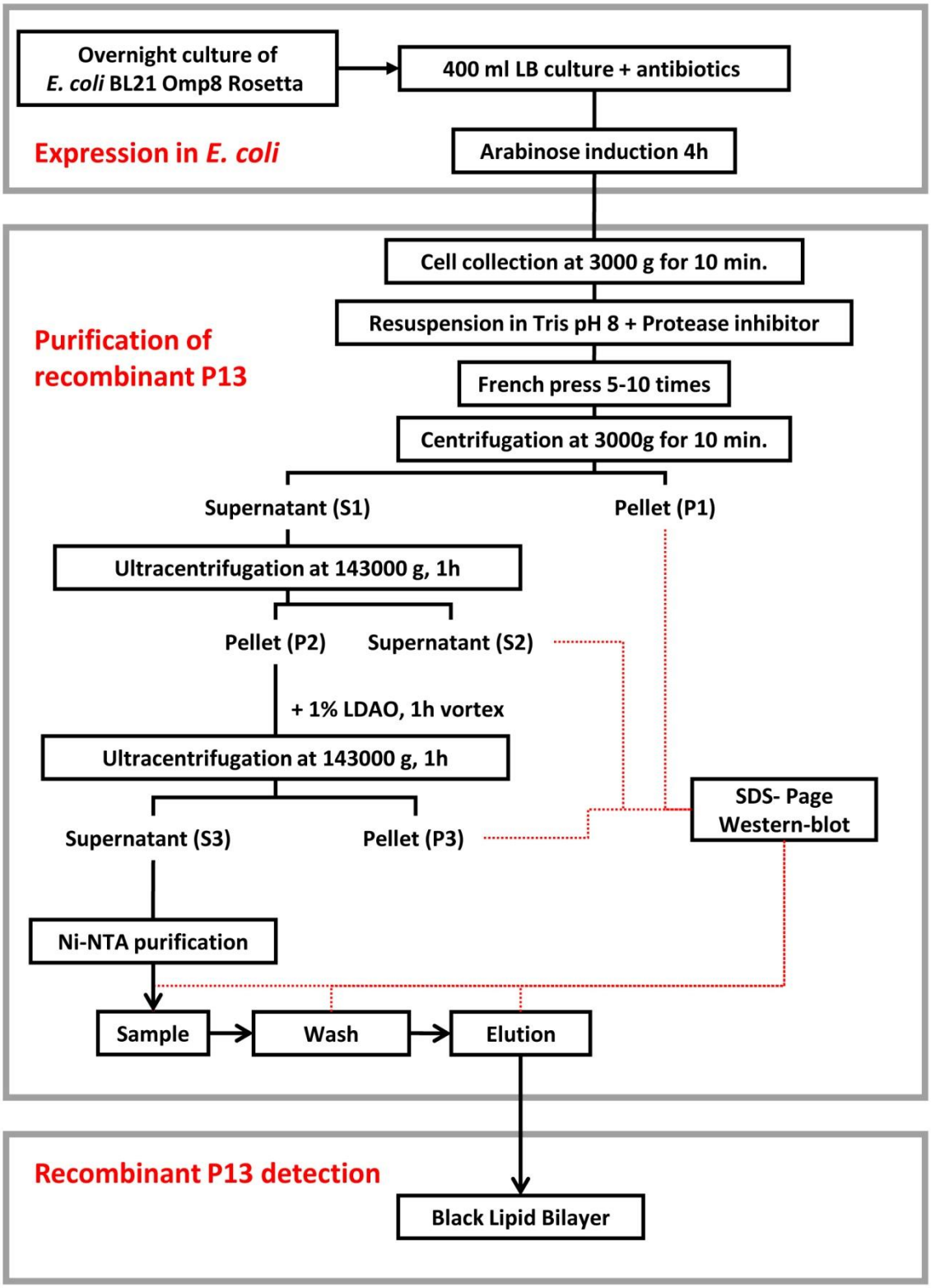

Fig. 2-12: Expression and purification of P13 in *E. coli*.

2.11.2 Protein induction

A day before expressing the desired protein, overnight cultures were set in 10 ml LB medium and incubated in a shaker at 37 °C. Also, 400 ml LB medium Erlenmeyer flasks were prepared to be used the next day. So many flasks were prepared as clones to be induced plus one to grow a negative control.

The next day, the optical density of the overnight cultures was checked. The volume of this culture needed to be added to the 400ml flask to have an initial optical density of 0.05 was calculated. This procedure enabled the cultures to grow at the same rate. The proper antibiotic must be added to the medium before adding the bacteria. Incubation took place at 37 °C with vigorous shaking.

The cultures were induced when they reached an optical density between 0.4 and 0.8. First, the cultures were placed 30 minutes at room temperature and then the arabinose was added to a 0.02% final concentration. After the induction with arabinose the flasks were placed in a room at 16 °C with vigorous shaking.

The cultures were centrifuged after 4 hours at 3000 g for 15 minutes. The supernatant was discarded and the pellets were frozen until the purification process began. Purification processes were required due to the big amount of other proteins and compounds produced by *E. coli*.

2.11.3 Protein extraction in *Escherichia coli*.

The cells were centrifuged down after inducing the expression of the recombinant protein. The pellet was resuspended in 10 ml 10 mM Tris pH 7.5. 100 µl of a protease inhibitor (Protease Inhibitor Cocktail Set II, Calbiochem) was immediately added after resuspension.

The cells were disrupted using a French Press. The sample was loaded 5 to 10 times in the piston and then forced at high pressure through a narrow valve.

The sample was centrifuged at 3000 g for 5 min at 4 °C to separate the proteins and membranes from the cell debris. The supernatant was ultracentrifuged in a Beckmann 90 Ti rotor at 143000 g and 4 °C during 1 hour. The ultracentrifuge tubes were tared with a 0.001 g maximal error. The cytoplasmic proteins stay in the supernatant and the pellet is formed by the membranes and its proteins. The supernatant was dismissed.

The pellet was resuspended using 10 mM Tris pH 7.5 plus 1% LDAO. The detergent makes the membrane proteins soluble and with a second ultracentrifugation they were separated from the rest of the membrane which formed the pellet. The supernatant containing the membrane proteins and the recombinant porin was keep at -20 °C until further purification.

2.12 Expression in *Nicotiana benthamiana*

2.12.1 *Agrobacterium* infiltration and virus expression

The expression in the tobacco plant is an expression system based in the infection with viral vectors that once inside the cell are replicated and infect the adjacent cells. The vector used in this thesis was developed from the potato virus X. The vector is first delivered into the tobacco cells by *A. tumefaciens* and confers to this bacterium a selective resistance against kanamycin.

The transformed *A. tumefaciens* strain containing the gen of interest were cultivated overnight in presence of kanamycin. To infiltrate the different strains two methods were used:

A syringe without needle was filled with the transformed strain and pressed against the inferior leaflet of the leaves where the stomata are. Carefully, the solution was injected to the leaf interior. A darker zone could be observed as the solution spread inside the leaf.

The second way to infiltrate the tobacco plants required less time and improved the infiltration. The *Agrobacterium* transformants were diluted in a big glass beaker and the plant was immersed in it upside down. Plant and beaker were introduced in a vacuum chamber. The air in the chamber was emptied establishing a negative pressure for a few seconds. Then the valve was opened letting the air to go back inside the chamber and establishing a positive pressure forcing the *Agrobacterium* solution into the plant through the stomata.

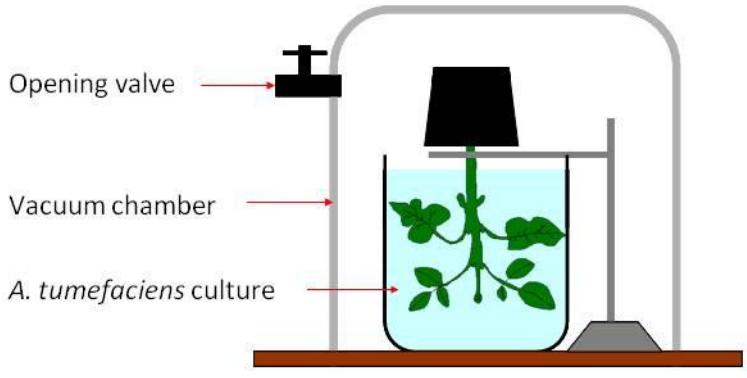

Fig. 2-13: Inoculation of *Agrobacterium* in tobacco plants using a vacuum chamber. When the atmospheric pressure is reestablished inside the chamber, the *Agrobacterium* solution is forced inside the leaves.

The recombinant protein expression worked better in younger leafs where larger amounts of recombinant protein were produced. The optimal expression time for P13 was between 8 and 10 days after infiltration. After that time, the leaves were collected and frozen at -80 °C until the extraction procedure started.

2.12.2 Protein extraction in *Nicotiana benthamiana*

Ten days after infiltration the recombinant protein expression was at its higher level. A positive control was used to confirm this expression. The green fluorescent protein gene was cloned in the pICH31160 vector. In this way, the plants infected with this control will fluorescent under black light, making possible to quantify the expression.

After checking the expression, the leaves were treated as following:

- The collected leaves were crashed to powder using liquid nitrogen and a mortar.
- 1 ml extraction buffer (see buffer section 7.5) was added to 500 mg plant powder. The mixture was let in a shaker overnight at 4 °C.
- The suspension was centrifuged in a table centrifuge at maximal speed and the supernatant was kept.
- The supernatant was filtered using a syringe connected to a 0.2 µl pore-diameter cellulose acetate filter.
- 200 µl of the sample were precipitated using the Wessel-Flügge protocol to do SDS-PAGE and WB against the recombinant protein.

2. 13 His-tag purification with Ni-NTA resins

One of the reasons to clone the desired gen in the pARAJS2 vector was to have a His-tag fragment in front of the *p13* gen.

Ni-NTA resins have a high affinity for histidine amino acids. While other proteins do not bind to the matrix, proteins with a His-tag remain stuck to the resin. Elution of those proteins will occur with increasing amounts of imidazole in the elution buffer.

To do this purification a commercial kit was used (Ni-NTA spin kit, QIAgen). The protocol used is a variant of the original supplied by the commercial brand, to maintain the native state of the protein:

- The Ni-NTA column was loaded with 600 µl of the sample and centrifuged 2 min. at 700 g. The process was repeated until the whole sample volume was filtered. The flow-through was saved to check binding efficiency.
- the column was washed twice with 600 µl of washing buffer and centrifuged 2 min. at 700 g. The flow-through was saved to check the binding efficiency.
- The His-tag protein was eluted twice with 200 µl of elution buffer. Centrifuge 2 min. at 700 g. Collect the flow-through where the recombinant protein is.

The sample and buffer that pass through the column in the first two steps were checked together with the elution sample using SDS-Page and WB. That way, the His-tag binding efficiency and the purity of the elution could be determined.

Ni Sepharose™ High Performance beads (GE Healthcare) were also used for the His-tag purification. The extraction buffer containing the plant proteins were cultivated in presence of the Ni Sepharose beads in a shaker overnight. The beads were recovered spinning down the samples at 700 g for 2 minutes. Several washing steps were carried out with increasing imidazole concentrations (up to 100 mM for *E. coli* samples and 70 mM for tobacco plant samples). The recombinant protein was eluted with 500 mM concentrations for samples produced in *E. coli* and with 80 mM for samples produced in *Nicotiana*.

During the process of purification with the Ni beads the supernatants were saved. The binding efficiency was tested with SDS-Page and WB.

Biophysical characterization of P66 in Lyme disease and relapsing fever species

Up to date, four porins have been described in the genus *Borrelia*. Three of them, P66, P13 and Oms28 have been found in the Lyme disease (LD) causing *B. burgdorferi*, the other one, Oms38, in species causing relapsing fever (RF).

P13 is a small protein of 13 kDa which monomer is too small to form a β-barrel like many porins do. Its structure and function in the biology of *Borrelia* is not very well understood. The function of Oms28 as porin has recently been called into question and Oms38 location in the outer membrane has still to be proved. On the other hand, P66 is the best studied porin in *Borrelia*, with a double function as porin and adhesin. It has an immunologic potential that can be used to develop new strategies for diagnose and to treat infections by *Borrelia*.

However, P66 has mainly been studied in *B. burgdorferi*, and little or nothing is known about its function in other species. To gain some knowledge about other *Borrelia* species, its pore forming properties were studied in six species, three belonging to the Lyme disease (LD) causing species (*B. burgdorferi*, *B. afzelii* and *B. garinii*) and three that cause relapsing fever (RF) (*B. duttonii*, *B. recurrentis* and *B. hermsii*).

B. burgdorferi, *B. afzelii* and *B. garinii* were chosen because they are the world distribution etiologic agent of the Lyme disease. *B. duttonii* and *B. hermsii* represent the main relapsing fever causing agents transmitted by ticks and *B. recurrentis* is the agent of the louse-borne relapsing fever.

3.1 Results

3.1.1 LD and RF P66 gene sequence comparison

The genome sequencing of many bacteria and its recent publication has made possible to obtain many *Borrelia* P66 gene sequences. The P66 sequences of the six chosen species (*B. burgdorferi* B31, *B. afzelii* PKo, *B. garinii* PBi, *B. duttonii* Ly, *B. recurrentis* A1 and *B. hermsii* HS1) were aligned (Fig. 3-1). The alignment showed highly conserved domains in all the sequences with an overall identity of 41%. Comparing only the LD sequences the homology increased to 90%. The same was done with the RF sequences and the homology reached only 67%. This fact is remarkable because *B. duttonii* and the *B. recurrentis* have a 98% sequence identity, pointing out the divergence of *B. hermsii* during evolution.

[Next Page] Fig. 3-1: Comparison of P66 sequences from three Lyme disease species (*B. burgdorferi*, *B. afzelii* and *B. garinii*) and three relapsing fever species (*B. duttonii*, *B. recurrentis* and *B. hermsii*). Conserved amino acids in all the species are indicated in green and amino acids conserved at least in three species are indicated in yellow. The red squares indicate predicted membrane-spanning β-sheet domains.

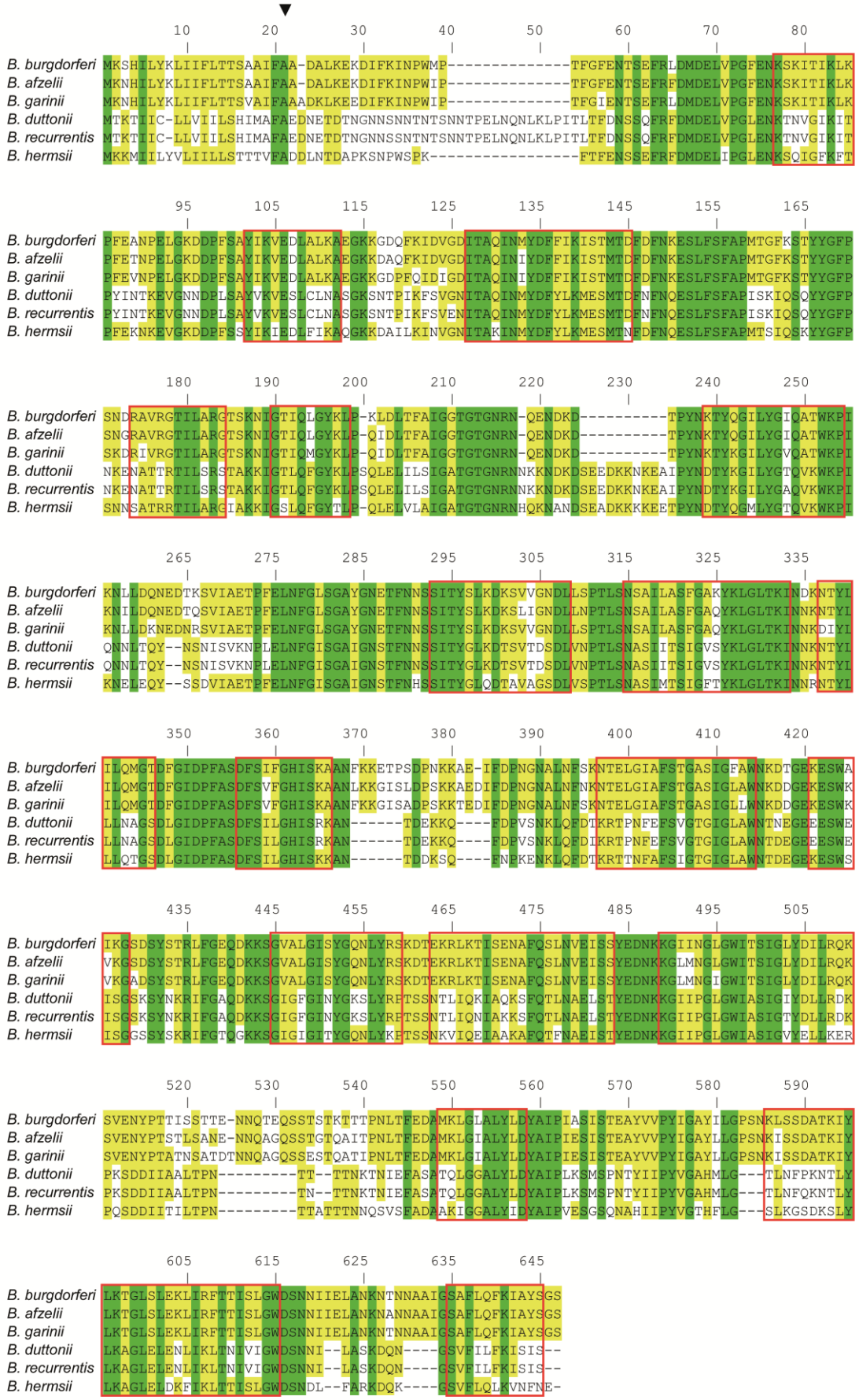
B. burgdorferi
B. afzelii
B. garinii
B. duttonii
B. recurrentis
B. hermsii

3.1.2 P66 secondary structure prediction

Computer programs were used to predict the secondary structure of P66. These predictions reflected a possible β-barrel composed of 20 to 22 transmembrane β-sheets in all the sequences. In Fig. 3-1 amino acids shared by all the sequences are marked in green while amino acids present in at least three sequences are marked in yellow. Predicted β-sheet regions are framed in red. All sequences posses a 21 amino acid signal sequence required for the transport trough the inner membrane in agreement with a location of P66 in the outer membrane.

3.1.3 Purification of the LD and RF P66 homologues

P66 was purified from B-fractions which contained the outer membrane proteins using a FPLC system with a MonoQ column. P66 and homologues eluted when the NaCl gradient reached 190 mM. In those cases where the P66 fraction contained other proteins, the process was repeated under the same conditions obtaining pure P66. To check P66 purity in the samples 12% SDS-Page were used. P66 and homologues appeared in a 66 KDa band and no contaminants were observed staining the gels with silver nitrate (Fig. 3-2). P66 and homologues were additionally tested in WB using an antibody against *B. burgdorferi* P66 (Fig. 3-2). While P66 and the LD homologues reacted positively against the antibody, only the homologue from *B. hermsii* showed a positive signal among the RF species. The WBs were repeated for *B. duttonii* and *B. recurrentis* using a higher concentration of the purified 66 KDa protein and increasing the P66 antibody concentration but none of them showed a positive signal. Finally the whole outer membrane protein fraction was tested to reject the idea of having isolated another 66 KDa protein. Again no positive signal was visible.

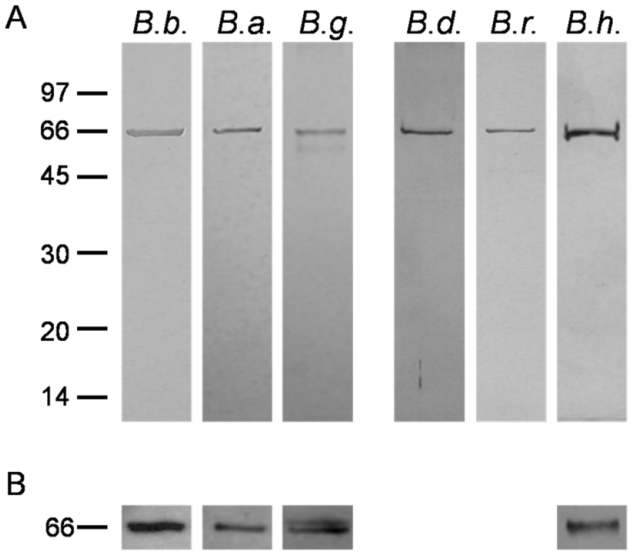

Fig. 3-2: SDS-Page (A) and WB against P66 (B) from different LD and RF *Borrelia* species. *B. burgdorferi* (B.b), *B. afzelii* (B.a) and *B. garinii* (B.g) belong to the Lyme disease species while *B. duttonii* (B.d), *B. recurrentis* (B.r) and *B. hermsii* (B.h) belong to the relapsing fever group. No WB signal against P66 was observed for *B. duttonii* and *B. recurrentis* (data not shown).

3.1.4 Single channel measurements of P66 and homologues

The pore forming activity of P66 from *B. burgdorferi* was previously shown with a surprising high single channel conductance of 9.6 nS in 1 M KCl [52]. To test if the P66 homologues had a similar pore forming activity the BLB assay was used. P66 was again tested to have comparable conditions with those used for the rest of the homologues. The purified proteins were added to a 1 M KCl solution and the permeabilization of the membrane was studied.

All the homologues excluding the one from *B. hermsii* exhibited step-like increases of the membrane conductance as the proteins inserted in the artificial membrane (Fig. 3-3).

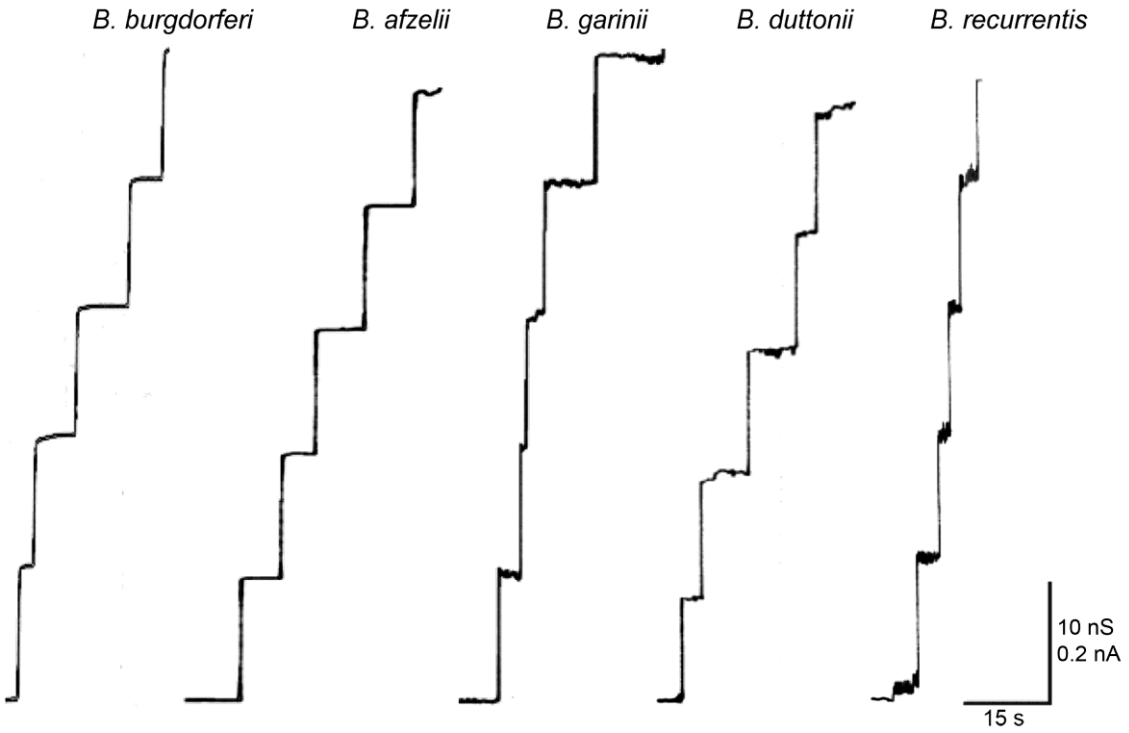

Fig. 3-3: Step-like increases of the membrane conductance as P66 and homologues inserted in the membrane. The salt solution in which the Diph-PC membranes were contained was 1M KCl and the temperature was 20 ˚C throughout.

The conductance range of the pores inserted in the membrane went from 7 to 13 nS in 1 M KCl (Fig. 3-4). The characteristic conductance for each protein was considered to be the most frequent value, differing here in some cases one from each other. *B. burgdorferi* and *B. garinii* had a typical single channel conductance of 11 nS while *B. afzelii* and *B. duttonii* had a 9 nS

conductance. *B. recurrentis* showed a similar conductance to *B. duttonii* of around 9.5 nS consistent with their high amino acid sequence homology.

Curiously, the homologue isolated from *B. hermsii* did not showed any pore forming activity when tested with the BLB assay. To make sure that the sample was not damaged a new outer membrane extraction was done. In addition, a different strain was used to reject a possible DNA mutation responsible for the P66 inactivation. Finally, an alternative extraction protocol described before was used [82]. None of these actions resulted in the observation of a pore forming activity from the *B. hermsii* P66 homologue.

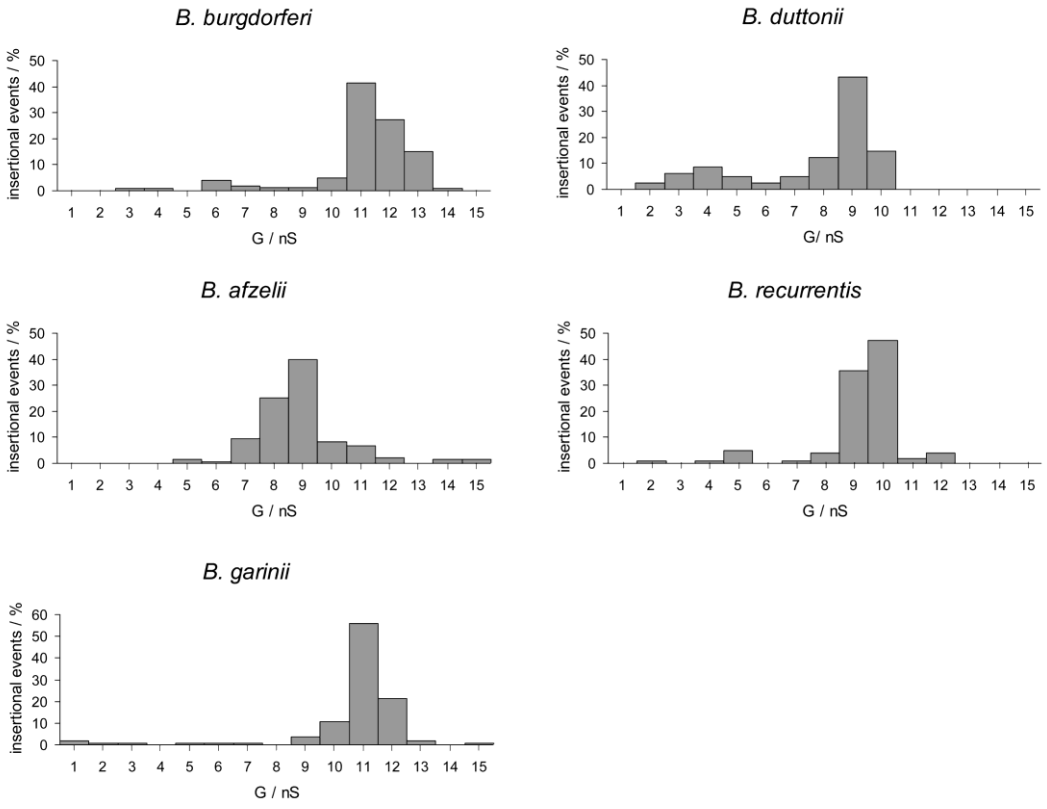

Fig. 3-4: Pore forming activity of purified P66 and homologues from LD and RF species. The histograms were created with at least 100 insertions for each sample. 1% DiphPC membranes in 1 M KCl were used for the experiments at room temperature.

In some cases, like shown in the histogram of *B. duttonii*, another group of pores with a conductance between 4 and 6 nS was observed. In principle, these pores do not correspond with the P66 pore conductance. As addressed later in the discussion and in the "*Analysis of*

outer membrane complexes using BN-Page" project in this thesis, these pores are believed to be related with P66.

The P66 proteins were tested in different KCl concentrations and in different electrolytes to gain some insight into the ion transport through them. The conductance of P66 and homologues was a linear function of the KCl concentration. This correlation is typical for diffusion porins which have no binding sites for anions or cations. Measurements with lithium chloride and potassium acetate, where anions and cations differ in size, showed a similar decrease in the single channel conductance. These results indicate that P66 channels have no apparent selectivity for ions or cations (Table 3-1).

		B. b.	B. a.	B. g.	B. d.	B. r.	B. h.
Electrolyte	Concentration (*M*) [γ]	*G* (*nS*)					
KCl	0.1 [0.77]	1.3	1.3	1.5	0.8	1.25	n.a.
	0.3 [0.68]	3.5	3.5	3.5	2.25	2.75	n.a.
	1 [0.6]	11.0	9.0	11.0	9.0	9.5	n.a.
	3 [0.56]	30	33	35	20	25	n.a.
LiCl	1 [0.77]	7.3	7.0	8.0	5.0	6.0	n.a.
KCH_3COO (pH 7)	1 [0.78]	6.7	6.5	6.5	4.0	5.0	n.a.

Table 3-1: Conductance of P66 and homologues in different concentrations of KCl and in different salt solutions. The ion activity coefficients are indicated in brackets [γ] next to the molarity (M). Samples from *B. hermsii* were not active in BLB (n.a.).

3.1.5 Selectivity measurements of P66 and homologues

Zero-current membrane potential measurements were carried out to define the ion selectivity of P66 and homologues more precisely. Membranes with more than hundred inserted P66 pores had been used to do the measurements. Five-fold gradients of potassium chloride,

lithium chloride and potassium acetate were established across the membranes. The results for KCl showed a small asymmetric negative potential at the diluted side of the membranes that reflects very light anion selectivity. When the KCl salt solution was replaced for LiCl the zero-current potential was more negative at the diluted side. When KCH_3COO was used a slightly positive asymmetry potential took place at the diluted side. All of these results support the idea of a diffusion channel without selectivity for anions or cations.

The permeability ratios shown in Table 3-2 for the different salt solutions were calculated using Eq. 5 indicated in the methods section (2.7.2).

	B. b.	B. a.	B. g.	B. d.	B. r.
Electrolyte	Permeability ratios P_c/P_a (V_m [mV])				
KCl	0.8 (-3.8)	1.0 (+0.6)	0.8 (-3.5)	0.9 (-1.8)	0.9 (-1.6)
LiCl	0.5 (-11.1)	0.7 (-6.1)	0.5 (-11.3)	0.6 (-9.8)	0.8 (-2.8)
KCH_3COO (pH 7)	1.5 (+6.5)	1.2 (+3.2)	1.4 (+5.6)	1.1 (+1.7)	1.2 (+3.5)

Table 3-2: Zero-current membrane potentials V_m (in brackets) and permeability ratios P_c/P_a of DiphPC membranes in presence of P66 and homologues measured for five-fold concentration gradients of three different electrolytes.

3.1.6 Voltage dependence measurements of P66 and homologues

As published elsewhere [52], P66 from *B. burgdorferi* possess a symmetric voltage dependency. In this previous study, a membrane saturated with P66 channels started to exhibit a decrease of the overall membrane conductance at voltages of about ±30 mV. The conductance of this membrane was reduced to half at ±70 mV and to 10% at ±100 mV or higher. To study if the homologues reacted in a similar way, voltage dependency measurements were performed. P66 from *B. burgdorferi* was again tested to have the same conditions for all proteins.

The pore closure was calculated measuring the conductance of the membrane immediately after applying a voltage and again after some time of stabilization where no further decrease in the membrane conductance was observed. In the first measurement the channels are

considered to be totally open. If the channel shows voltage dependency it will show a determined closure that will reach a state of equilibrium some time after. The conductance at this point is considered to be final conductance. Comparing initial and final conductance, the percentage of pore closure can be calculated for each applied voltage. In Fig. 3.5 the pore closure at each voltage is shown for P66 and homologues.

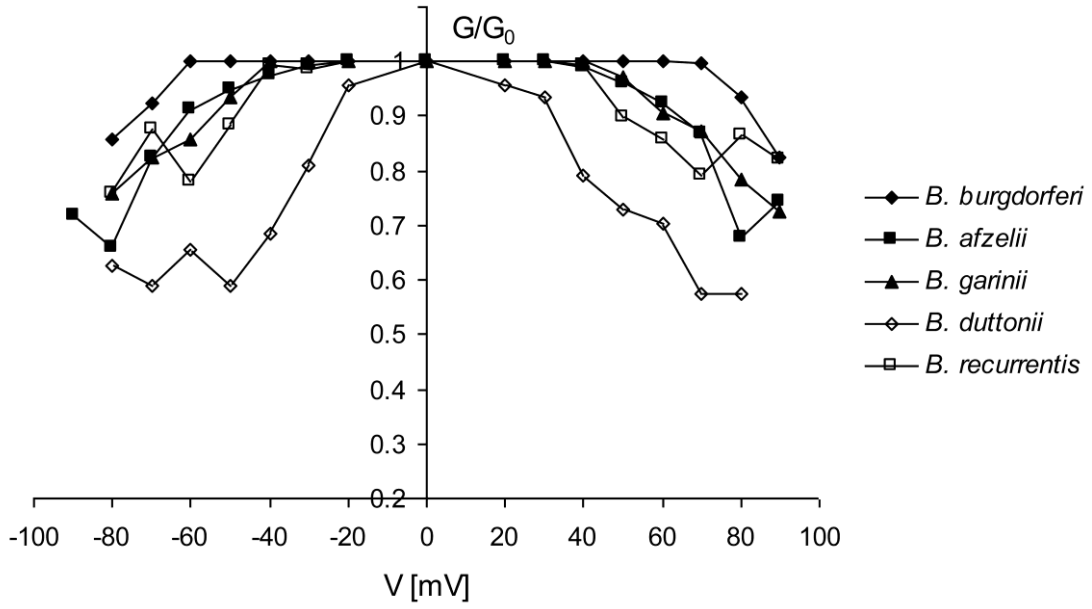

Fig. 3-5: Voltage dependency for P66 and its homologues in other species. After application of voltage and stabilization of the channels, the conductance of the membrane was measured (G) and divided by the initial conductance measured immediately after turning on the voltage (G_o). The salt solution used was 1 M KCl at room temperature. The standard deviations did not exceed 0.03.

Some of the homologues reacted strongly to the applied voltage like *B. duttonii*, showing some closure starting at ±20 mV. Many of them, like the homologues from *B. afzelii*, *B. garinii* and *B. recurrentis* started showing channel closure at voltages of around ±50 mV. The P66 protein from *B. burgdorferi* was the pore forming protein that showed a higher resistance against voltage-closure (70 mV). This result is in contrast with the previous study where the closure of P66 from *B. burgdorferi* started at ±30 mV. In addition, the overall closure of P66 is clearly smaller than the previous published reaching only a reduction of 20% at 90 mV.

3.2 Discussion

3.2.1 P66 homologues are present in LD and RF species

Up to date, the biology of the genus *Borrelia* was based on studies carried out in *B. burgdorferi*. *Borrelia* includes many species with different vectors and life cycles. To analyze if the different way of life could be related with differences in composition or function of the surface proteins, studies using other species of this genus are needed. Porins are among the outer membrane proteins and they have an important role in the exchange of different substances with the environment. One of the best known porins in *Borrelia* is P66, but the vast majority of the experiments dealing with this porin have been done in *B. burgdorferi*.

In the present work six species of *Borrelia* were compared. Three of them caused the Lyme disease and are responsible for the global distribution of the disease. The other three were the main relapsing fever causative agents.

The recent publication of some genomes in the net during the realization of this work made allowed doing a gene alignment for these six species. The P66 gene was found in all of them, showing a high conservation among homologues. The three species producing Lyme disease seem to be closer in the evolution sharing a 90% sequence homology while the RF species studied here differ to a larger extend. *B. duttonii* and *B. recurrentis* seem to be species extremely close related while *B. hermsii* had gene regions that are not shared with the other two RF species.

In SDS gels all the homologues purified appeared to have a similar molecular weight of around 66 KDa and seem to elute at similar salt gradients. The antibodies for the immunoassays were obtained from rabbits immunized with P66 from *B. burgdorferi.* Differences in the amino acid chain from *B. duttonii* and *B. recurrentis* could explain the absence of signal in the WB when using these antibodies. Nevertheless the high conserved regions between sequences and a single channel conductance in the same atypical range of P66 lead to the assumption that those two proteins are homologues of P66. In contrast, the homologue from *B. hermsii* reacted with the P66 antibody. Conserved amino acids between *B. hermsii* shared with LD but not with the RF species where the P66 antibody may bind could explain this fact.

3.1.2 Biophysical characterization of P66 and homologues

Corresponding with the homology of the proteins, almost all of them showed membrane channel formation. The pores had a high single channel conductance in a range between 9 and 11 nS.

Only the homologue from *B. hermsii* lacks this channel formation ability after purification. Disruption of the protein during the purification was rejected testing the whole B-fraction in BLB assays. Using the whole outer membrane protein content displayed no single channel activity above 2 nS. One of the reasons for this lack of activity could be a bigger sensibility to detergents which are required to extract the outer membrane or the loss of the porin function due to amino acids mutations during the evolution process. In any case, further experiments are required to clarify why P66 shows no pore forming activity in this species. The results presented in this thesis are contrary to a previous study where outer membrane protein preparations were tested in artificial membranes showing a conductance of 7.2 nS among others [82]. No relation was shown in this study between this conductance and a possible P66 homologue. In the present work whenever B-fractions from *B. hermsii* were tested such a single channel activity was not observed.

P66 and the other four homologues showed similar biophysical characteristics. They seem to be water filled diffusion channels with no selectivity for anions or cations. All of them showed voltage dependency at voltages lower than 100 mV. Therefore these proteins seem to have a similar behavior and probably a similar function in all the species.

P66 channel diameter estimation using non-electrolytes

P66 is a protein situated in the outer membrane of *B. burgdorferi* [83] with pore forming properties [52]. P66 is also present in other Lyme disease (LD) species and relapsing fever (RF) species with a similar porin activity [51]. It has an unusual high single conductance of 11 nS [51], which was previously thought to be indicative of a big diameter channel. Previous theoretical estimations of the P66 channel diameter lead to an estimate of 2.6 nm [52], which it is a rather large diameter compared to other pore forming outer membrane proteins [84]. If this would be the case, these big channels would allow a free molecule exchange between the environment and the periplasmic space, a fact that could impair the defense function of the outer membrane. A better understanding of the structure of the P66 porin could help to understand why the outer membrane of certain *Borrelia* strains contain small pores, such as Oms38 [62], next to big channels like P66.

Therefore, an applied method using non-electrolytes (NEs) with known hydrodynamic radii [78] was used to calculate the real diameter of P66. This method was used before successfully [78, 85-93] and should provide a more accurate estimate of the P66 channel diameter using a biophysical approach.

4.1 Results

4.1.1 P66 pore diameter estimation

The estimation of a channel diameter using NEs is a method based on the fact that small non-electrolytes that penetrate in a channel will reduce its conductance due to an increase in the solution viscosity that will make the ion flux more difficult. That way, the conductance of a pore is measured in a salt solution containing each time a different NE with increasing

hydrodynamic radius. As the diameter of the NE is increased, a point will be reached where it will not be able to enter the channel. From that point on, NEs with a larger radius will not enter the channel and the channel interior will be free of NEs. The conductance of the pore will be in those cases equal to the original measured in the salt solution. It is possible then to correlate the hydrodynamic radius of the smallest NE that do not enter the pore with the diameter of the pore.

P66 from *B. burgdorferi* was measured in a salt solution (1 M KCl) each time with a different NE (20%). The P66 conductance for the independent measurements is summarized in the next table (Table 4-1). The molecular mass and hydrodynamic radius of the NEs and the conductance of the solutions are also indicated in the table.

Non-electrolyte	Mr (g/mol)	*r* (*nm*)	*G* (*nS*)	X (mS cm^{-1})
None	-	-	11.0	110.3
Ethylene glycol	62	0.26	6.5	57.2
Glycerol	92	0.31	5.5	49.1
Arabinose	150	0.34	7.0	63.7
Sorbitol	182	0.39	7.5	57.8
Maltose	360	0.50	8.0	73.8
PEG 300	300	0.60	7.5	45.5
PEG 400	400	0.70	0.9	46.4
PEG 600	600	0.80	0.9	54.1
PEG 1000	1000	0.94	12.0	49.5
PEG 3000	3000	1.44	10.5	48.9
PEG 6000	6000	2.50	10.5	50.5

Table 4-1: Non-electrolytes used to determine the P66 diameter. The molecular weight (*Mr*) and the radius (*r*) are indicated together with the conductance of P66 (*G*) and the conductivity of the solution (X) in presence of each NE.

Examples of the measurements performed in the BLB assay in presence of different NEs are shown in the next figure (Fig. 4-2). In presence of maltose, the conductance of P66 was reduced to some extent (to approximately 70%). This decrease is in relation with the decrease

of the salt solution conductivity in presence of the NE. With PEG 400 and PEG 600 an unexpected big reduction in the P66 conductance and increase of noise was observed. This effect cannot be explained with the reduction of the salt solution conductivity and is later further discussed. P66 shows no conductance reduction in presence of PEG 1000 showing that this NE had no access to the channel interior.

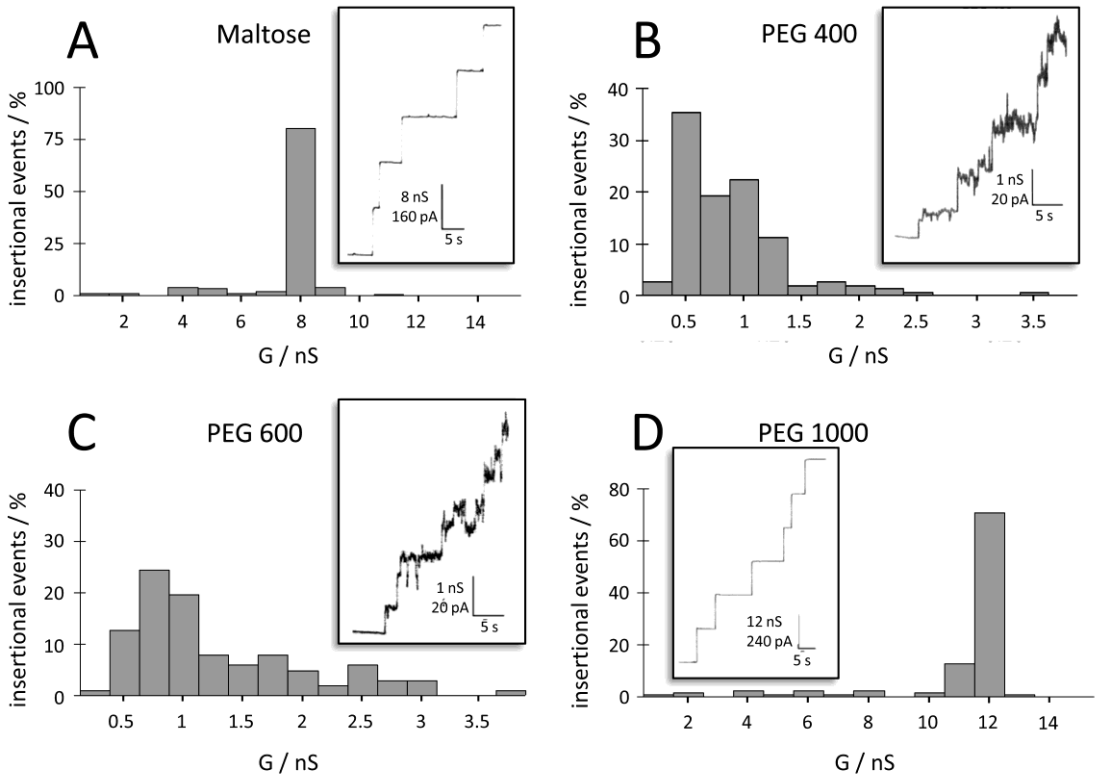

Fig 4-2: Four examples of BLB measurements of P66 in presence of different NEs. The histograms were done with at least hundred P66 individual insertions in presence of maltose (A), PEG 400 (B), PEG 600 (C) and PEG 1000 (D). Next to each histogram and example of P66 insertions in artificial membranes is shown.

As summarized in the Table 4-1, NEs with a hydrodynamic radius of 0.94 nm or bigger were not able to get inside the channel showing P66 no reduction in its conductance (around 11 nS). Those NEs were PEG 1000, PEG 3000 and PEG 6000. In contrast, NEs with a hydrodynamic radius of 0.8 nm or smaller got inside the channel showing P66 the corresponding conductance reduction. The NEs used were ethylene glycol, glycerol, arabinose, sorbitol, maltose, PEG 300, PEG 400 and PEG 600. These results are again clearly summarized in the next figure (Fig. 4-1).

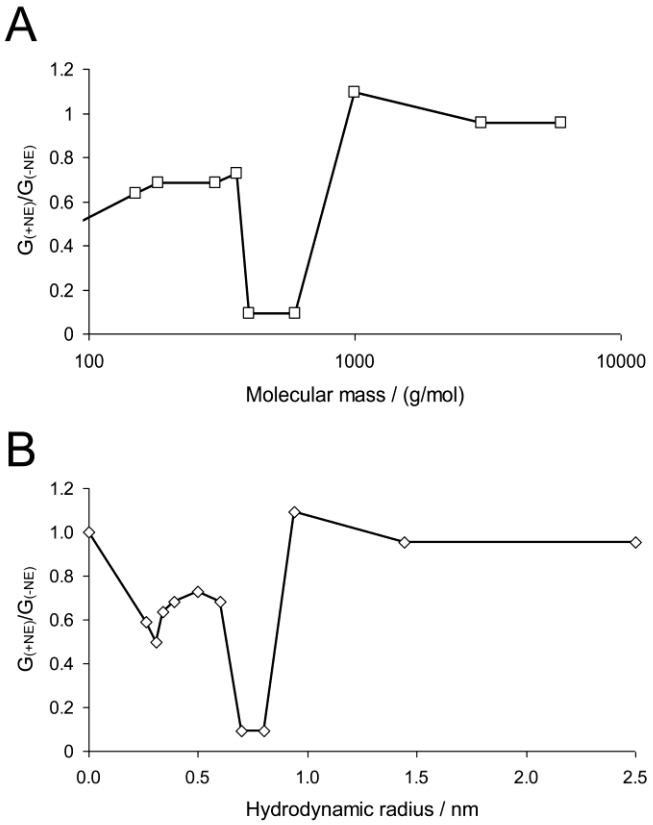

Fig. 4-1: Influx of NE with diferent molecular mass (A) and different hydrodinamic radius (B) in the P66 conductance. Each point in the plot represents the most frequent conductance for P66 in the presence of a determined NE.

The entrance radius of a pore forming protein is considered to be equal to the radius of the smallest NE that does not reduce its conductance. In the case of P66 this NE was PEG 1000, in which presence the P66 conductance was again around 11 nS. Therefore the P66 entrance radius is estimated to be 0.9 nS.

A pore forming protein could be considered as a perfect cylinder or what it is more likely to happen in the nature a cylinder with irregularities in the channel interior. In the case of a perfect cylinder, the NEs will either fill the channel completely when they are small enough to enter the channel or not at all if they are too big. But in the case of having an inner constriction inside the channel, another event is possible. NEs small enough to enter the channel but too big to pass all the way trough it will be present only in a fraction of the channel. To analyze the idea of a possible constriction inside the channel the filling concept was introduced. This concept and the formulas to calculate the channel filling (Eq. 8 and Eq. 9) are explained with more detail in the methods section 2.7.6. This concept establishes that the radius of a

constriction zone should be equal to the radius of the smallest NE that do not pass freely through the channel and fill it only partially.

In the measurements done using P66 from *B. burgdorferi*, NEs like ethylene glycol, glycerol and arabinose showed a channel filling close to 100%. NEs like sorbitol and PEG 300 filled the channel only partially. And NEs like PEG 1000, PEG 3000 and PEG 6000 didn´t fill the channel at all (*F%* values in Table 4-2). The smallest NE that did not fill the channel completely was sorbitol. Therefore the radius of the P66 constriction zone is considered to be equal to the sorbitol hydrodynamic radius, which is 0.39 nm.

Non-electrolyte	*r* (*nm*)	F	F%
Ethylene glycol	0.26	0.75	96.8
Glycerol	0.31	0.80	106.7
Arabinose	0.34	0.78	100.6
Sorbitol	0.39	0.51	65.8
Maltose	0.50	0.76	98.1
PEG 300	0.60	0.33	42.6
PEG 400	0.70	nl.	nl.
PEG 600	0.80	nl.	nl.
PEG 1000	0.94	-0.07	9.0
PEG 3000	1.44	0.04	5.2
PEG 6000	2.50	0.04	5.2

Table 4-2: P66 channel filling with different NEs. The hydrodynamic radius (*r*) of the different non-electrolytes are shown together with the P66 channel filling (*F*) and the channel filling expressed in percentage (*F%*). The formulas used to calculate *F* and *F%* are indicated in the methods section 2.7.6.

The presence of PEG 400 and PEG 600 in the salt solution resulted in an unexpected reduction of P66 conductance close to 1 nS with a lot of noise and a contradictory channel filling higher than 100%. This decrease in conductance, which should be between 45 and 75 % of the original when using 1M KCl, is not in accordance with the reduction of the salt solution conductivity in presence of NEs.

The channel filling with maltose was close to 100%. However, smaller NEs like sorbitol do not fill the channel completely. To test if that effect was due to an interaction of the maltose with the channel interior, another NE with the same hydrodynamic radius (PEG 200) was tested. PEG 200 showed as well a reduced conductance of 6.5 nS with a channel filling of 64.1% which is in concordance with the rest of the measurements.

4.1.2 Interactions of NEs with the P66 channel.

To help understanding the interaction between maltose, PEG 400 and PEG 600 with this channel, multi-channel titration experiments with these and other NEs were performed. To do these experiments P66 was added to a 0.1 M KCL solution without NEs. When the pore forming activity reached a stationary phase with at least 100 pores inserted in the membrane a small amount of a NE was added.

The NEs selected were maltose, PEG 400, PEG 600, maltohexaose, fructose, glucose, sucrose and related carbohydrates. An effect could only be seen after addition of PEG 400, PEG 600 and maltohexaose. Those NEs caused a dose-dependent blockage of the channel conductance. The P66 conductance was blocked approximately 80 % after addition of 4.5 mM PEG 400 and PEG 600, and approximately 90 % after addition of 45 mM maltohexaose (Fig. 4-3). The blockage kinetics of PEG 400 and PEG 600 compared to maltohexaose were different. While the channel blockage after addition of maltohexaose was relatively fast, after addition of PEG 400 and PEG 600 it took between 10 and 30 minutes to reach a stationary phase. Titrations with other NEs like glucose and maltose did not lead to any blockage of the P66 channel conductance (results not shown).

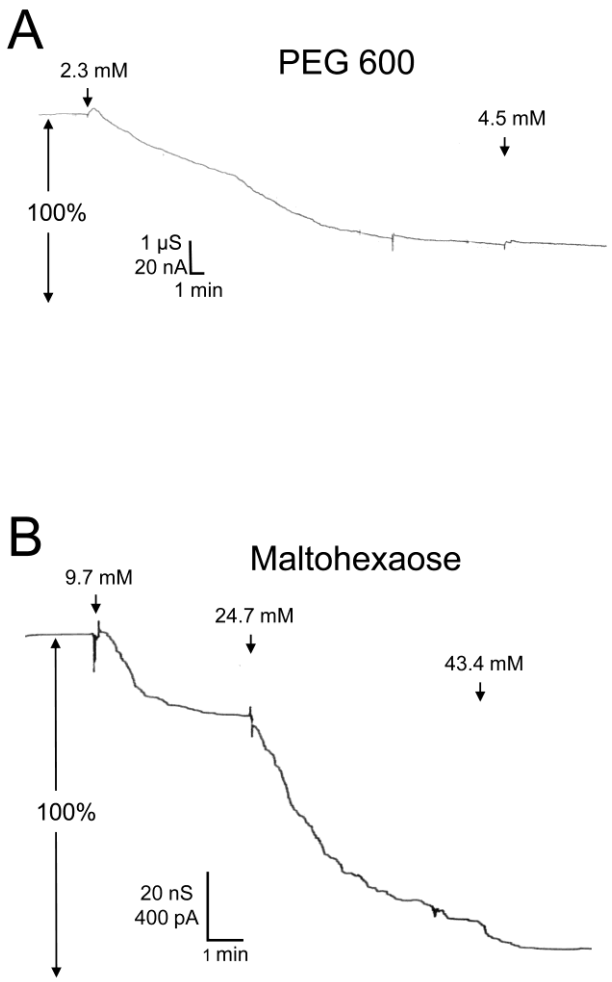

Fig. 4-3: Titrations of P66 with PEG 600 and maltohexaose. Membranes permeabilized with at least hundred P66 units were titrated adding PEG 600 and maltohexaose to a 0.1 M KCl solution. Additions of the NE are indicated with arrows together with the final concentration of the NE in the salt solution. Similar effects of those observed for PEG 600 were observed for PEG 400.

4.1.3 Effect of PEG 400 and PEG 600 on a P66 single channel

The blockage pattern of a single P66 unit could give important information about the organization of this porin. For example, trimeric porins like LamB form three independent channels, and its blockage with maltose occurs in three conductance decreasing steps. In the same way, blockage of one single P66 complex could give insight in its possible multi-channel organization.

In order to have just one single P66 unit inserted in the membrane, the sample was diluted to a great extend (1:10000) before adding a few microliters to the salt solution in the Teflon chamber. After getting the first insertion of a P66 channel in the membrane, the PEG 400 or PEG 600 was immediately added to the salt solution. Shortly after the addition the conductance through the membrane started to decrease. This decrease of conductance

happened in form of small steps down reducing the conductance. These steps are usually indicative of a protein complex where each step down represents a monomer being blocked. The P66 blockage occurred in approximately eight regular 1.5 nS steps (Fig. 4-4).

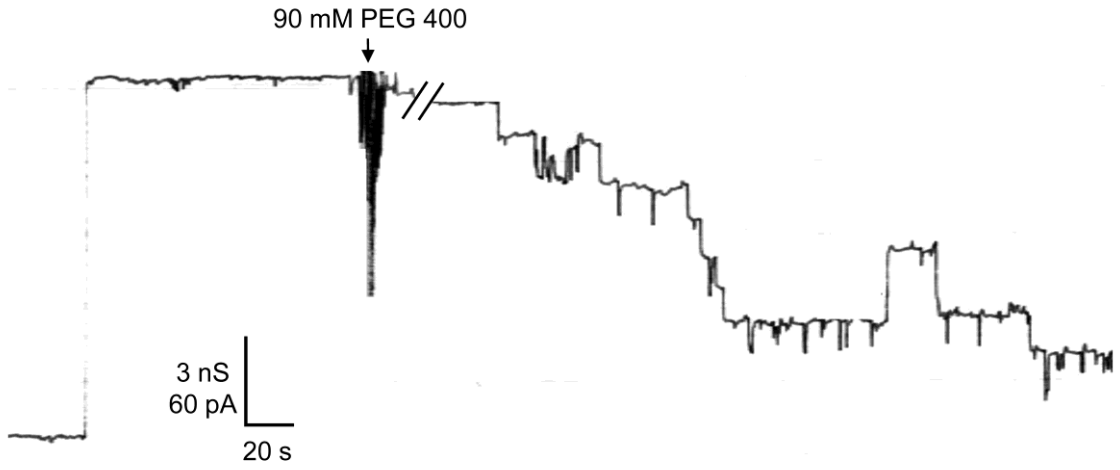

Fig. 4-4: Blockage of a single P66 unit with PEG 400. After insertion of a P66 pore in the membrane 90 mM PEG 400 was added to the salt solution (indicated by an arrow).

4.1.4 Current noise of P66 in presence of PEG 400, PEG 600 and Maltohexaose

To investigate in detail the possibility of a P66 binding site for PEG 400, PEG 600 and maltohexaose the current noise of the blocked P66 channels was studied.

Parallel to the titration measurements, the frequency-dependence of the spectral density of the current noise was analyzed using fast Fourier transformation. Fig 4-5 illustrates an example of a measurement with PEG 600. Before addition of NEs, a reference spectrum was taken to obtain the current noise of the open P66 channel, which exhibited 1/f -noise in the frequency range between 10 Hz and 100 Hz (Fig. 4-5, trace 1). The increase of the spectral density at frequencies above 200 Hz was caused by intrinsic noise of the preamplifier that produces a frequency-dependent current noise through the membrane capacity C_m. The reference spectrum was subtracted from each spectrum taken after the successive addition of NEs in increasing concentrations. In Fig. 4-5, trace 2 shows a spectrum taken after addition of PEG 600 (9.6 mM; the reference spectrum of trace 1 was subtracted). The current noise spectrum of P66 after addition of PEG 600 could be fitted to a 1/f-function and is shifted to higher spectral density as compared to the reference spectrum (Fig. 4-5, trace 2). In further

measurements, the concentration of PEG 600 was increased in defined steps. At other concentrations of PEG 600 (18.7 mM and 30.0 mM) the power density spectrum corresponded to that of traces 3 and 4, respectively, in Fig. 4-5, which also could be fitted to a 1/f-function. This type of noise is expected for diffusion processes through open channels [76, 77]. The spectral density of current noise through P66 channels could also be fitted to 1/f functions after addition of PEG 400 and maltohexaose.

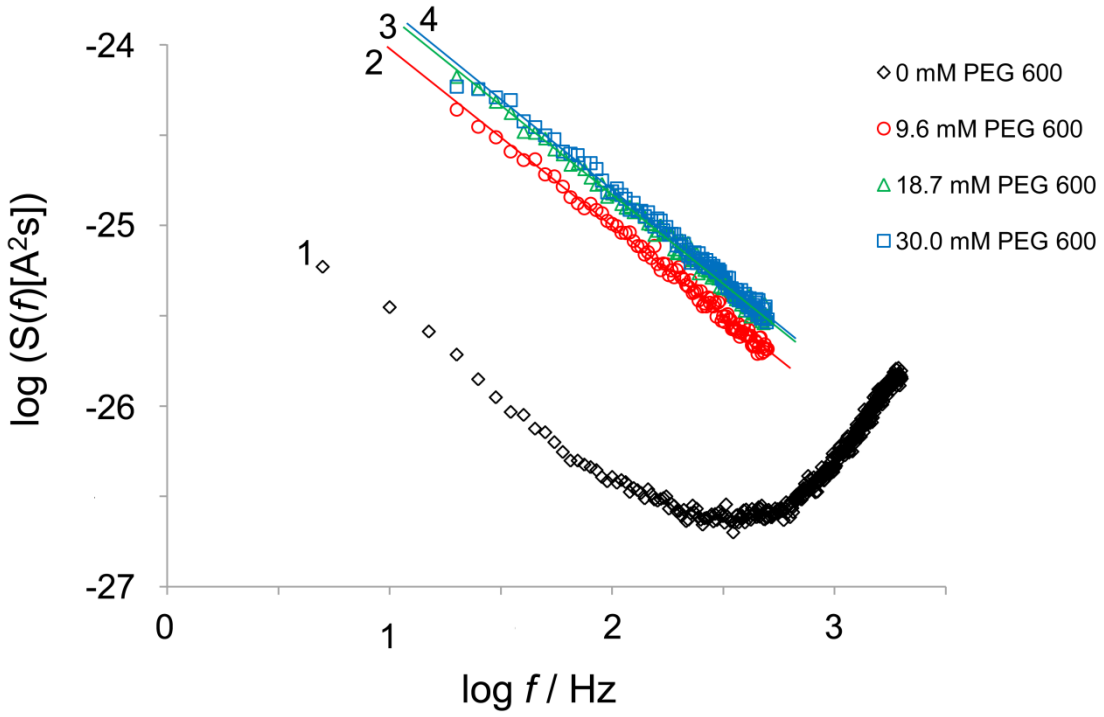

Fig. 4-5: Power density spectrum of PEG 600 induced current noise of P66. Trace 1 shows the noise of P66 in 1 M KCl salt solution without PEG 600. Traces 2-4 show the power density spectra of P66 in presence of increasing concentrations of PEG 600.

4.1.5 Blue Native Page analysis of the P66 complex

Previously, samples analyzed with SDS-Page did not show any oligomeric association of this protein. SDS is an ionic detergent which can cause the dissociation of protein complexes. To avoid denaturation of P66 samples, they were analyzed using BN-Page [70, 71].

In this native gels stained with silver nitrate only one band was observed. This band had an estimated molecular weight of around 460 kDa. Since the proteins maintain their native conformation, the size estimation may have an expected error of around 15% [94]. The real molecular weight of the P66 complex should be in a range between 390 and 530 kDa.

This band was blotted to a PVDF membrane and incubated with P66 antibodies. The band reacted positively in this immunoassay showing the presence of P66 in this protein complex.

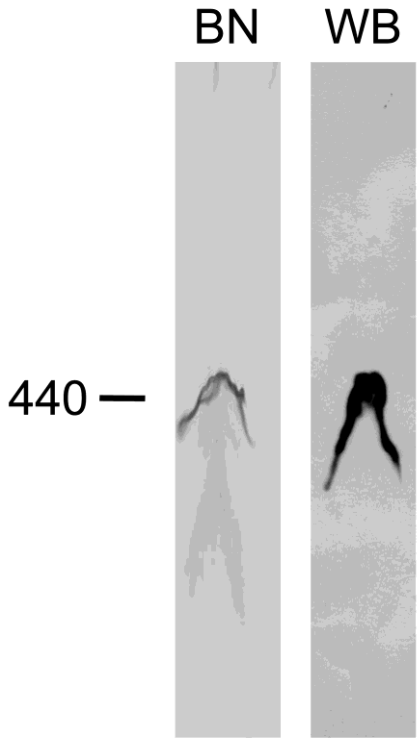

Fig. 4-6: Blue Native Page (left) and WB (right) of a pre-purified P66 sample. P66 was obtained from a B-fraction sample purified by FPLC using a MonoQ column. The molecular weight used was NativeMark Unstained, Invitrogen and is indicated in kDa to the left.

4.2 Discussion

4.2.1 Pore estimation

Previous studies tried to determine the P66 channel radius using only a theoretical approach [52]. The P66 conductance was considered to be equal to the conductivity of a simple cylinder of aqueous salt solution where the length of the cylinder was considered equal to the membrane thickness. The predicted diameter for P66 channel was estimated to be 2.6 nm[52]. This kind of estimation can only be considered preliminary because it does not take into account important parameters like charge and hydrophobic interactions inside the channel or oligomeric conformation.

The existence of a huge hole in the outer membrane of *Borrelia burgdorferi* is difficult to imagine. These pores could definitely impair the protection function of this membrane allowing the transport of harmful substances to the periplasmic space. In addition to that, it is also difficult to understand the presence of small porins like Oms38 described in *B. duttonii* [62] next to P66. Therefore, in order to study the P66 channel diameter in an objective experimental way the use of NEs was thought to be a good approach.

The use of different NE to determine the channel diameter of pore forming proteins has been reported previously. The channel diameter of PA_{63} from *Bacillus anthracis* [95], the α-toxin from *Staphylococcus aureus* [92] and the colicin Ia channel from *Escherichia coli* [78] have been successfully estimated using this method. Because NEs are uncharged molecules, they avoid attraction/repulsion forces between ions and the channel interior charges. Additionally, the determination of the channel diameter using NEs is not influenced by oligomeric conformations which are usual for porins.

Analyzing the results of the measurements in presence of different NEs it can be concluded that P66 has an entrance pore diameter of approximately 1.9 nm with a 0.8 nm inner constriction. An estimated error of 0.1 nm can be considered caused by a smearing in the molecular weight of the NEs and therefore their hydrodynamic radius [92, 95]. This size is in accordance with other porin diameters and is much smaller than the previously predicted value of 2.6 nm. A 0.8 nm constriction diameter does not allow an indiscriminate transport across the outer membrane rejecting the idea of a huge channel but does not explain the discrepancy between the diameter and the channel conductance. The oligomeric constitution of P66 could play a major role as discussed below in more detail.

PEG 400 and PEG 600 blocked the channel in an unexpected way reducing the conductance to approximately 10 % of the original measured in 1M KCl. This effect is difficult to explain and is probably caused by the occlusion of the channel when a molecule gets blocked somewhere along the channel interior. This effect allowed gaining some insight in the arrangement of the P66 complex studying the single channel blockage of P66.

4.2.2 Interactions of NEs with the P66 channel

The drastic reduction of P66 conductance due to the addition of 20% PEG 400 and PEG 600 to the salt solution does not correspond to the decrease in the bulk conductivity of the salt solution which should be between 40 and 70 %. The multi-channel titration measurements

with PEG 400 and PEG 600 showed a P66 conductance reduction of 80-90 %. This blockage was surprisingly slow taking 10-30 minutes to reach a stationary phase after addition of the PEGs. This kind of slow blockage is not usual for substrate-binding porins. Because of that fact and to clarify if there was some kind of interaction with the channel interior the P66 current noise through opened and NE-induced closed state was measured.

Current noise measurements and the subsequent analysis of the power density spectra obtained by Fourrier-transformation permitted the identification of binding sites in specific porins. In the case of a porin being specific for a substrate the noise is of Lorentzian type [96-99]. In contrast, specific channel without substrate and diffusion porins show a $1/f$- noise [76, 77, 100]. In current noise measurements, P66 showed a $1/f$- noise not only in the open state in absence of NEs, but also in presence of PEG 400, PEG 600 and maltohexaose. Well studied specific porins showed always the Lorentzian noise type and therefore the blockage of P66 by these NEs cannot be explained with specific binding sites. PEG 400 and PEG 600 probably diffuse through the channel getting stuck along the way due to their size.

The blockage effect of those NEs also allowed studying the blockage of a single P66 channel. After the insertion of one single P66 channel in the membrane, PEG400 or PEG 600 was added to the salt solution. P66 conductance was blocked in about eight similar progressive steps. This blockage was reversible and some of the steps fluctuated between the opened and closed state. These effect leads to the idea of P66 being a bundle of channels rather than a huge channel as it was predicted before. In that case, P66 could build an unusual oligomeric channel conformation no described before for any organism. Some other porins with high single channel conductance have been described in spirochetes, like those from *Spirochaeta aurantia* and *Treponema denticola* [101, 102]. A possible gene homology and a similar organization as a bundle of pores must be studied. These studies might reveal a specific protein complex important for the spirochetes biology.

4.2.3 Blue Native Page analysis of the P66 complex

The results obtained with Blue Native gels confirmed an oligomeric conformation of P66. The P66 complex appeared as a 460 kDa band. Because the BN-Page separates proteins in their native state and the structure of different proteins can differ enormously a molecular weight error must be considered. This error is estimated to be around 15% [94]. Therefore, it can only be concluded that P66 is a big protein complex with a molecular weight in a range from 390

kDa to 530 kDa. Probably P66 is an octamer, but in any case indications described in the next chapter support the idea of a symmetric complex (hexamer, octamer or decamer) that can be divided in two equal parts as explained in the section 6 in detail.

Recombinant P13 in *Escherichia coli* and *Nicotiana benthamiana*

One of the main aims of this thesis was the production of an outer membrane protein from *B. burgdorferi* that could be used in the diagnosis and treatment of *Borrelia* infections. The chosen protein was P13 as it is proved to be surface exposed and because researches in genome databanks revealed no homologues in other bacterial genera, even in the close related *Treponema* [103]. This protein is possibly involved in functions that are specific for the *Borrelia* pathogenesis and its production and isolation could help to clarify its structure and function which is not completely understood.

Large amounts of the chosen protein are needed to develop these new strategies. *Borrelia* cells grow very slow and entail an infection risk. For those reasons, the recombinant expression of P13 seems to be the optimal approach for its production. In order to find the best expression system and to optimize the expression levels of the recombinant protein, two organism were selected: first, the well known *E. coli* used before successfully to express many other proteins, and second, a new system in the tobacco plant *N. benthamiana* which has been employed previously with *Borrelia* proteins with the possibility of a large-scale and cost-saving production [104].

P13 is an outer membrane protein with an N-terminal signal sequence processed on its way through the inner membrane. It has also been described that the C-terminus is cleaved somewhere between the periplasmic space and the outer membrane [103, 105]. P13 has pore forming activity [56] but it is unknown if the C-terminus is required for the pore formation [105]. To look deeper into this question, two DNA fragments were designed to be cloned in *E. coli*. One of the inserts was the P13 gene with neither the N-terminus nor the C- terminus and the other one was the P13 gene only with the C-terminus. Both structures included an *E. coli* signal sequence from one of its outer membrane proteins (OmpF) to cross the inner membrane and a His-tag residue to facilitate purification of the recombinant protein.

Only one construct was designed to be cloned in the tobacco plant, the processed P13 protein with a His-tag for later purification. The aim of this cloning was to establish an easy and fast production of the protein in big amounts and at low cost.

5.1 Results

5.1.1 *p13* expression in *Escherichia coli*

After inducing the production of rP13 in *E. coli* and breaking the cells using a French press the cell debris was spun down (P1). The cell membranes with its embedded proteins and the cytoplasmic proteins were located in the supernatant (S1). The S1 was ultracentrifugated at 143000 g for 1 hour. From this ultracetrifugation a pellet (P2) and a supernatant (S2) were obtained. The cytoplasmic proteins were found in the supernatant S2, while the membranes with its proteins were located in the pellet (P2). After discarding the S2, the P2 was resuspended in a Tris solution with 1% LDAO. After the addition of the detergent, the membrane proteins were soluble. A second ultracentrifugation at 143000 g was required to separate solubilized proteins from unsolubilized membrane patches and other components. The membrane proteins were then in the supernatant (S3). An overview of the whole cell fractionation is described in the next figure (Fig. 5-1).

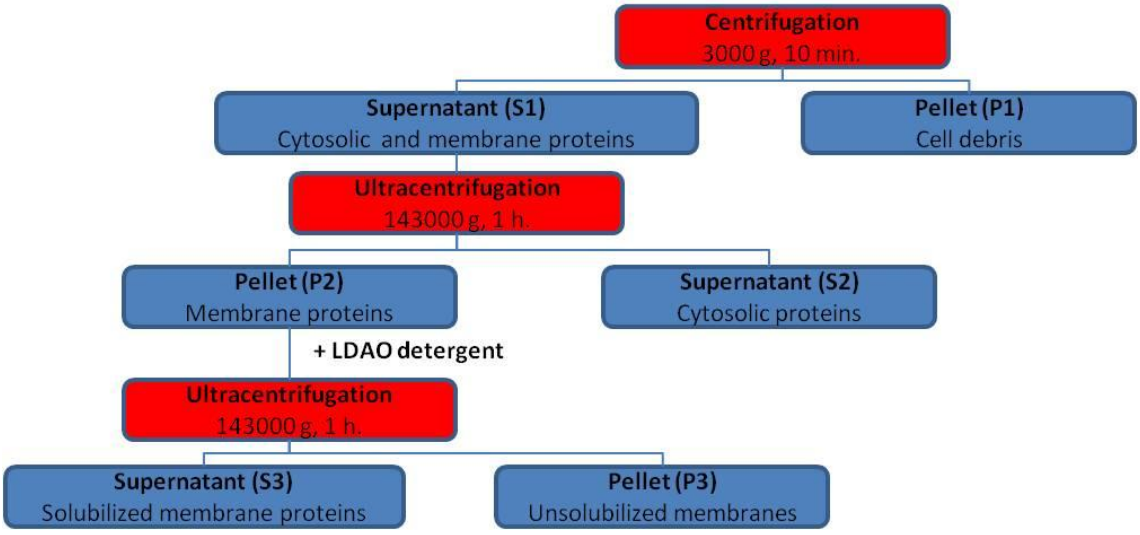

Fig. 5-1: Cell fractionation of *E. coli* cells. The centrifugation steps are shown in red squares while the products obtained are detailed in the blue squares.

To check if the protein was expressed during the induction and if the cell fractionation was correct, different samples were collected during the process and tested in a WB. The WB was performed without any further purification, and therefore the samples contained a high amount of *E. coli* proteins. A clear positive reaction against the P13 antibody could be observed in S3 as expected but part of the recombinant protein remained in P1 and P3 (Fig. 5-2).

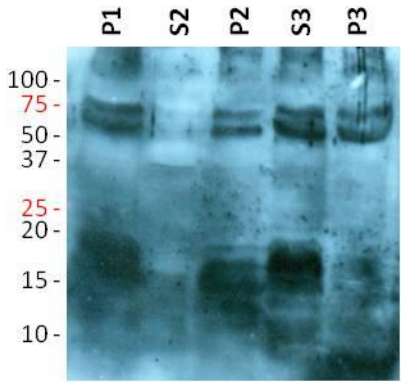

Fig. 5-2: WB against P13 from the *E. coli* cell fractionation of construct 1. The marker is indicated right in kDa (Precision Plus Protein Prestained Standards Dual Color, BioRad). The different fractions are indicated above, and the origin of each one is explained in the Fig. 5-1. Similar results were obtained for construct 2.

Using Ni-NTA Sepharose beads the protein content in the S3 was further purified. The recombinant protein had a polyhistidine-tag that binds strongly to the column matrix and it was eluted with an increase in the imidazole concentration. The different washing steps and the elution were tested in a WB. In Fig. 5-3 is possible to see how the recombinant protein eluted after the several washing steps when the imidazole concentration reached 500 mM. In the elution fractions several bands reacted against the P13 antibody in each construct sample. A 13 and a 17 kDa band were observed in the construct 1 sample. For the construct 2 sample, also two bands were visible, one that was approximately 13 kDa and a second one that reached 20 kDa. A third 30 kDa band was also present in all the elutions, even in the negative control. In the upper part of the WB two bands can be observed for const. 1 and 2. The height of these bands corresponds with the loading pockets of the gel showing some protein aggregation that hinder the entry of part of the recombinant protein in the gel.

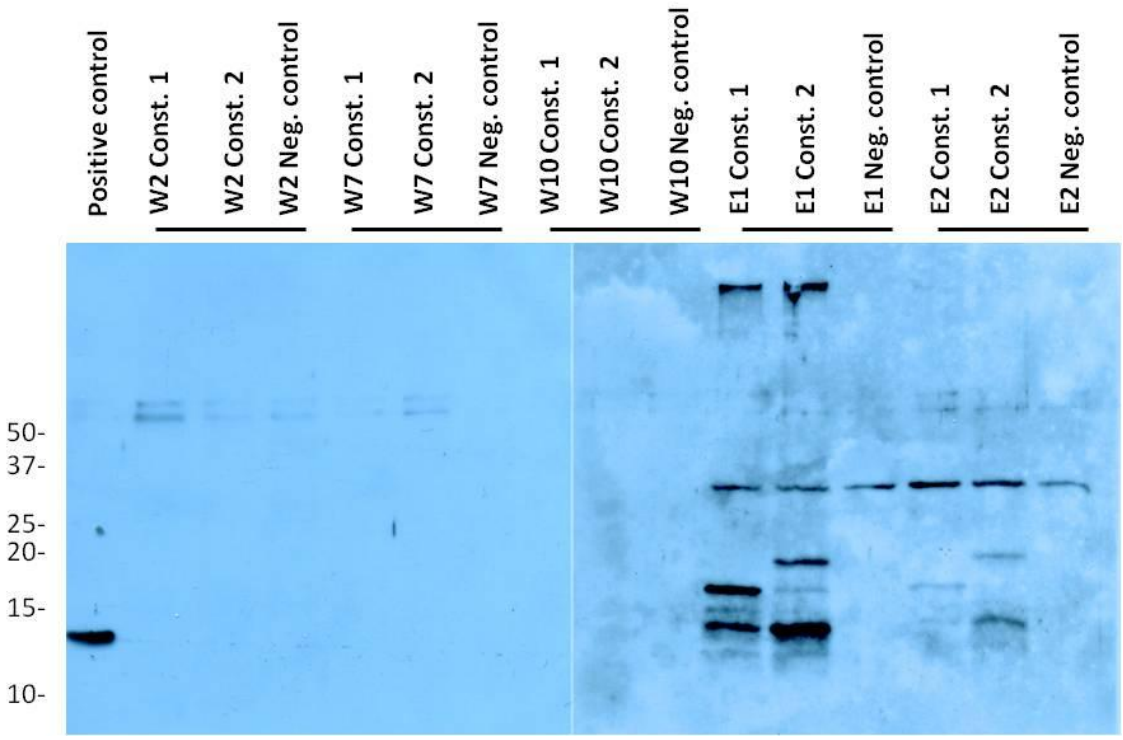

Fig. 5-3: WB from the P13 purification using Ni-NTA Sepharose beads. Several washing steps (W2, W7 and W10) were checked to confirm that no premature elution occurred. W1-W9 were done with 50 mM imidazole and W10 with 100 mM imidazole. The two elution steps (E1 and E2 were done with a 500 mM imidazole concentration. The protein marker used was Precision Plus Protein™ standards Kaleidoscope (BioRad).

5.1.2 *p13* expression in *Nicotiana benthamiana*

The expression process in the tobacco plants differs from the expression in *E. coli*. After infiltration of *A. tumefaciens* through the stomata in the tobacco leafs a production time was required. After that period, the leaves were collected and immediately crushed to powder using a mortar and liquid nitrogen.

The powder obtained with the previous step was mixed with an extraction buffer. The mixture was incubated over night under vigorous shaking at 4 °C. The cell debris and other insoluble components were spun down. The extract was tested in SDS-Page and WB to prove the presence of rP13 (Fig. 5-4).

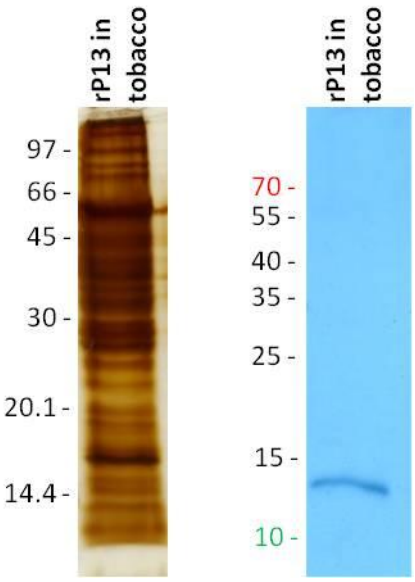

Fig. 5-4: SDS-Page and WB against P13 from the plant extract. The SDS-Page was stained with silver nitrate and the molecular weight is indicated in kDa.

Great amount of plant proteins extracted together with the recombinant protein were visible on the SDS-Page making necessary further purification steps. The presence of rP13 was evidenced by the 13 kDa band that reacted against the P13 antibody in the WB.

The remaining solution was incubated overnight in presence of Ni-NTA Sepharose beads for the purification. The His-tag in the recombinant protein bound to the beads and those were collected by centrifugation. Posterior washing steps with increasing concentrations of imidazole lead to purification of rP13. A SDS-Page and a WB were done to analyze the loss of protein during the washing steps and the purity of the protein in the elution fraction (Fig. 5-5).

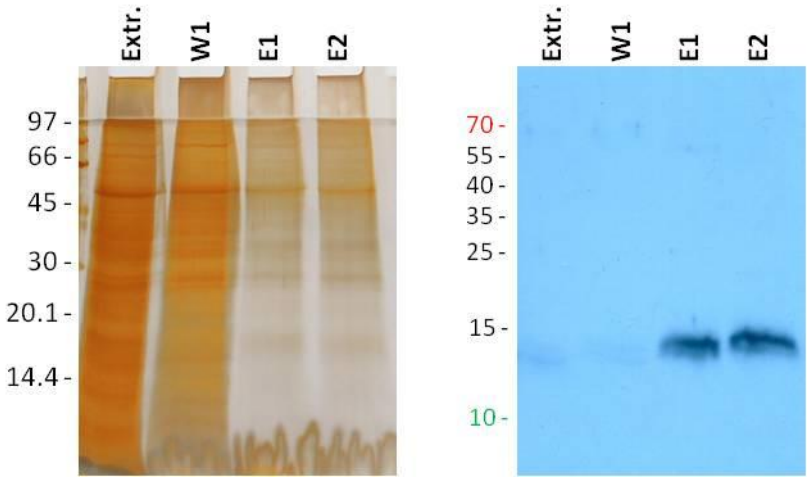

Fig. 5-5: SDS-Page and WB against P13 from the purification realized using the protein extract from tobacco plants. In the first lane, the extract solution after incubation with Ni-NTA Sepharose beads is found (Extr.). W1 in the second lane is a wash step realized with 20 mM imidazole. E1 and E2 are successive elution steps with a 250 mM imidazole.

5.1.3 Pore forming activity of rP13 in black lipid bilayers

The two structures produced in *E. coli* were tested in artificial membranes to further characterize their pore forming activity. Additionally, a negative control without the pARAJS2 plasmid was measured in BLB. The results are shown in the next Fig. 5-6.

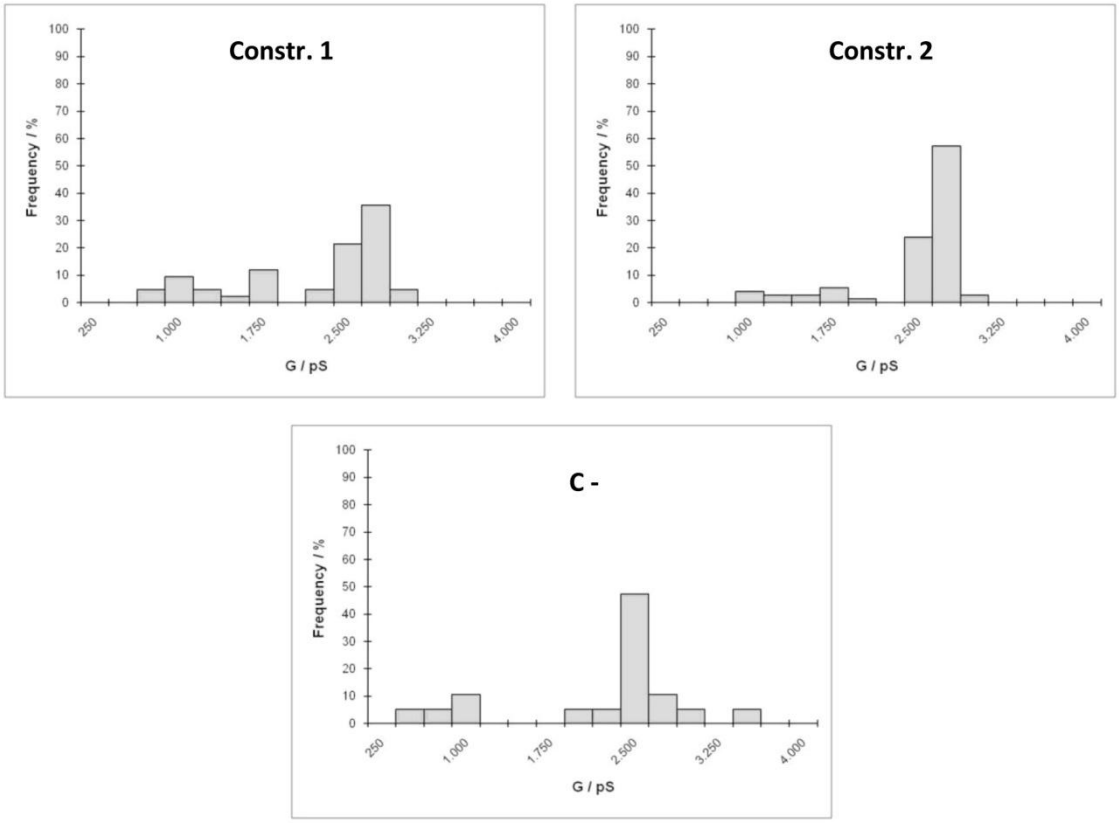

Fig. 5-6: Pore forming activity of purified rP13 produced in *E. coli*. The samples were measured with the BLB assay in 1 M KCL. A negative control (C-) was measured under the same conditions as construct 1 and 2.

A main activity was observed in both constructs with a prevalent conductance of 2.75 nS and a secondary activity of 1 nS. The negative control displayed a similar pore forming activity with a main conductance of 2.5 nS and the same residual conductance of 1 nS.

The voltage dependency of the 2.75 nS pore was measured to discern between a possible *E. coli* porin and rP13. The samples showed a voltage dependency around 100 mV (data not shown). rP13 voltage dependency was measured before determining that P13 was voltage independent at least until ±150 mV [56].

More rigorous purification processes lead to a loss in the amount of rP13 in the samples. After those processes no pore forming activity close to that described for P13 could be observed in the samples.

In the construct produced in *N. benthamiana* no activity close to 3.5 nS was observed (data not show) and therefore no further work was done with this construct in artificial bilayers.

A possible explanation for the absence of P13 activity in the samples will be discussed in the next chapter, where another conductance was observed for P13 when extracting it from a BN-Page.

5.2 Discussion

5.2.1 Production of P13 in *E. coli*

Two constructs of P13 were produced in *E. coli*. One included a C-terminus which function is unknown and the other one contained the mature P13 protein without this C-terminus. These two constructs were produced in *E. coli* to evaluate if this C-terminus was somehow involved in the pore formation or had any other function.

C-terminal processing of P13 is accomplished by a carboxyl-terminal protease designated CtpA [105]. CtpA belongs to a protease family first described in the cyanobacterium *Synechocystis* [106, 107]. Examples of *ctpA* homologues are present in Gram negative and Gram positive bacteria [108], chloroplast of algae [109], higher plants [110] and even in humans [111]. In prokaryotes the C-terminal processing is not well understood but there are some examples known of such proteins in different organism [112-116].

Recombinant expression of P13 was successful in *E. coli* as it can be observed in the WB shown in Fig. 5-3. However, two bands were observed for each construct in the WB against P13. For construct 1, a 15 and an 18 kDa band could be observed. For construct 2, the bands had a molecular weight of approximately 15 and 21 kDa.

In the samples, proteins from the outer and inner membrane may be found together since the cell fractionation only separates membrane proteins from cytosolic proteins. Outer membrane proteins present in the inner membrane waiting to be translocated may still have the signal sequence attached. This fact could explain the two molecular weights observed for each construct. One should correspond with the N-terminal processed protein and the other one

will still have the signal sequence. The unprocessed rP13 constructs should produce an 18.5 kDa protein in the case of construct 1 and a 21.5 kDa protein for the construct number 2. Processed proteins should have a molecular weight of 16.2 kDa and 19.2 kDa for constructs 1 and 2 respectively. The theoretical values of those bands are in agreement with what it is seen in the WB except in the case of processed construct 2.

The processed construct 2 should have a His-tag and P13 including its C-Terminus with an approximate molecular weight of 19 kDa. However, in the WB the observed band had approximately 15 kDa. A possible P13 C-terminal processing in *E. coli* might be responsible for this discrepancy. A C-terminal protease is known in *E. coli* with a certain grade of homology to CtpA in *Borrelia* [105]. The major site of cleavage for this protein called Tps seems to be the amino acid alanine [116]. This fact coincide with the predicted cleave of P13 by CtpA. The C-terminal processed construct 2 would have a 16 kDa molecular weight which is in agreement with the results observed in the WB.

The amount of protein recovered after purification was enough to study its pore forming activity in artificial bilayers. The results for both constructs show an activity of around 2.75 nS. Unfortunately, the negative control displayed a very similar conductance. Previous studies done in the research group of Prof. Dr. Roland Benz in the Biotechnology Department of the University of Wuerzburg showed that untransformed *E. coli* BL21 Omp8 Rosetta used for the production of recombinant porins retained a similar pore forming activity even after rigorous purification with Ni-NTA resins (data not published). Therefore, the voltage dependency of the samples was tested to verify if indeed the activity came from an *E. coli* porin. The pores started to close at voltages near to 100 mV while P13 is described to be voltage independent at least up to ±150 mV voltages. That way, the 2.75 nS activity is believed to come from an unidentified *E. coli* porin.

5.3.2 Production of P13 in *Nicotiana benthamiana*

The expression of the processed P13 in the tobacco plant was thought to be a good expression system to get high amounts of the protein at low cost. Recombinant protein expressions in tobacco plants have successfully been achieved before [104, 117-119]. Therefore, the processed form of P13 was expressed with this method to be used afterwards as a possible vaccine candidate.

The expression of P13 in *N. benthamiana* was successful as determined by WB. The purification eliminated many of the other plant proteins contained in the sample as shown in the E1 and E2 in the SDS-Page from Fig. 5-5. Unfortunately, the expression yield was not as high as expected. Big amounts of plant material needed to be processed to get visible signals in WB. Because of the low amount of P13, the 13 kDa band was not clearly visible in SDS-Page stained with silver nitrate. The fact that P13 is a small hydrophobic protein makes the protein run in fuzzy bands in SDS gels and its observation much more difficult.

The rP13 protein expressed in *N. benthamiana* showed no activity close to 3.5 nS in BLB. A lack of activity in the sample is difficult to explain. The right folding of the protein needs sometimes the help of chaperones or other complexes like Omp85 in bacteria [120]. Maybe *Borrelia* and *Nicotiana* are organisms so apart from another that they differ greatly in the folding machinery and therefore some proteins could be improperly folded losing their functionality. The same could also happen with *E. coli* which is not the closest bacteria to *Borrelia*.

P13 is a *Borrelia* outer membrane protein with a described pore forming activity of 3.5 nS [56]. Tests done in BLB with rP13 were focused to try to find a similar activity that might be in a way influenced by the His-tag producing some conductance variance. But no activity close to the mentioned before was observed. The next chapter deals with the *Borrelia* outer membrane complexome where two complexes were clearly observed, one of them probably related with P13 and which elution showed a very different conductance for P13 than the published elsewhere before [56].

Analysis of Outer Membrane Complexes using Blue Native Page

Blue Native Page (BN-Page) is a kind of polyacrylamide gel with a neutral pH that allow the separation of protein complexes in their native state. BN-Page allows getting a molecular weight estimation of protein complexes with a standard deviation up to 15 %. The SDS detergent, which usually breaks the complexes, is substituted by Coomassie blue G-250 as charge-shift molecule. The Coomassie G-250 confers a negative charge to the proteins without any denaturation.

BN-Page is also conceived to isolate proteins in their functional state and study the composition of macro complexes resolving them in a second dimension SDS-Page (2D SDS-Page).

6.1 Results

6.1.1 Separation of the B-fraction from *B. burgdorferi* in BN-Page

The B-fraction of *Borrelia burgdorferi* was studied using BN-Page to identify possible outer membrane complexes. B-fraction proteins were diluted in different concentrations of digitonin to find the optimal concentration for solubilization. Digitonin is a soft, non ionic detergent that maintains the complexes in its functional state.

In Fig. 6-1 a digitonin dilution series was carried out to find the optimal detergent concentration to solubilize the B-fraction of *B. burgdorferi*.

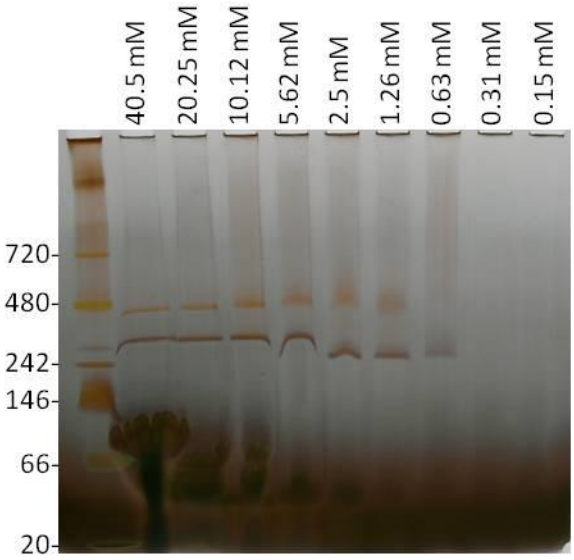

Fig. 6-1: *B. burgdorferi* B-fraction solubilized in different concentrations of digitonin and separated in a 4-16% BN-Page. The different concentrations of digitonin used to solubilize the outer membrane proteins are indicated in the upper part. On the left side the molecular weight marker (NativeMark Unstained, Invitrogen) is shown in kDa.

As shown in the gel above, two main complexes appeared in the BN-Page stained with silver nitrate. The bigger one had a molecular weight of approximately 480 KDa and the small one around 350 kDa.

In BN-Page, it is important to find the optimal concentration of detergent to solubilize the membrane proteins [69]. The detergent concentration must be the lowest possible without loss of any band. At this detergent concentration the bands have to appear well defined and straight. At a certain detergent concentration, vesicles formed during the process of solubilization will appear at the bottom of the gel (visible in the 40.5 and 20.25 mM digitonin lanes, Fig. 6-1). At or above this detergent concentration should not be worked. Taking all of this in consideration the optimal detergent concentration to solubilize outer membrane proteins from the B-fraction of *B. burgdorferi* seems to be around 10.12 mM digitonin.

To further investigate if these complexes had a relation with P13 and P66, two of the main transmembrane proteins in *B. burgdorferi*, Western blots (WB) were carried out using antibodies against them. Again, all the detergent concentrations were tested to observe possible protein complex fragmentation. The results are shown in the next figure (Fig. 6-2).

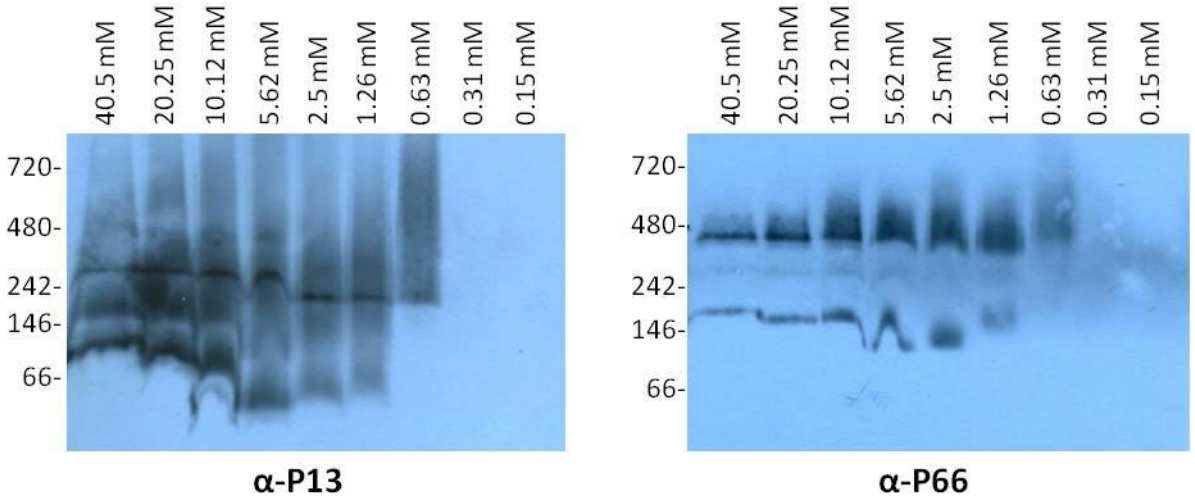

Fig. 6-2: Western blots against P13 and P66 using BN-Page to separate proteins from the B-fraction of *B. burgdorferi* solubilized in different concentrations of digitonin. In the upper part the concentration of digitonin for each sample is indicated. On the left side, the protein marker is shown in kDa (NativeMark Unstained, Invitrogen). The proteins were blotted at 30 mV const. during 60 min. to a PVDF membrane.

In the WB against P13 one band reacts intensely with the antibody. The band corresponds to the 350 kDa band previously observed in the BN Page. The same WB was done for P66. In this case the antibodies reacted mainly against the 480 KDa band also observed in the BN-Page previously. In this WB, it is also possible to observe a second band that reacted with the P66 antibody with a molecular weight of around 200 kDa.

The WB of the dilution series corroborates that samples solubilized with 10.12 mM digitonin have an optimal detergent concentration where the antibody signal appears with the highest definition.

6.1.2 Second dimension SDS-Page from BN-Page

Second dimension gels were done to obtain a better understanding of the composition of these complexes. In the first dimension, the B-fraction proteins were separated in a BN-Page (4-16% acrylamide) using a 10.12 mM concentration of digitonin. After that, a strip/lane was cut from the gel and treated with three denaturing solutions (reducing, alkylating and

quenching solution) as described by the manufacturer to break the complexes into monomers [67]. The results of this second dimension are show in Fig. 6-3.

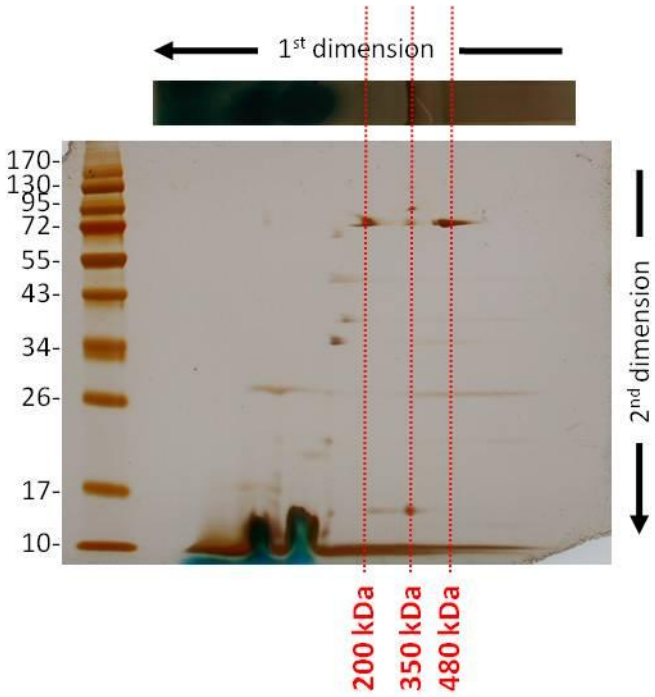

Fig. 6-3: 2D SDS-Page from a BN-Page used in the first dimension. The B-fraction from *B. burgdorferi* was solubilized with 10.12 mM digitonin and separated in a BN-Page (4-16 % acrylamide). The BN-Page strip was pretreated with denaturing solutions as described by the manufacturer [67] and separated in a SDS-Page (NuPAGE® Novex 12% Bis-Tris Gel 1.0 mm, 2D well, Invitrogen). The gel was silver stained. The protein marker is indicated on the left side in kDa (PageRuler™ Prestained Protein Ladder, Fermentas).

As show in the 2D gel, the 480 kDa band was disrupted only in one component, a protein of approximately 66 KDa. As well, the band of around 200 kDa seemed to be composed only by a 66 kDa protein. These results are in concordance with the WB shown in Fig. 6-2 that identifies P66 as component of these two complexes.

The 350 kDa band broke down in different possible monomers. Different spots appeared in the same vertical line with different molecular weights of 14, 72 and 95 KDa approximately. In the previous WB shown in Fig. 6-2, P13 was identified as one of the possible components of this complex, but the identity of the 72 and 95 kDa components was unknown.

Other complexes smaller than 200 kDa seem to appear in the BN-Page. These complexes were difficult to see when the gel was stained with silver nitrate and therefore they were not further characterized.

P13 and P66 presence was again tested by WB of the second dimension gels. This experiment was mainly carried out to observe the correct division of the complexes into their monomers, especially in the case of the 350 kDa complex. As done before in the first dimension with the BN-Page, the proteins separated by 2D gels were transferred to PVDF membranes.

Immunoblots against P13 and P66 were completed with these membranes. The results are shown in Fig. 6-4.

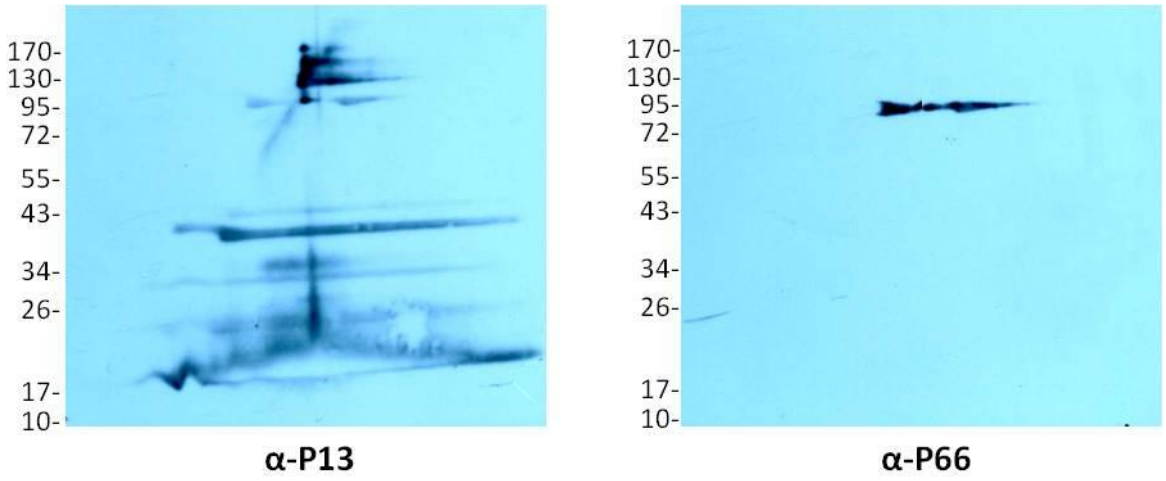

Fig. 6-4: WB against P13 and P66 realized from the 2D SDS-Page from the BN-Page in the first dimension. The first dimension run from right to left as shown in the previous figure. The molecular weight is indicated in kDa on the left side (PageRuler^{TM} Prestained Protein Ladder, Fermentas).

The 480 and 200 kDa complexes reacted against the P66 antibody, making apparent the formation of these complexes by P66.

The 350 kDa band seems to decompose in many spots with different molecular weights as shown in the 2D gels stained with silver nitrate (Fig.6-3). In the WB, many spots in the same vertical line reacted strongly with the P13 antibody, including the 72 and 95 kDa dots. Some other new dots not visible in gels stained with silver nitrate appeared in the WB

6.1.3 Mass Spectrometry of the 350 and 480 kDa bands

Since the bands identity was still not clear enough, especially in the case of the 350 KDa band, some samples were prepared and sent for mass spectrometry analysis. Both bands were excised from BN-Page and digested afterwards with trypsin. The results pointed the presence of OspC, a lipoprotein from *B. burgdorferi*, in the 350 KDa complex while the expected P13 presence was not detected. The band of 460 KDa was indeed composed of P66.

6.1.4 Analysis of different *B. burgdorferi* mutants B-fractions by BN-Page

To further analyze the OspC participation in the complex, different *B. burgdorferi* strains were tested in BN Page. *B. burgdorferi* B31 which is a wild type, *B. burgdorferi* B313 which does not express four lipoproteins (OspA, OspB, OspC and OspD)[121] and *B. burgdorferi* P13-18 which is a mutant for *p13* [122]. In all cases, different concentrations of outer membrane proteins where solubilized in 10.12 mM digitonin and the remaining unsolubilized protein was removed from the sample by centrifugation as described in the methods. The gel was stained with silver nitrate .The results are presented in Fig. 6-5.

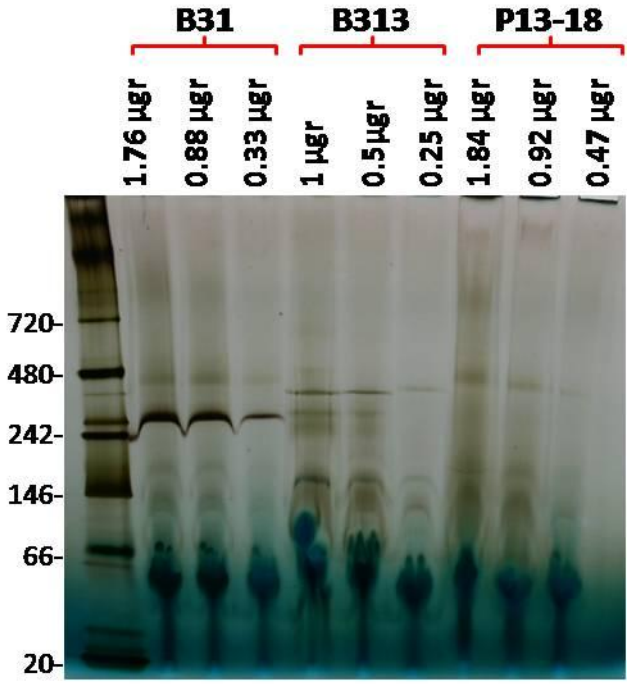

Fig. 6-5: BN-Page from the B-fraction of *B. burgdorferi* B31 (wild type), *B. burgdorferi* B313 (Δ *OspA, -B, -C, -D*) and *B. burgdorferi* P13-18 (Δ *p13*). On the right side the protein molecular weight is indicated in kDa. On the upper side the strain is indicated and the concentration of the B fraction solubilized in 10.12 mM digitonin.

In the gel, the thick 350 kDa band is visible in the B-fraction from *B. burgdorferi* B31. This band is much lighter in the outer membrane fraction from the B313 strain where a light band appears after developing the gel for a long time before stopping the staining process. The 350 kDa band disappears completely in the *p13* mutant where the P13 protein is not expressed. The observation of a 150 kDa band that appears much stronger in the lipoproteins deficient mutant is also remarkable.

A WB from the same gel against P13 was carried out. The results are shown in Fig. 6-6.

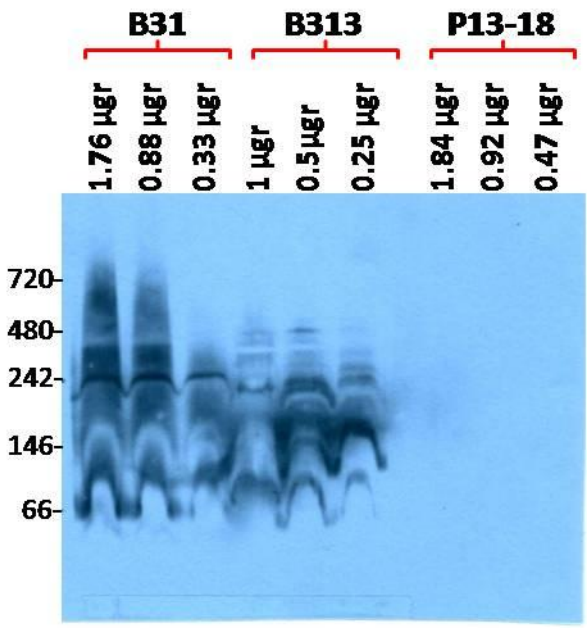

Fig. 6-6: WB against P13 using different B-fractions from *B. burgdorferi* B31, *B. burgdorferi* B313, *B. burgdorferi* P13-18 separated in a BN-Page. The different concentrations of B fraction solubilized in 10.12 mM digitonin are indicated on the upper part. The marker is shown on the right side in kDa.

The WB shows in the B31 strain a strong reaction of the P13 antibody with the 350 KDa bands. In the B313 strain, where many lipoproteins are knocked out, the signal is much fainter. In this strain a 150 kDa band mentioned before appears to react much stronger against the P13 antibodies. In the case of the P13-18 stain the signal is completely nonexistent rejecting the hypothesis of a possible cross reaction of the P13 antibody with other *B. burgdorferi* outer membrane proteins.

6.1.5 Pore forming activity of the 350 and 480 kDa bands

In *Borrelia*, there are two main integral proteins described, P13 and P66. Both are described as pore forming proteins. Since the biggest membrane proteins complexes in the outer membrane of *B. burgdorferi* seemed to be composed at least partially by P13 and P66, their pore forming activity was assessed. To evaluate the activity of both bands in artificial lipid membranes, a BN Page was run using *B. burgdorferi* B31 B-fraction solubilized previously in 10.12 mM digitonin. The 480 and 350 kDa bands were excised with a scalpel and crashed into little pieces. A 1% Genapol X-80 solution was added twice the weight of the gel and incubated over night at 4 °C with vigorous shaking. Further dilutions to reduce the activity whenever needed were also done with a 1% Genapol X-80 solution.

After the proteins were extracted from the gel the activity in BLB was measured. A summary of these activities is presented in Fig. 6-7.

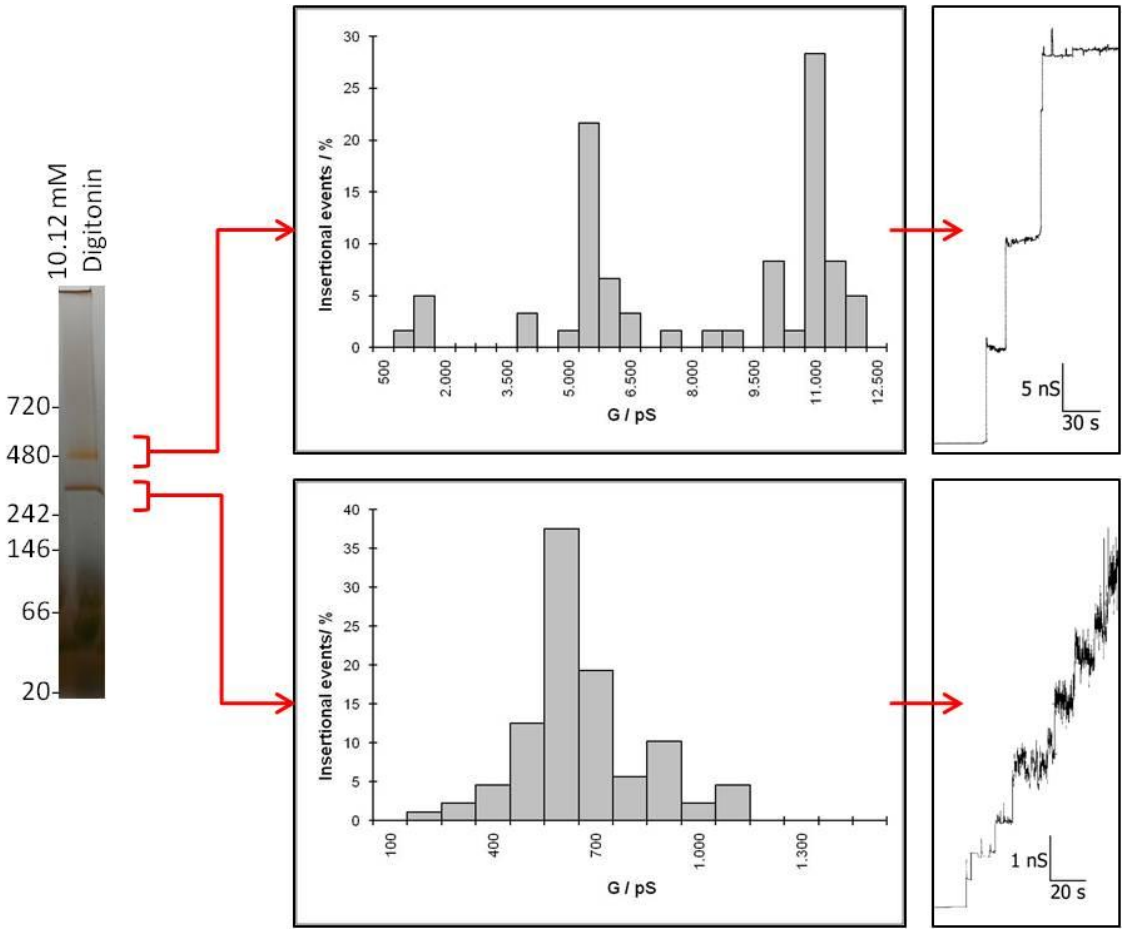

Fig. 6-7: Pore forming activity of the 480 and 350 kDa bands. The bands were cut and eluted in 1% Genapol from a BN-Page. In the upper row appears the activity from the 480 kDa band and in the lower row the activity measured for the 350 kDa band. The activity was measured using the BLB assay. The results are summarized in a histogram where the insertional events (approx. 100 pores) are indicated in percentage in the Y-axis and the conductance in pS in the X-axis. To the right an example of the step-like pore formation was included with a conductance-time scale. The salt solution used was 1 M KCl, with an applied voltage of 20 mV and a amplification factor of 10^9 V/A.

As shown in the upper histogram, the 480 kDa band elution exhibited a well defined 11 nS pore forming activity in artificial membranes. A second conductance peak was observed in this sample with a lower frequency and a conductance of 6 nS. The steps formed in the register

were clear and reproducible in different measurements using different sample preparations. When the 350 kDa band activity was tested in BLB, a 0.6 nS activity was observed. In this case the steps were well defined at the beginning but with increasing noise after three or four insertions. At this point it was difficult to identify the exact single channel conductance of each new insertion (lower picture, right). Therefore, the histogram was done taking only into account the first clear pore insertions in the membranes. When the noise reached high levels, a new membrane was established. This procedure was repeated until the intersectional events were enough to perform a histogram (approx. 100 pores).

6.1.6 BN-Page from rP13 produced *N. benthamiana*

In the previous project P13 was recombinant expressed in the tobacco plant, *Nicotiana benthamiana*. The samples obtained in the tobacco plants were tested in BN-Page to study the oligomerization of P13. The recombinant protein was extracted and pre-purified with Ni-NTA resins. Although the samples still contained plant proteins no further purifications were done to avoid loss of rP13. The sample was tested with WBs from the SDS-Page and BN-Page as shown in the next figure (Fig. 6-8).

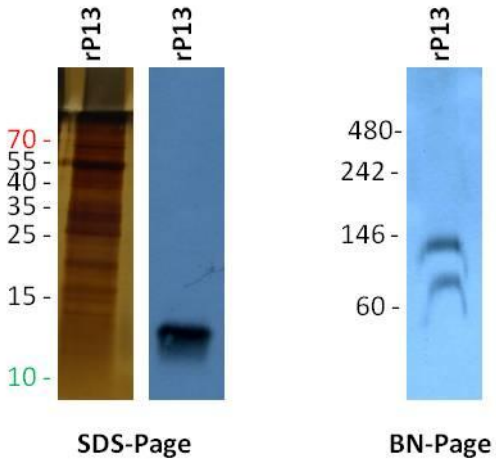

Fig. 6-8: SDS-Page and WB from rP13 expressed in tobacco plants and the WB from the same sample in a BN-Page. The sample for the SDS-Page was boiled 10 min. Markers are indicated in kDa.

The sample was pre-purified with Ni-NTA and eluted with 80 mM imidazole without washing steps avoiding any lost of rP13. The reduction in plant proteins was obvious but further purifications are required to get a clean rP13 sample. The SDS-Page was run under denaturing conditions (Redmix reducing sample buffer and boiled at 100 °C, 10 min.). The plant proteins present in the sample are shown in the gel stained with silver nitrate. The presence of rP13 is

revealed by the 13 kDa band that reacted with the P13 antibody. No other plant protein reacted against the antibody rejecting a possible cross reaction between the P13 antibody and those proteins.

On the right WB, the same sample was separated in a BN-Page. Two bands clearly reacted with P13 antibody, one around 80 kDa and the other one close to 150 kDa. This last one showed a more intensive antibody signal.

6. 2 Discussion

Borrelia is usually included in the group of Gram negative bacteria as it possesses two membranes. However, this genus has many distinctive characteristics that differ from the general Gram negative model. *Borrelia* has a more fluid outer membrane that lacks lipopolysaccharides. In addition, the exterior leaflet of the outer membrane has a high number (> 150) of lipoproteins that comprise the bacterium's primary interface with its host [36, 123]. This outer membrane contains a very low density of membrane-spanning proteins. Two of these proteins are P13 and P66 which show a high preponderance in the outer membrane. P13 and P66 have been described as proteins with porin properties. But both, P13 and P66, differ from the typical porin structure in Gram negative bacteria.

Many porins have a tertiary structure composed of a β-barrel. In some cases, they associate in oligomers, often in trimers, to gain stability. In the case of P13, a monomer due its small molecular weight is not enough to form a pore. Its pore forming activity can only be explained by an association of different monomers to form an oligomer. Also its secondary structure in α-helix differs from the typical β sheet found in other porins [56, 103]. P66 forms channels with a very high single channel conductance of 11 nS which is very rare in porins [51]. As described in a previous chapter of this thesis (*P66 channel diameter estimation using non-electrolytes*) P66 could associate in an oligomeric protein complex formed possibly by eight independent channels. This association of so many channels together has not been shown before for any other described porin.

The BN Page used in this chapter is a technique that has gained more importance in the past years to characterize protein complexes and protein interactions. It provides not only a close estimation of the molecular weight of a protein complex but also the opportunity to isolate protein complexes in a native state retaining their biological functions. Therefore, this

technique is a useful tool to study the arrangement and function of outer membrane proteins in *Borrelia*.

6.2.1 Protein complexes in the B-fraction from *B. burgdorferi*

When the B-fraction containing the outer membrane proteins of *Borrelia* is separated using a BN-Page mainly two big complexes were observed (Fig. 6-1). Their molecular weights were approximately 480 and 350 kDa. Proteins separated in BN-Page run folded in their native state and they are not linearized like in SDS-Page. Consequently, the number of shift molecules bound to the protein complexes depends on how the protein is folded. As well, the proteins will run differently depending on the shape of the complex. Globular or elongated complexes might run in a different way. Taken all together, the maximal molecular weight deviation of the BN-Page is estimated to be 15% for proteins that either bind Coomassie or have a isoelectric point (pI) below 5.4 [67].

In fig. 6-2, the same BN-Page stained previously with silver nitrate was used to do two WBs using antibodies against P13 and P66. Those two proteins were described previously as porins, and hence they were a main subject of study in this work. Surprisingly the WB for P13 showed a strong reaction of the antibody against the 350 kDa band, while the P66 antibody reacted very strong against the 480 kDa band. These results manifested some kind of involvement of P66 in the 480 kDa complex and P13 in the 350 kDa complex.

In the WB done with P13 antibodies (Fig. 6-2) the samples seemed to smear all the way through the lane. This effect was probably caused by the high hydrophobicity of P13 [124] that binds strongly to the detergent or Coomassie dye leaving a black background in the WB. A stronger signal was appreciated in the band where P13 possibly formed a complex.

In the P66-WB a second band reacted positively against the P66 antibody with a molecular weight of around 200 kDa, approximately half of the MW of the 480 kDa complex. This band was probably a fragment of the 480 kDa complex dissociated due to the membrane solubilization with detergents. In previous BLB experiments using fractions from a FPLC purification a 6 nS activity was often found (data not shown). A 6 nS activity could come from the disruption of the P66 complex in two halves retaining enough stability to form independent channels in membranes. This idea was supported by the observation of a 6 nS activity when extracting the 480 kDa complex from the BN-Page with detergents as shown in the Fig. 6-7.

The second dimension gels proved that the 480 kDa complex was composed exclusively of a 66 kDa monomer, identified in the WB of this second dimension as P66. The 200 kDa complex, which is thought to be a fragment of the 480 kDa complex, was only constituted by P66 as well. No other protein seems to be associated to P66 to form the 11 nS channel in the outer membrane of *B. burgdorferi*. The number of monomers involved in the formation of the channel is thought to be between 6 and 8. If the BN-Page results are compared to the PEG blockage of the P66 channel in 8 steps (Fig. 4-4), the P66 complex could probably form an octamer of 528 kDa. An octamer is within the molecular weight range of 480±72 kDa estimated using BN-Page.

In the case of the 350 kDa complex, the second dimension gel contained three possible monomers with different molecular weights (13, 72 and 95 kDa) which could form part of the complex. One of them, the 13 kDa protein was not always visible when the gels were stained with silver nitrate. The P13-WB done using the second dimension gel showed that all the dots corresponding to the 13, 74 and 95 kDa and other dots not visible in the 2D-gel reacted against the P13 antibody. The denaturation solutions where the BN-Page strip was denatured were probably not sufficient to completely break down the complex to its monomers.

Surprisingly, the mass spectrometry analysis showed no presence of P13 due to a high contamination with keratin but identified OspC as a possible second component of the complex. This association between transmembrane proteins and lipoproteins had already been observed in *Borrelia*. For example, the association between P66 and OspA was established in a former study [125]. OspA was postulated to act as a protective lipoprotein that limits the access to P66 and reduce its exposure to the host immune system.

In the gel done with different strains of *B. burgdorferi* (Fig. 6-5), a thick 350 kDa band was seen in the B31 wild type strain. This band disappeared completely in the P13-18 samples where P13 is knock-out. P13 seems to be definitely a component of this complex.

One last problem must be addressed concerning the P13-18 strain. This mutant was made from *B. burgdorferi* B31-A, a noninfectious high-passage B31 clone [126]. Plasmids are often lost during in vitro cultivation of *B. burgdorferi* [127, 128]. OspC is contained in the cp26 plasmid. This plasmid encodes essential proteins like ResT and other proteins and cannot be displaced [129]. Therefore cp26 is present in all natural isolates and has never been lost during in vitro cultivation [3, 130-132]. The loss of the 350 kDa band cannot be attributed to the loss of the cp26 plasmid. In the same way, the absence of the band due the loss of proteins from other plasmids or the influx of those in the OspC expression cannot totally be excluded.

A faint 350 kDa band can be also noticed in the B313 samples. OspC is not present in this strain and consequently if it is part of the complex, the band should have disappeared completely in this strain. However, there are studies where it is claimed that other lipoproteins with similar molecular weight and structure like VslE, could replace OspC [133, 134]. This could be an explanation for the appearance of the faint 350 kDa band.

The difference in the 350 kDa band intensity when comparing B313 to B31 samples cannot be attributed to a different protein concentration between samples. The samples were centrifuged preceding the load of the gel and pellets were visible. This indicates an excess of protein that could not be solubilized by the detergent. This fact should equalize to a certain extend the protein concentration between samples.

In the B313 strain is also noteworthy the apparition of a 150 kDa band (Fig. 6-5). In the P13-WB from the same gel (Fig. 6-6), this band reacted strongly with the P13 antibody. If the 350 kDa band is a complex formed by P13 and OspC, the 150 kDa band may be the part of this complex formed by P13. The association with OspC might explain the increase in molecular weight. This hypothesis is supported by the surprising observation of a 150 kDa band in a sample from tobacco plants where rP13 was expressed. This band together with another one of approximately half the molecular weight reacted against the P13 antibody.

To sum up, the 480 kDa complex seems to be composed only by P66. The band clearly bound Coomassie stain and P66 has a pI of 5.3. Fulfilling these two characteristics the maximal deviation calculated for the BN-Page is 15 %. Therefore the real molecular weight for the P66 complex should be 480±72 kDa. In contrast, if the 350 kDa band is a complex formed at least in part for P13 which pI is 9.5, the determination of its real molecular weight could vary to a greater extend. A previous molecular weight calibration of BN-Page showed that some extremely basic proteins like P13 had a lower migration distances in BN-Page appearing to have a higher molecular weight [94]. Therefore, a concrete range value of the molecular weight of the P13 complex cannot be given.

6.2.2 Pore forming activity of the 350 and 480 kDa bands

The pore forming activity of both complexes could be measured in BLB experiments. Previous studies proclaimed that P66 and P13 formed holes in the outer membrane of *Borrelia*. The conductance for the pore formed by P66 was estimated to be between 9 and 11 nS in 1 M KCl [51, 52] while in the same salt solution P13 had a conductance of 3,5 nS [56, 57]. To confirm

this pore forming activity the 480 and 350 kDa band were excised from the gel and eluted in a detergent containing solution.

Both samples exhibited pore forming activities in artificial membranes. The P66 complex showed an 11nS activity and a 5.5 nS activity in a lower frequency. This observation reinforce the hypothesis of P66 being a symmetric complex that can be separated in half by solubilization with detergents. This is not only supported by an activity with half of the conductance but also by the observation of a band with approximately half of the MW in the BN-Page WB for P66.

In regards to the P13 band extraction a 3.5 nS activity was expected. However, none of the different samples isolated from different BN-Page showed a similar activity. The BLB measurements of the 350 kDa band and the realization of the corresponding histogram revealed a 0.6 nS activity. This find is in high contrast with the previous pore forming activity characterization of P13 published elsewhere [56]. The pores observed from the elution of the 350 kDa band had some noise and after 3 or 4 insertions it was difficult to differentiate the exact conductance of new insertions. Although the noise was very high from that point on, the conductance of the membrane increased constantly.

A 0.6 nS pore forming activity was previously described together with a 12.6 nS activity in outer membrane vesicles from *B. burgdorferi* B31 [135]. The 0.6 nS activity was afterwards attributed to Oms28 by the same group [59]. But recent studies show the lack of porin-like properties in Oms28 [61]. The existence of a protein in the outer membrane of *Borrelia* with a 0.6 nS pore forming activity has been observed several times when B-fractions were analyzed with the BLB assay. The 350 KDa complex isolated from BN-Page where P13 is involved have a pore forming activity with the same conductance and therefore is a candidate to be the protein responsible for such activity.

An unproven explanation for the 3.5 nS activity attributed previously to P13 could be a further disruption of the P66 complex. In the same way as observed before, P66 could not only break in two halves, but maybe in four, producing smaller complexes with a pore conductance of around 3 nS. A previous observation when the B-fraction from a *p66* knock-out was measured in BLB could support this hypothesis. This B-fraction showed no 3.5 nS activity at all and a double *p13/p66* knock-out reduced the conductance of the porins in the sample to 300 pS or below [122].

If the association between P13 and OspC to form the 350 kDa complex is confirmed, further studies will be required to clarify if OspC forms part of the channel or it has another function, like for example the protection of P13 from the host immune system.

Equipment, Materials and buffers

7.1 Lab equipment

Autoclave	KSG
Balance	Kern
"Black Lipid Bilayer" device	own fabrication
BLB Amplifier	own fabrication
BLB Electrodes	Metrohm
BLB Electrometer	Keithley 617
BLB Magnetic stirrer	Hanna Instruments
BLB Oscilloscope	OWON
BLB Recorder	Rikadenki
BLB Teflon chamber	Own fabrication
BLB telescope	Spindler und Hoyer
BLB voltage source	own fabrication
Centrifuge, cooled 15/50 ml tubes	Beckmann, Heraeus
Centrifuge (Table)	Eppendorf
Centrifuge (Ultracentrifuge)	Beckmann
French press	SLM Instruments, Inc.
FPLC	Amersham Biosciences
Gel-fotography / UV cabinet	LTF Labortechnik
Gel voltage source	Bio-Rad
Laminar flow cabinet	Gelaire
Magnetic stirrer	Hartenstein
Microwave	Moulinex
PCR machine	Perkin Elmer, Eppendorf

pH meter	WTW
Pipettes	Eppendorf, Gilson, SLG, Brand
Precision balance	Sartorius
Protein electrophoresis chamber	Bio-Rad, Invitrogen
Shaker	GFL
Shaker (vascular movement)	Heidolph
Spectrophotometer	Amersham Biosciences
Stove	Memmert
Vortex	Hartenstein
Water purifier	Millipore
Western-blots device	Bio-Rad, Invitrogen

7.2 Materials

The experiments to elaborate this thesis were done with materials bought by the Biotechnology Department of the University of Wuerzburg.

- Chemical products: Sigma, Roth, Merck, Bio-Rad, Difco.
- Lipids to form artificial membranes: Avanti Polar Lipids.
- Restriction Endonucleases: Fermentas GmbH, NEB
- PVDF membranes: Roth
- Disposable materials: Falcon, Greiner, Eppendorf, Fortuna, Primo, Roth, etc.

7.3 Commercial Kits

Kits used in this work:

"QIAquick Gel Extraction Kit Qiagen"- DNA purification from Agarose gels.

"QIAquick PCR Purification Kit Qiagen" – Purification and concentration of PCR products.

"QIAprep Spin Miniprep Kit Qiagen" – Bacterial DNA isolation.

"Ni-NTA Spin Kit Qiagen" – "His-tag" protein purification.

"ECL- detection kit" GE Healthcare – Western blot development.

"TOPO TA Cloning® Kit" Invitrogen – Cloning and transformation of *E. coli* cells

"Taq- Kit Fermentas Polymerase" – PCR components

"Pfu- Kit Fermentas Polymerase" – PCR components

7.4 Molecular weight markers.

DNA molecular weight markers:

GeneRuler™ 100bp Marker (Fermentas)

MassRuler™ DNA Ladder Mix (Fermentas)

Protein molecular weight markers:

LMW-Marker (Amersham Biosciences)

Precision Plus Protein Prestained Standard (Dual Color) (Bio-Rad)

PageRuler™ Prestained Protein Ladder, Fermentas

NativeMark Unstained, Invitrogen

7.5 .Buffers and Solutions

Whenever the pH needed to be corrected, HCl (1M and 5M) and NaOH (1M) solutions were used.

- Media and buffers to prepare the outer membrane of *Borrelia*.

BSK II médium to cultivate *Borrelia*.

TSM Buffer	10 mM Tris (pH 7,5)
	150 mM NaCl
	1 M $MgCl_2$

TSEA Buffer	10 mM Tris (pH 7,5)
	150 mM NaCl
	10 mM EDTA
	0,05 % NaN_3

- Buffer to prepare *Agrobacterium* competent cells:

TE Buffer	10 mM Tris (pH 5, HCl)
	1 mM EDTA

- Extraction buffer for *Nicotiana benthamiana*:

50 mM NaH_2PO_4
50mM NaCl
50 mM Ascorbate
0.4 % LDAO
pH 8

- Buffers and solutions for SDS-PAGE:

	Stacking gel (5 %)	***Separation gel (12 %)***
H_2O_{dd}	1.72 ml	3.3 ml
30% Polyacrylamide	0.76 ml	4.0 ml
1 M Tris (pH 6,8)	0.76 ml	---
1,5 M Tris (pH 8,8)	---	2.5 ml
10% SDS	0.03 ml	0.1 ml
10% APS	0.03 ml	0.1 ml
TEMED	0.006 ml	0.008 ml

* The indicated volumes are enough to prepare 2 SDS-Page, 1mm.

SDS-Page Running Buffer (1x Laemmli Buffer)	3.1 g Tris
	1.0 g SDS
	14.4 g Glycine
	up to 1000 ml H_2O_{dd}
MOPS SDS-Page Running Buffer (1x)	10.4 g MOPS
	6 g Tris Base
	1 g SDS
	0.3 g EDTA
	up to 1000 ml H_2O_{dd}
REDMIX Sample buffer (4x)	2.5 ml 0,5 M Tris (pH 6,8)
	4.0 ml 10 % SDS
	1.0 ml ß-Mercaptoethanol
	2.0 ml Glycerol
	0.01 % Bromophenol blue

- Silver nitrate staining solutions:

Solution A (1x)	20 ml Ethanol
	25 µl formaldehyde (37%)
	up to 50 ml H_2O_{dd}
Solution B (5x)	0.5 g $Na_2S_2O_3$
	up to 500 ml H_2O_{dd}
Solution C (1x)	0.05-0.08 g $AgNO_3$
	up to 50 ml H_2O_{dd}

Solution D (5x)	75 g Na_2CO_3
	up to 50 ml H_2O_{dd}

- Western Blot Buffers

Towbin Buffer	3.03 g Tris
	14.4 g Glycine
	200 ml Methanol
	1 g SDS
	up to 1000 ml H_2O_{dd}
Nu-Page Transfer Buffer	4.8 gr Bicine
	5.2 g Bis-Tris
	0.3 g EDTA
	200 ml Methanol
	up to 1000 ml H_2O_{dd}
TBS Buffer (10X)	24.2 g Tris
	80 g NaCl
	38 ml HCl (1M)
	up to 1000 ml H_2O_{dd}
TBS + Tween Buffer (1X)	100 ml 10x TBS buffer
	1 ml Tween 20
	up to 1000 ml H_2O_{dd}
Milk/BSA Buffer (5%)	0.5 g BSA
	up to 10 ml Buffer TBS (1X)

- FPLC Buffers

MonoQ

Low salt concentration buffer (Inlet A)	10 mM Tris (pH 8)
	0.4 % LDAO
High salt concentration buffer (Inlet B)	10 mM Tris (pH 8)
	0.4 % LDAO
	1 M NaCl

Superdex

	10 mM Tris (pH 8)
	150 mM NaCl
	0.4 % LDAO

- Buffers and solutions for the agarose gel electrophoresis:

Agarose gel (1%)	2 g agarose
	up to 200 ml H_2O_{dd}
TAE buffer (50x)	242 g Tris
	57.1 ml Acetic acid
	100 ml 0.5 M EDTA
	up to 1000 ml H_2O_{dd}
Ethidium bromide bath	10 mg/ml ethidium bromide

7.6 Culture media and agar plates:

LB (Luria Bertani) medium	10 g Bactotryptone 5 g yeast extract 10 g NaCl up to 1.000 ml H_2O_{dd}
LB plates	15 g Agar up to 1.000 ml LB medium
LB/Amp plates	15 g Agar 1.000 µl (100 mg/ml) Ampicillin up to 1.000 ml LB medium
Amp/IPTG/X-Gal Plates	15 g Agar 1.000 µl Ampicillin (100 mg/ml) 20 µl IPTG (200 mM) 40 µl X-Gal up to 1.000 ml LB medium

7.7 Bacterial strains

-Strains used to compare the porin content in different species or strains within the genus *Borrelia*:

B. burgdorferi B31 (ATCC 35210), P13-18 [122], B313 [121]

B. afzelii K78 [136]

B. garinii PBi [137]

B. duttonii 1120K3 [138]

B. hermsii HS1 (ATCC 35209)

B. recurrentis A1 [139]

- Bacterial species/strains used to obtain rP13:

E. coli One Shot® TOP10F'

E. coli BL21 Omp8 Rosetta

Agrobacterium tumefaciens

7.8 Plasmids, primers and gene sequences.

Plasmids:

• pCR®2.1-TOPO® (Invitrogen) (Clonning vector)

Size: 3.9 kb

Important fragments: *lac*Zα, f1 ori, kanamycin resistance, Ampicillin resistance,

pUC ori, P_{lac}

• pARAJS2 (expression vector)

Size: 5.942 kb

Important fragments: ampicillin resistance

• pICH31660 (expression vector in the tobacco plant)

Size: 6440 bp

Important fragments: kanamycin resistance.

• Rosetta

Important fragments: tRNA genes for the following codons: AGG, AGA, AUA, CUA, CCC, GGA.

Chloranphenicol resistance (This plasmid was obtained from *E. coli* Rosetta (DE3) pLys)

Color caption for DNA and protein sequences:

P13 mature gen	P13 C-terminus	Histidine-tag
E. coli signal sequence	Factor Xa Protease	**Restriction site**
Start/Stop codon	Primer	

Primers:

Primer E	CAACATCAACTCGAGGTTCTAGACCTCATTAAGCTACAT
Primer F	GACTCGAGGCAATCTAGAATTGCAATCAC
Primer G	CTAGCCATGGTCAAGCTAATGATTCTAAAAATG
Primer H	TTTGGTCTCAAGGTATGCGGGCGAAACTCCTAGGAATAG
MIp13F	TTTGGTCTCAAGGTATGCATCACCATCACCATCACGGCATTGAAGGCCGCA CTCAAGCTAATGATTCTAAAAATGGTG
MIp13R:	TAGGGTCTCAAAGCTCTAGATTAAGCTACATTAAGGCTATTTTTTAGC

DNA - Construct 1 in pCR®2.1-TOPO vector (primers G and E):

CTAGCCATGGTCAAGCTAATGATTCTAAAAATGGTGCGTTTGGGATGAGTGCTGGAGAAAAACTTTTG
GTTTATGAAACTAGCAAGCAAGATCCTATTGTACCATTTTTATTGAACCTTTTTTTAGGGTTTGGAATAG
GCTCCTTTGCTCAAGGAGATATTCTTGGAGGTTCTCTTATTCTTGGATTTGATGCGGTTGGTATAGGGCT
TATACTTGCGGGGGCTTATTTGGATATCAAAGCGCTTGATGGTATTACTAAAAAAGCTGCTTTTCAATG
GACTTGGGGTAAGGGAGTTATGTTAGCAGGTGTGGTTACTATGGCTGTGACAAGATTAACAGAAATTA
TTCTTCCATTTACATTTGCTAATAGTTATAATAGGAAGCTAAAAAATAGCCTTAATGTAGCTTAATGAGG
TCTAGAACCTCGAGTTG

DNA - Construct 1 in the pARAJS2 vector (primers H and E):

TTTGGTCTCAAGGTATGCGGGCGAAACTCCTAGGAATAGTCCTGACAACCCCTATCGCGATCAGCTCTT
TTGCGTCGACGCATCATCACCATCACCATCACCATCACCACGGCGCCGAAGGCCGCCCCGGGATCCATG
GTCAAGCTAATGATTCTAAAAATGGTGCGTTTGGGATGAGTGCTGGAGAAAAACTTTGGTTTATGAAA
CTAGCAAGCAAGATCCTATTGTACCATTTTTATTGAACCTTTTTTTAGGGTTTGGAATAGGCTCCTTTGCT

CAAGGAGATATTCTTGGAGGTTCTCTTATTCTTGGATTTGATGCGGTTGGTATAGGGCTTATACTTGCG
GGGGCTTATTTGGATATCAAAGCGCTTGATGGTATTACTAAAAAAGCTGCTTTTCAATGGACTTGGGGT
AAGGGAGTTATGTTAGCAGGTGTGGTTACTATGGCTGTGACAAGATTAACAGAAATTATTCTTCCATTT
ACATTTGCTAATAGTTATAATAGGAAGCTAAAAAAATAGCCTTAATGTAGCTTAATGAGGTCTAGAACCT
CGAGTTG

Protein - Construct 1:

MRAKLLGIVLTTPIAISSFASTHHHHHHHHHHGAEGRPGIHGQANDSKNGAFGMSAGEKLLVYETSKQDPI
VPFLLNLFLGFGIGSFAQGDILGGSLILGFDAVGIGLILAGAYLDIKALDGITKKAAFQWTWGKGVMLAGVVT
MAVTRLTEIILPFTFANSYNRKLKNSLNVA-

DNA - Construct 2 in the pCR®2.1-TOPO vector (primers G and F):

CTAGCCATGGTCAAGCTAATGATTCTAAAAATGGTGCGTTTGGGATGAGTGCTGGAGAAAAACTTTTG
GTTTATGAAACTAGCAAGCAAGATCCTATTGTACCATTTTTATTGAACCTTTTTTTAGGGTTTGGAATAG
GCTCCTTTGCTCAAGGAGATATTCTTGGAGGTTCTCTTATTCTTGGATTTGATGCGGTTGGTATAGGGCT
TATACTTGCGGGGGCTTATTTGGATATCAAAGCGCTTGATGGTATTACTAAAAAAGCTGCTTTTCAATG
GACTTGGGGTAAGGGAGTTATGTTAGCAGGTGTGGTTACTATGGCTGTGACAAGATTAACAGAAATTA
TTCTTCCATTTACATTTGCTAATAGTTATAATAGGAAGCTAAAAAATAGCCTTAATGTAGCTTTAGGAGG
ATTTGAACCTAGTTTTGATGTTGCAATGGGCCAATCCAGTGCTCTTGGGTTTGAACTGTCTTTCAAAAAA
AGCTATTAATTTTATTTATTACAAAAATGGGTGATTGCAATTCTAGATTGCCTCGAGTC

DNA - Construct 2 in the pARAJS2 vector (primers H and F):

TTTGGTCTCAAGGTATGCGGGCGAAACTCCTAGGAATAGTCCTGACAACCCCTATCGCGATCAGCTCTT
TTGCGTCGACGCATCATCACCATCACCATCACCATCACCACGGCGCCGAAGGCCGCCCCGGGATCCATG
GTCAAGCTAATGATTCTAAAAATGGTGCGTTTGGGATGAGTGCTGGAGAAAAACTTTTGGTTTATGAAA
CTAGCAAGCAAGATCCTATTGTACCATTTTTATTGAACCTTTTTTTAGGGTTTGGAATAGGCTCCTTTGCT
CAAGGAGATATTCTTGGAGGTTCTCTTATTCTTGGATTTGATGCGGTTGGTATAGGGCTTATACTTGCG
GGGGCTTATTTGGATATCAAAGCGCTTGATGGTATTACTAAAAAAGCTGCTTTTCAATGGACTTGGGGT
AAGGGAGTTATGTTAGCAGGTGTGGTTACTATGGCTGTGACAAGATTAACAGAAATTATTCTTCCATTT
ACATTTGCTAATAGTTATAATAGGAAGCTAAAAAATAGCCTTAATGTAGCTTTAGGAGGATTTGAACCT

AGTTTTGATGTTGCAATGGGCCAATCCAGTGCTCTTGGGTTTGAACTGTCTTTCAAAAAAAGCTATTAAT

TTTATTTATTACAAAAATGGGTGATTGCAATTCTAGATTGCCTCGAGTC

Protein - Construct 2:

MRAKLLGIVLTTPIAISSFASTHHHHHHHHHHGAEGRPGIHGQANDSKNGAFGMSAGEKLLVYETSKQDPI

VPFLLNLFLGFGIGSFAQGDILGGSLILGFDAVGIGLILAGAYLDIKALDGITKKAAFQWTWGKGVMLAGVVT

MAVTRLTEIILPFTFANSYNRKLKNSLNVALGGFEPSFDVAMGQSSALGFELSFKKSY-

DNA in pICH31160 (primers MIp13F and MIp13R):

TTT*GGTCTC*AAGGTATGCATCACCATCACCATCACGGCATTGAAGGCCGCACTCAAGCTAATGATTCTA

AAAATGGTGCGTTTGGGATGAGTGCTGGAGAAAAACTTTTGGTTTATGAAACTAGCAAGCAAGATCCT

ATTGTACCATTTTTATTGAACCTTTTTTTAGGGTTTGGAATAGGCTCCTTTGCTCAAGGAGATATTCTTGG

AGGTTCTCTTATTCTTGGATTTGATGCGGTTGGTATAGGGCTTATACTTGCGGGGGCTTATTTGGATATC

AAAGCGCTTGATGGTATTACTAAAAAAGCTGCTTTTCAATGGACTTGGGGTAAGGGAGTTATGTTAGCA

GGTGTGGTTACTATGGCTGTGACAAGATTAACAGAAATTATTCTTCCATTTACATTTGCTAATAGTTATA

ATAGGAAGCTAAAAAATAGCCTTAATGTAGCTTAA*TCTAGA*GCTTTGAGACCCTA

Protein – Tobacco plants:

MHHHHHHGIEGRTQANDSKNGAFGMSAGEKLLVYETSKQDPIVPFLLNLFLGFGIGSFAQGDILGGSLILGF

DAVGIGLILAGAYLDIKALDGITKKAAFQWTWGKGVMLAGVVTMAVTRLTEIILPFTFANSYNRKLKNSLNV

A-

7.9 PCR preparation

- Cloning PCR

Master Mix	2.5 µl	Pfu-Buffer
	0.5 µl	100 pM forward primer
	0.5 µl	100 pM reverse primer
	2.5 µl	2 mM dNTPs
	0.5 µl	Pfu-Polymerase
	200-300 ng	*Borrelia* DNA
	up to 25 µl	H_2O_{dd}

Step PCR temperature parameters:

Const. 1	5 min, 95 °C	
	1 min, 95 °C	5 cycles
	1 min, 50 °C	
	2 min, 72 °C	
	1 min, 95 °C	25 cycles
	1 min, 55 °C	
	2 min, 72 °C	
	10 min, 72 °C	
	∞ 4 °C	

Const. 2	5 min, 95 °C	
	1 min, 95 °C	5 cycles
	1 min, 45 °C	
	2 min, 72 °C	
	1 min, 95 °C	25 cycles
	1 min, 50 °C	
	2 min, 72 °C	
	10 min, 72 °C	
	∞ 4 ºC	

- Standard (Check) PCR

Master Mix	14.9 µl	H_2O_{dd}
	2.5 µl	10x Buffer (+KCl −$MgCl_2$)
	1.5 µl	25 mM $MgCl_2$
	0.5 µl	100 pM forward primer
	0.5 µl	100 pM reverse primer
	2.5 µl	2 mM dNTPs
	0.5 µl	Taq- Polymerase
	1	Colony

Std PCR temperature parameters	5 min 95 °C 1 min 95 °C 1 min 55 °C 2 min 72 °C 10 min 72 °C ∞ 4 ºC	25 cycles

7.10 Antibodies

Name	***Directed against***	***Dilution in TBS***	***Producer***
α- P66 mAb	P66	1:500	Dep. Microbiol. Umeå
α- P13 rAb	P13	1:3000	Dep. Microbiol. Umeå
α- mouse IgG	mouse antibodies	1:3000	GE Healthcare
α- rabbit IgG	rabbit antibodies	1:3000	GE Healthcare

Abbreviations

A	A	Adenine
	Ag	Silver
	AgCl	silver chloride
	$AgNO_3$	silver nitrate
	Amp	Ampicillin
	APS	Ammonium persulfate
	A. tumefaciens	*Agrobacterium tumefaciens*
B	B.	*Borrelia*
	B.a	*Borrelia afzelii*
	B.b	*Borrelia burgdorferi*
	B.d	*Borrelia duttonii*
	B.g	*Borrelia garinii*
	B.h	*Borrelia hermsii*
	bp	base pair
	B.r	*Borrelia recurrentis*
	BSA	Bovine Serum Albumin
C	C	Cytosine
	Cl^-	Chlorine anion
D	DNA	Deoxyribonucleic acid
	dNTP	Deoxyribonucleotide triphosphate

E	*E. coli*	*Escherichia coli*
	ECL	Enhanced Chemiluminescence
	ESS	*Escherichia* Signal Sequence
F	Fig.	Figure
	FPLC	Fast Performance Liquid Chromatography
G	G	Guanosine
	g	Gravity acceleration constant
H	H_2O_{dd}	Double distilled water
	HCl	Hydrochloric acid
I	IPTG	Isopropyl-β-D-Thiogalactopyranoside
K	KCl	Potassium chloride
	kDa	Kilodalton
L	LB	Luria-Bertani
	LDAO	Lauryl Dimethyl Ammonium Oxide
	LMW	Low Molecular Weight
M	mA	Miliampere
	mg	Milligram
	$MgCl_2$	Magnesium chloride
	min	Minute
	ml	Milliliter
	mM	Millimolar
	mV	Millivolts

N	NaCl	Sodium chloride
	Na_2CO_3	Sodium carbonate
	NaH_2PO_4	Sodium dihydrogen phosphate
	NaN_3	Sodium azide
	NaOH	Sodium hydroxide
	$Na_2S_2O_3$	Sodium thiosulphate
	Ni-NTA	Nickel-nitrilotriacetic acid
	ng	Nanogram
	nS	Nanosiemen
O	OD	Optical density
P	pA	Picoampere
	Page	Polyacrylamide gel electrophoresis
	PCR	Polymerase Chain Reaction
	Prof.	Professor
	pM	Picomolar
	pS	Picosiemens
	Pfu	Pyrococcus furiosus
	PVDF	Polyvinylidene fluoride
R	rP13	recombinant P13
	rpm	Revolutions per minute
S	SDS	Sodium dodecyl sulphate
T	T	Thymine
	TAE	Tris-Acetat-EDTA
	Taq	Thermus aquaticus
	TBS	Tris Buffered Saline

	TEMED	N,N,N´-Tetramethylenediamine
	Tris	Trishydroxymethylaminomethane
U	UV	Ultraviolet
W	WB	Western-blot
X	X-gal	5-Bromo-4-Chloro-3-Indolyl-β-D-Galactoside
α	α-mouse	mouse antibodies
	α-rabit	rabbit antibodies
	α-P13	Antibodies against P13
	α-P66	Antibodies against P66
µ	µgr	Microgram
	µl	Microliter
	µm	Micrometer

References

1. Johnson, R.C., *The spirochetes.* Annu Rev Microbiol, 1977. **31**: p. 89-106.
2. Fraser, C.M., et al., *Genomic sequence of a Lyme disease spirochaete, Borrelia burgdorferi.* Nature, 1997. **390**(6660): p. 580-6.
3. Casjens, S., et al., *A bacterial genome in flux: the twelve linear and nine circular extrachromosomal DNAs in an infectious isolate of the Lyme disease spirochete Borrelia burgdorferi.* Mol Microbiol, 2000. **35**(3): p. 490-516.
4. Madigan, M.T., J.M. Martinko, and J. Parker, eds. *Brock Mikrobiologie*. 2001, Spektrum Akademischer Verlag Heidelberg. Deutschland.
5. Shamaei-Tousi, A., *Pathobiological effects of erythrocyte-rosetting Borrelia crocidurae*, in *Department of Molecular Biology*. 2000, Umeå University.
6. Satz, N., ed. *Klinik der Lyme-Borreliose.* 2. Auflage ed. 2002, Verlag Hans Huber.
7. Oschmann, P. and P. Kraiczy, eds. *Lyme-Borreliose und Fhühsommer-Meningoenzephalitis*. 1998, Uni-Med Verlag.
8. Barbour, A.G. and S.F. Hayes, *Biology of Borrelia species.* Microbiol Rev, 1986. **50**(4): p. 381-400.
9. Goldstein, S.F., K.F. Buttle, and N.W. Charon, *Structural analysis of the Leptospiraceae and Borrelia burgdorferi by high-voltage electron microscopy.* J Bacteriol, 1996. **178**(22): p. 6539-45.
10. Motaleb, M.A., et al., *Borrelia burgdorferi periplasmic flagella have both skeletal and motility functions.* Proc Natl Acad Sci U S A, 2000. **97**(20): p. 10899-904.
11. Shi, W., et al., *Chemotaxis in Borrelia burgdorferi.* J Bacteriol, 1998. **180**(2): p. 231-5.
12. Barbour, A.G., *Isolation and cultivation of Lyme disease spirochetes.* Yale J Biol Med, 1984. **57**(4): p. 521-5.
13. Plank, L.D. and J.D. Harvey, *Generation time statistics of Escherichia coli B measured by synchronous culture techniques.* J Gen Microbiol, 1979. **115**(1): p. 69-77.
14. Barbour, A.G., *Antigenic variation of a relapsing fever Borrelia species.* Annu Rev Microbiol, 1990. **44**: p. 155-71.
15. Woese, C.R., *Bacterial evolution.* Microbiol Rev, 1987. **51**(2): p. 221-71.
16. Steere, A.C., et al., *Lyme arthritis: an epidemic of oligoarticular arthritis in children and adults in three connecticut communities.* Arthritis Rheum, 1977. **20**(1): p. 7-17.
17. Buchwald, A., *Ein Fall von diffuser idiopathischer Haut-Artrophie.* Archives of dermatological research, 1883: p. 553-556.
18. Afzelius, A., *Erythema migrans.* Acta Derm Venereol 1921. **2**: p. 120-125.
19. Burgdorfer, W., et al., *Lyme disease-a tick-borne spirochetosis?* Science, 1982. **216**(4552): p. 1317-9.
20. Burgdorfer, W., *Discovery of the Lyme disease spirochete and its relation to tick vectors.* Yale J Biol Med, 1984. **57**(4): p. 515-20.
21. Cutler, S.J., *Possibilities for relapsing fever reemergence.* Emerg Infect Dis, 2006. **12**(3): p. 369-74.
22. Bryceson, A.D., et al., *Louse-borne relapsing fever.* Q J Med, 1970. **39**(153): p. 129-70.
23. Obermeier, O., Zentbl. med. Wiss., 1873. **10**: p. 145.
24. Dutton, J. and J. Todd, *The nature of tick fever in the eastern part of the Congo Free State.* BMJ., 1905. **ii**: p. 1259–60.

25. Cutler, S.J., *Relapsing fever--a forgotten disease revealed.* J Appl Microbiol, 2010. **108**(4): p. 1115-22.
26. Doury, P., *[Henry Foley and the discovery in 1908 of the role played by the louse in the transmission of relapsing fever].* Hist Sci Med, 1996. **30**(3): p. 363-9.
27. Goubau, P.F., *Relapsing fevers. A review.* Ann Soc Belg Med Trop, 1984. **64**(4): p. 335-64.
28. Fournier, P.E., et al., *Human pathogens in body and head lice.* Emerg Infect Dis, 2002. **8**(12): p. 1515-8.
29. Sonenshine, D.E., *Biology of Ticks*. Vol. I. 1997: Oxford University Press.
30. Dupont, H.T., et al., *A focus of tick-borne relapsing fever in southern Zaire.* Clin Infect Dis, 1997. **25**(1): p. 139-44.
31. Mitani, H., A. Talbert, and M. Fukunaga, *New World relapsing fever Borrelia found in Ornithodoros porcinus ticks in central Tanzania.* Microbiol Immunol, 2004. **48**(7): p. 501-5.
32. CDC. *Epidemiology and repoting of tick-borne relapsing fever.*; Available from: www.cdc.gov.
33. Belisle, J.T., et al., *Fatty acids of Treponema pallidum and Borrelia burgdorferi lipoproteins.* J Bacteriol, 1994. **176**(8): p. 2151-7.
34. Takayama, K., R.J. Rothenberg, and A.G. Barbour, *Absence of lipopolysaccharide in the Lyme disease spirochete, Borrelia burgdorferi.* Infect Immun, 1987. **55**(9): p. 2311-3.
35. Brandt, M.E., et al., *Immunogenic integral membrane proteins of Borrelia burgdorferi are lipoproteins.* Infect Immun, 1990. **58**(4): p. 983-91.
36. Radolf, J.D., et al., *Analysis of Borrelia burgdorferi membrane architecture by freeze-fracture electron microscopy.* J Bacteriol, 1994. **176**(1): p. 21-31.
37. Walker, E.M., et al., *Analysis of outer membrane ultrastructure of pathogenic Treponema and Borrelia species by freeze-fracture electron microscopy.* J Bacteriol, 1991. **173**(17): p. 5585-8.
38. Trias, J., V. Jarlier, and R. Benz, *Porins in the cell wall of mycobacteria.* Science, 1992. **258**(5087): p. 1479-81.
39. Zeth, K. and M. Thein, *Porins in prokaryotes and eukaryotes: common themes and variations.* Biochem J, 2010. **431**(1): p. 13-22.
40. Benz, R., *Solute uptake through bacterial outer membranes.*, in *Bacterial Cell Wall*, J.M. Ghuysen and R. Hakenbeck, Editors. 1994, Elsevier Science. p. 397-423.
41. Achouak, W., T. Heulin, and J.M. Pages, *Multiple facets of bacterial porins.* FEMS Microbiol Lett, 2001. **199**(1): p. 1-7.
42. Ye, J. and B. van den Berg, *Crystal structure of the bacterial nucleoside transporter Tsx.* EMBO J, 2004. **23**(16): p. 3187-95.
43. Basle, A., et al., *Crystal structure of osmoporin OmpC from E. coli at 2.0 A.* J Mol Biol, 2006. **362**(5): p. 933-42.
44. Koronakis, V., et al., *Crystal structure of the bacterial membrane protein TolC central to multidrug efflux and protein export.* Nature, 2000. **405**(6789): p. 914-9.
45. Benz, R., *Structure and function of porins from gram-negative bacteria.* Annu Rev Microbiol, 1988. **42**: p. 359-93.
46. Maier, C., et al., *Pore-forming activity of the Tsx protein from the outer membrane of Escherichia coli. Demonstration of a nucleoside-specific binding site.* J Biol Chem, 1988. **263**(5): p. 2493-9.
47. Benz, R., et al., *Characterization of the nucleoside-binding site inside the Tsx channel of Escherichia coli outer membrane. Reconstitution experiments with lipid bilayer membranes.* Eur J Biochem, 1988. **176**(3): p. 699-705.
48. Benz, R., A. Schmid, and G.H. Vos-Scheperkeuter, *Mechanism of sugar transport through the sugar-specific LamB channel of Escherichia coli outer membrane.* J Membr Biol, 1987. **100**(1): p. 21-9.
49. Hancock, R.E. and R. Benz, *Demonstration and chemical modification of a specific phosphate binding site in the phosphate-starvation-inducible outer membrane porin protein P of Pseudomonas aeruginosa.* Biochim Biophys Acta, 1986. **860**(3): p. 699-707.

50. Kim, B.H., C. Andersen, and R. Benz, *Identification of a cell wall channel of Streptomyces griseus: the channel contains a binding site for streptomycin.* Mol Microbiol, 2001. **41**(3): p. 665-73.
51. Barcena-Uribarri, I., et al., *P66 porins are present in both Lyme disease and relapsing fever spirochetes: a comparison of the biophysical properties of P66 porins from six Borrelia species.* Biochim Biophys Acta, 2010. **1798**(6): p. 1197-203.
52. Skare, J.T., et al., *The Oms66 (p66) protein is a Borrelia burgdorferi porin.* Infect Immun, 1997. **65**(9): p. 3654-61.
53. Coburn, J., et al., *Characterization of a candidate Borrelia burgdorferi beta3-chain integrin ligand identified using a phage display library.* Mol Microbiol, 1999. **34**(5): p. 926-40.
54. Coburn, J. and C. Cugini, *Targeted mutation of the outer membrane protein P66 disrupts attachment of the Lyme disease agent, Borrelia burgdorferi, to integrin alphavbeta3.* Proc Natl Acad Sci U S A, 2003. **100**(12): p. 7301-6.
55. Defoe, G. and J. Coburn, *Delineation of Borrelia burgdorferi p66 sequences required for integrin alpha(IIb)beta(3) recognition.* Infect Immun, 2001. **69**(5): p. 3455-9.
56. Ostberg, Y., et al., *Elimination of channel-forming activity by insertional inactivation of the p13 gene in Borrelia burgdorferi.* J Bacteriol, 2002. **184**(24): p. 6811-9.
57. Pinne, M., et al., *The BBA01 protein, a member of paralog family 48 from Borrelia burgdorferi, is potentially interchangeable with the channel-forming protein P13.* J Bacteriol, 2006. **188**(12): p. 4207-17.
58. Pinne, M., et al., *Molecular analysis of the channel-forming protein P13 and its paralogue family 48 from different Lyme disease Borrelia species.* Microbiology, 2004. **150**(Pt 3): p. 549-59.
59. Skare, J.T., et al., *Porin activity of the native and recombinant outer membrane protein Oms28 of Borrelia burgdorferi.* J Bacteriol, 1996. **178**(16): p. 4909-18.
60. Cluss, R.G., D.A. Silverman, and T.R. Stafford, *Extracellular secretion of the Borrelia burgdorferi Oms28 porin and Bgp, a glycosaminoglycan binding protein.* Infect Immun, 2004. **72**(11): p. 6279-86.
61. Mulay, V., et al., *Borrelia burgdorferi BBA74, a periplasmic protein associated with the outer membrane, lacks porin-like properties.* J Bacteriol, 2007. **189**(5): p. 2063-8.
62. Thein, M., et al., *Oms38 is the first identified pore-forming protein in the outer membrane of relapsing fever spirochetes.* J Bacteriol, 2008. **190**(21): p. 7035-42.
63. Magnarelli, L.A., J.F. Anderson, and A.G. Barbour, *Enzyme-linked immunosorbent assays for Lyme disease: reactivity of subunits of Borrelia burgdorferi.* J Infect Dis, 1989. **159**(1): p. 43-9.
64. Wessel, D. and U.I. Flugge, *A method for the quantitative recovery of protein in dilute solution in the presence of detergents and lipids.* Anal Biochem, 1984. **138**(1): p. 141-3.
65. Laemmli, U.K., *Cleavage of structural proteins during the assembly of the head of bacteriophage T4.* Nature, 1970. **227**(5259): p. 680-5.
66. Schagger, H. and G. von Jagow, *Blue native electrophoresis for isolation of membrane protein complexes in enzymatically active form.* Anal Biochem, 1991. **199**(2): p. 223-31.
67. Invitrogen, *NativePAGE™ Novex® Bis-Tris Gel System. A system for native gel electrophoresis*. 2006.
68. Reisinger, V. and L.A. Eichacker, *Solubilization of membrane protein complexes for blue native PAGE.* J Proteomics, 2008. **71**(3): p. 277-83.
69. Reisinger, V. and L.A. Eichacker, *How to analyze protein complexes by 2D blue native SDS-PAGE.* Proteomics, 2007. **7 Suppl 1**: p. 6-16.
70. Wittig, I., H.P. Braun, and H. Schagger, *Blue native PAGE.* Nat Protoc, 2006. **1**(1): p. 418-28.
71. Schagger, H., *Tricine-SDS-PAGE.* Nat Protoc, 2006. **1**(1): p. 16-22.
72. Blum, H., H. Beier, and H.J. Gross, *Improved silver staining of plant proteins, RNA and DNA in polyacrylamide gels.* Electrophoresis, 1987. **8**(2): p. 93-99.
73. Benz, R., et al., *Formation of large, ion-permeable membrane channels by the matrix protein (porin) of Escherichia coli.* Biochim Biophys Acta, 1978. **511**(3): p. 305-19.

74. Benz, R., K. Janko, and P. Lauger, *Ionic selectivity of pores formed by the matrix protein (porin) of Escherichia coli.* Biochim Biophys Acta, 1979. **551**(2): p. 238-47.
75. Ludwig, O., et al., *Pore formation by the mitochondrial porin of rat brain in lipid bilayer membranes.* Biochim Biophys Acta, 1986. **860**(2): p. 268-76.
76. Bezrukov, S.M. and M. Winterhalter, *Examining noise sources at the single-molecule level: 1/f noise of an open maltoporin channel.* Phys Rev Lett, 2000. **85**(1): p. 202-5.
77. Wohnsland, F. and R. Benz, *1/f-Noise of open bacterial porin channels.* J Membr Biol, 1997. **158**(1): p. 77-85.
78. Krasilnikov, O.V., et al., *A novel approach to study the geometry of the water lumen of ion channels: colicin Ia channels in planar lipid bilayers.* J Membr Biol, 1998. **161**(1): p. 83-92.
79. Towbin, H., T. Staehelin, and J. Gordon, *Electrophoretic transfer of proteins from polyacrylamide gels to nitrocellulose sheets: procedure and some applications.* Proc Natl Acad Sci U S A, 1979. **76**(9): p. 4350-4.
80. Prilipov, A., et al., *Coupling site-directed mutagenesis with high-level expression: large scale production of mutant porins from E. coli.* FEMS Microbiol Lett, 1998. **163**(1): p. 65-72.
81. Hofgen, R. and L. Willmitzer, *Storage of competent cells for Agrobacterium transformation.* Nucleic Acids Res, 1988. **16**(20): p. 9877.
82. Shang, E.S., et al., *Isolation and characterization of the outer membrane of Borrelia hermsii.* Infect Immun, 1998. **66**(3): p. 1082-91.
83. Bunikis, J., et al., *A surface-exposed region of a novel outer membrane protein (P66) of Borrelia spp. is variable in size and sequence.* J Bacteriol, 1998. **180**(7): p. 1618-23.
84. Benz, R., *Porin from bacterial and mitochondrial outer membranes.* CRC Crit Rev Biochem, 1985. **19**(2): p. 145-90.
85. Rostovtseva, T.K., E.M. Nestorovich, and S.M. Bezrukov, *Partitioning of differently sized poly(ethylene glycol)s into OmpF porin.* Biophys J, 2002. **82**(1 Pt 1): p. 160-9.
86. Berestovsky, G.N., V.I. Ternovsky, and A.A. Kataev, *Through pore diameter in the cell wall of Chara corallina.* J Exp Bot, 2001. **52**(359): p. 1173-7.
87. Kaulin, Y.A., et al., *Cluster organization of ion channels formed by the antibiotic syringomycin E in bilayer lipid membranes.* Biophys J, 1998. **74**(6): p. 2918-25.
88. Ternovsky, V.I., Y. Okada, and R.Z. Sabirov, *Sizing the pore of the volume-sensitive anion channel by differential polymer partitioning.* FEBS Lett, 2004. **576**(3): p. 433-6.
89. Vodyanoy, I. and S.M. Bezrukov, *Sizing of an ion pore by access resistance measurements.* Biophys J, 1992. **62**(1): p. 10-1.
90. Holz, R. and A. Finkelstein, *The water and nonelectrolyte permeability induced in thin lipid membranes by the polyene antibiotics nystatin and amphotericin B.* J Gen Physiol, 1970. **56**(1): p. 125-45.
91. Sabirov, R.Z., et al., *Relation between ionic channel conductance and conductivity of media containing different nonelectrolytes. A novel method of pore size determination.* Gen Physiol Biophys, 1993. **12**(2): p. 95-111.
92. Krasilnikov, O.V., et al., *A simple method for the determination of the pore radius of ion channels in planar lipid bilayer membranes.* FEMS Microbiol Immunol, 1992. **5**(1-3): p. 93-100.
93. McKim, S. and J.F. Hinton, *Evidence of xenon transport through the gramicidin channel: a 129Xe-NMR study.* Biochim Biophys Acta, 1994. **1193**(1): p. 186-98.
94. Schagger, H., W.A. Cramer, and G. von Jagow, *Analysis of molecular masses and oligomeric states of protein complexes by blue native electrophoresis and isolation of membrane protein complexes by two-dimensional native electrophoresis.* Anal Biochem, 1994. **217**(2): p. 220-30.
95. Nablo, B.J., et al., *Sizing the Bacillus anthracis PA63 channel with nonelectrolyte poly(ethylene glycols).* Biophys J, 2008. **95**(3): p. 1157-64.
96. Andersen, C., et al., *Study of sugar binding to the sucrose-specific ScrY channel of enteric bacteria using current noise analysis.* J Membr Biol, 1998. **164**(3): p. 263-74.

97. Andersen, C., M. Jordy, and R. Benz, *Evaluation of the rate constants of sugar transport through maltoporin (LamB) of Escherichia coli from the sugar-induced current noise.* J Gen Physiol, 1995. **105**(3): p. 385-401.
98. Jordy, M., et al., *Rate constants of sugar transport through two LamB mutants of Escherichia coli: comparison with wild-type maltoporin and LamB of Salmonella typhimurium.* J Mol Biol, 1996. **259**(4): p. 666-78.
99. Orlik, F., C. Andersen, and R. Benz, *Site-directed mutagenesis of tyrosine 118 within the central constriction site of the LamB (maltoporin) channel of Escherichia coli. II. Effect on maltose and maltooligosaccharide binding kinetics.* Biophys J, 2002. **83**(1): p. 309-21.
100. Denker, K., et al., *Site-directed mutagenesis of the greasy slide aromatic residues within the LamB (maltoporin) channel of Escherichia coli: effect on ion and maltopentaose transport.* J Mol Biol, 2005. **352**(3): p. 534-50.
101. Egli, C., et al., *Pore-forming properties of the major 53-kilodalton surface antigen from the outer sheath of Treponema denticola.* Infect Immun, 1993. **61**(5): p. 1694-9.
102. Kropinski, A.M., et al., *Isolation of the outer membrane and characterization of the major outer membrane protein from Spirochaeta aurantia.* J Bacteriol, 1987. **169**(1): p. 172-9.
103. Noppa, L., et al., *P13, an integral membrane protein of Borrelia burgdorferi, is C-terminally processed and contains surface-exposed domains.* Infect Immun, 2001. **69**(5): p. 3323-34.
104. Glenz, K., et al., *Production of a recombinant bacterial lipoprotein in higher plant chloroplasts.* Nat Biotechnol, 2006. **24**(1): p. 76-7.
105. Ostberg, Y., et al., *Pleiotropic effects of inactivating a carboxyl-terminal protease, CtpA, in Borrelia burgdorferi.* J Bacteriol, 2004. **186**(7): p. 2074-84.
106. Anbudurai, P.R., et al., *The ctpA gene encodes the C-terminal processing protease for the D1 protein of the photosystem II reaction center complex.* Proc Natl Acad Sci U S A, 1994. **91**(17): p. 8082-6.
107. Shestakov, S.V., et al., *Molecular cloning and characterization of the ctpA gene encoding a carboxyl-terminal processing protease. Analysis of a spontaneous photosystem II-deficient mutant strain of the cyanobacterium Synechocystis sp. PCC 6803.* J Biol Chem, 1994. **269**(30): p. 19354-9.
108. Mazmanian, S.K., H. Ton-That, and O. Schneewind, *Sortase-catalysed anchoring of surface proteins to the cell wall of Staphylococcus aureus.* Mol Microbiol, 2001. **40**(5): p. 1049-57.
109. Trost, J.T., et al., *The D1 C-terminal processing protease of photosystem II from Scenedesmus obliquus. Protein purification and gene characterization in wild type and processing mutants.* J Biol Chem, 1997. **272**(33): p. 20348-56.
110. Inagaki, N., et al., *Carboxyl-terminal processing protease for the D1 precursor protein: cloning and sequencing of the spinach cDNA.* Plant Mol Biol, 1996. **30**(1): p. 39-50.
111. Islam, M.R., J.H. Grubb, and W.S. Sly, *C-terminal processing of human beta-glucuronidase. The propeptide is required for full expression of catalytic activity, intracellular retention, and proper phosphorylation.* J Biol Chem, 1993. **268**(30): p. 22627-33.
112. Gollin, D.J., L.E. Mortenson, and R.L. Robson, *Carboxyl-terminal processing may be essential for production of active NiFe hydrogenase in Azotobacter vinelandii.* FEBS Lett, 1992. **309**(3): p. 371-5.
113. Hara, H., et al., *Cloning, mapping, and characterization of the Escherichia coli prc gene, which is involved in C-terminal processing of penicillin-binding protein 3.* J Bacteriol, 1991. **173**(15): p. 4799-813.
114. Hatchikian, E.C., et al., *Carboxy-terminal processing of the large subunit of [Fe] hydrogenase from Desulfovibrio desulfuricans ATCC 7757.* J Bacteriol, 1999. **181**(9): p. 2947-52.
115. Rossmann, R., et al., *Maturation of the large subunit (HYCE) of Escherichia coli hydrogenase 3 requires nickel incorporation followed by C-terminal processing at Arg537.* Eur J Biochem, 1994. **220**(2): p. 377-84.
116. Silber, K.R., K.C. Keiler, and R.T. Sauer, *Tsp: a tail-specific protease that selectively degrades proteins with nonpolar C termini.* Proc Natl Acad Sci U S A, 1992. **89**(1): p. 295-9.

117. Gils, M., et al., *High-yield production of authentic human growth hormone using a plant virus-based expression system.* Plant Biotechnol J, 2005. **3**(6): p. 613-20.
118. Giritch, A., et al., *Rapid high-yield expression of full-size IgG antibodies in plants coinfected with noncompeting viral vectors.* Proc Natl Acad Sci U S A, 2006. **103**(40): p. 14701-6.
119. Marillonnet, S., et al., *In planta engineering of viral RNA replicons: efficient assembly by recombination of DNA modules delivered by Agrobacterium.* Proc Natl Acad Sci U S A, 2004. **101**(18): p. 6852-7.
120. Bos, M.P., V. Robert, and J. Tommassen, *Biogenesis of the gram-negative bacterial outer membrane.* Annu Rev Microbiol, 2007. **61**: p. 191-214.
121. Sadziene, A., D.D. Thomas, and A.G. Barbour, *Borrelia burgdorferi mutant lacking Osp: biological and immunological characterization.* Infect Immun, 1995. **63**(4): p. 1573-80.
122. Pinne, M., et al., *Elimination of channel-forming activity by insertional inactivation of the p66 gene in Borrelia burgdorferi.* FEMS Microbiol Lett, 2007. **266**(2): p. 241-9.
123. Radolf, J.D. and M.J. Caimano, *The long strange trip of Borrelia burgdorferi outer-surface protein C.* Mol Microbiol, 2008. **69**(1): p. 1-4.
124. Nilsson, C.L., et al., *Characterization of the P13 membrane protein of Borrelia burgdorferi by mass spectrometry.* J Am Soc Mass Spectrom, 2002. **13**(4): p. 295-9.
125. Bunikis, J. and A.G. Barbour, *Access of antibody or trypsin to an integral outer membrane protein (P66) of Borrelia burgdorferi is hindered by Osp lipoproteins.* Infect Immun, 1999. **67**(6): p. 2874-83.
126. Bono, J.L., et al., *Efficient targeted mutagenesis in Borrelia burgdorferi.* J Bacteriol, 2000. **182**(9): p. 2445-52.
127. Barbour, A.G., *Plasmid analysis of Borrelia burgdorferi, the Lyme disease agent.* J Clin Microbiol, 1988. **26**(3): p. 475-8.
128. Schwan, T.G., W. Burgdorfer, and C.F. Garon, *Changes in infectivity and plasmid profile of the Lyme disease spirochete, Borrelia burgdorferi, as a result of in vitro cultivation.* Infect Immun, 1988. **56**(8): p. 1831-6.
129. Jewett, M.W., et al., *Genetic basis for retention of a critical virulence plasmid of Borrelia burgdorferi.* Mol Microbiol, 2007. **66**(4): p. 975-90.
130. Byram, R., P.E. Stewart, and P. Rosa, *The essential nature of the ubiquitous 26-kilobase circular replicon of Borrelia burgdorferi.* J Bacteriol, 2004. **186**(11): p. 3561-9.
131. Marconi, R.T., M.E. Konkel, and C.F. Garon, *Variability of osp genes and gene products among species of Lyme disease spirochetes.* Infect Immun, 1993. **61**(6): p. 2611-7.
132. Tilly, K., L. Lubke, and P. Rosa, *Characterization of circular plasmid dimers in Borrelia burgdorferi.* J Bacteriol, 1998. **180**(21): p. 5676-81.
133. Eicken, C., et al., *Crystal structure of Lyme disease variable surface antigen VlsE of Borrelia burgdorferi.* J Biol Chem, 2002. **277**(24): p. 21691-6.
134. Stewart, P.E., et al., *Delineating the requirement for the Borrelia burgdorferi virulence factor OspC in the mammalian host.* Infect Immun, 2006. **74**(6): p. 3547-53.
135. Skare, J.T., et al., *Virulent strain associated outer membrane proteins of Borrelia burgdorferi.* J Clin Invest, 1995. **96**(5): p. 2380-92.
136. Asbrink, E., B. Hederstedt, and A. Hovmark, *The spirochetal etiology of erythema chronicum migrans Afzelius.* Acta Derm Venereol, 1984. **64**(4): p. 291-5.
137. Wilske, B., et al., *An OspA serotyping system for Borrelia burgdorferi based on reactivity with monoclonal antibodies and OspA sequence analysis.* J Clin Microbiol, 1993. **31**(2): p. 340-50.
138. Ras, N.M., et al., *Phylogenesis of relapsing fever Borrelia spp.* Int J Syst Bacteriol, 1996. **46**(4): p. 859-65.
139. Cutler, S.J., et al., *Borrelia recurrentis characterization and comparison with relapsing-fever, Lyme-associated, and other Borrelia spp.* Int J Syst Bacteriol, 1997. **47**(4): p. 958-68.

Acknowledgements

I would like to thank...

... especially Prof. Dr. Roland Benz for giving me the opportunity to do my Doctoral Thesis in his laboratory and for being a very supportive and comprehensive person. Thank you also for making possible all the wonderful trips to Sweden, Moscow, Los Angeles and all those wonderful Biotechnology seminars.

... to Prof. Sven Bergström and his team for the great moments together in Umeå, for the accomplished work together and the great discussions...

... to Prof. Dr. Miquel Viñas Ciordia for his selfless support.

... to Dr. Marcus Thein, probably the person that have help me the most during my PhD, for his great advice, his friendship, and the hard work together... and also those great “Snickers breaks”..., since you are gone I have lost a lot of weight!!!

... to my first “Maecenas”, Teresa Camy, for helping me to start my scientific career.

... also to all my lab coworkers, specially Christoph Beitzinger and Angelika Kronhardt for help me with the improvement and correction of my Thesis and to Elke Maier for BLB advice. Thank you for putting up with my mood swings during the writing process (and maybe some other days, :)).

I would like to dedicate this Thesis to...

... my Spanish doctoral friends in Wuerzburg, for sharing with me this wonderful experience of doing the doctoral thesis in Germany, for all the good moments, the trips and experiences...

... my family; my two great brothers, Asier and Pablo and to my father whom I would love to have here today with me to enjoy this “Victory”.

...and above all, I dedicate this thesis to my mother. As the first page says in her language (Basque) because she always was and still is there to help me keep waking ahead...